Resilient Vertical Forest Renovation of Reinforced Concrete Structures in Seismic Prone Areas

(H.F.R.I. Project Number 015376)

Designs and photos of detailing and instrumentation and structural, energy, forestry retrofit of renovated 3d VF structure

Deliverable D2.2   Work package 2

Funding source

"Hellenic Foundation for Research & Innovation (H.F.R.I.)

Greece 2.0

Basic Research Financing Action"

Host Organization

Democritus University of Thrace (DUTH)

Collaborating Organizations

Aristotle University of Thessaloniki (AUTH)

June 2025

Funded by the European Union NextGenerationEU

The research project is implemented in the framework of H.F.R.I call “Basic research Financing (Horizontal support of all Sciences)” under the National Recovery and Resilience Plan “Greece 2.0” funded by the European Union – NextGenerationEU (H.F.R.I. Project Number: 015376)

Version	Date	Comments-Modifications
1	June 2025	Final Version
2		

Suggested citation:

Rousakis T., Voutetaki M., Kellis S., Zapris A., Lappa M., Xynopoulos I., Karabini M. Sapidis G., Papadopoulos N., Mallinis G., Stefanidou M., Theodoridou I., Kytinou V., Chalioris C., 2025. *Designs and photos of detailing and instrumentation and structural, energy, forestry retrofit of renovated 3d VF structure*. Greenergy-Resilient Vertical Forest Renovation of Reinforced Concrete Structures in Seismic Prone Areas (H.F.R.I. Project Number 015376). Deliverable D2.2 Democritus University of Thrace, Xanthi.

Project Title	Resilient Vertical Forest Renovation of Reinforced Concrete Structures in Seismic Prone Areas
Acronym	GREENERGY
HFRI Project Number	015376
Call identifier	Basic Research Financing (Horizontal support for all Sciences), National Recovery and Resilience Plan (Greece 2.0) / Sub-action 2. Funding Projects in Leading-Edge Sectors – RRFQ: Basic Research Financing (Horizontal support for all Sciences)
Thematic area	ThA1. Physical Sciences, Engineering Sciences and Technology, Environment and Energy
Thematic Field	1.16 Smart Cities
Host Organization	Democritus University of Thrace
Collaborating Institutions	Aristotle University of Thessaloniki
Project starting date	13/3/2024
Project Principal Investigator	**Dr. Theodoros Rousakis**
Affiliation	**Democritus University of Thrace / Department of Civil Engineering**
Email	**trousak@civil.duth.gr**
Telephone	25410 79645, 461 / 6977421569
Deliverable number and title	*D2.2* Designs and photos of detailing and instrumentation and structural, energy, forestry retrofit of renovated 3d VF structure
Related work package	**WP2** – Experimental dynamic assessment of physical model structure towards holistic renovation
Authors	Theodoros Rousakis, Maristella Voutetaki, Stefanos Kellis, Adamantis Zapris, Martha Lappa, Ioannis Xynopoulos, Martha Karabini, Georgios Sapidis, Nikolaos Papadopoulos, (DUTh) Violetta Kytinou, Constantin Chalioris. Georgios Mallinis, Maria Stefanidou, Ifigeneia Theodoridou (AUTh)

Τίτλος Έργου	Ανθεκτική Αντισεισμική Ανακαίνιση Κατασκευών από Ωπλισμένο Σκυρόδεμα σε Κάθετο Δάσος
Ακρωνύμιο	GREENERGY
Αριθμός Έργου ΕΛΙΔΕΚ	015376
Δράση	Χρηματοδότηση Βασικής Έρευνας (Οριζόντια υποστήριξη όλων των Επιστημών), Εθνικό Σχέδιο Ανάκαμψης και Ανθεκτικότητας (Ελλάδα 2.0)
Θεματική Περιοχή	ΘΠ1. Φυσικές Επιστήμες, Επιστήμες Μηχανικού και Τεχνολογίας, Περιβάλλον και Ενέργεια
Θεματικό Πεδίο	1.16 Έξυπνες Πόλεις
Φορέας Υποδοχής	Δημοκρίτειο Πανεπιστήμιο Θράκης
Συνεργαζόμενος Φορέας	Αριστοτέλειο Πανεπιστήμιο Θεσσαλονίκης
Ημερομηνία έναρξης Έργου	13/3/2024
Επιστημονικά Υπεύθυνος Έργου	**Δρ. Θεόδωρος Ρουσάκης**
Ίδρυμα / Τμήμα	**Δημοκρίτειο Πανεπιστήμιο Θράκης / Πολιτικών Μηχανικών**
Email	**trousak@civil.duth.gr**
Τηλέφωνα	25410 79645, 461 / 6977421569
Αριθμός και Τίτλος Παραδοτέου	***Π2.2*** *Σχέδια και Φωτογραφίες λεπτομερειών και ενοργάνωσης καθώς και της δομικής, ενεργειακής και δασικής αναβάθμισης της ανακαινισμένης 3Δ κατασκευής με ΚΔ.*
Σχετική Ενότητα Εργασίας	**ΕΕ2** – Πειραματική δυναμική αποτίμηση του φυσικού προσομοιώματος της κατασκευής προς την ολιστική ανακαίνιση
Συγγραφείς	Θεόδωρος Ρουσάκης, Μαριστέλλα Βουτετάκη, Στέφανος Κέλλης, Αδαμάντης Ζάπρης, Μάρθα Λάππα, Ιωάννης Ξυνόπουλος, Μάρθα Καραμπίνη, Γεώργιος Σαπίδης, Νικόλαος Παπαδόπουλος, (ΔΠΘ), Βιολέτα Κυτίνου,, Κωνσταντίνος Χαλιορής Γιώργος Μαλλίνης, Μαρία Στεφανίδου, Ιφιγένεια Θεοδωρίδου (ΑΠΘ)

ACKNOWLEDGEMENTS

This project is carried out within the framework of the National Recovery and Resilience Plan Greece 2.0, funded by the European Union – NextGenerationEU (Implementation body: HFRI).

TABLE OF CONTENTS

LIST OF TABLES

LIST OF FIGURES

LIST OF ACRONYMS

VF	Vertical Forest
RC	Reinforced Concrete
PZT	Piezoelectric sensors or piezoelectric transducers
3D	3 Dimensions
etc	et cetera
D22	Deliverable 22
e.g.	exempli gratia (for example)
PFJ	Polymer Flexible Joints
PUFJ	Polyurethane Flexible Joints
SHM	Structural Health Monitoring
EMI	Electromechanical Impedance
DUTH	Democritus University of Thrace
SG	Strain gauges
AUTH	Aristotle University of Thessaloniki

ABSTRACT

GREENERGY aims to investigate Reinforced Concrete Structure in Seismic Prone Areas after Resilient Vertical Forest Renovation. This report focuses on the retrofitting process of the columns and brick infills of the test specimen, along with the modifications and additions made to receive Vertical Forest (VF) renovations. Special constructions are attached on the structure to simulate eight cases of vertical living walls attachments with different detailing as well as five critical cases of anchoring of simulated planters with wooden trees. The mass and stiffness of the VF constructions and their interfaces are presented in detail. The report outlines, step by step, the applied renovation techniques.

In addition to the extensive instrumentation presented in previous reports of workpackage 2, PZT sensors have been installed in the lightweight PU flexible joint (PUFJ) regions between the brick walls and the concrete columns, on the lightweight external PU glass grid jackets (FRPU jackets) as well as on the basalt rope confinement of columns. Further, PZT sensors instrumented the bottom steel anchors of the vertical living walls as well as their top basalt rope anchor detailing. The PUFJs and the top basalt rope anchors of the vertical living walls received in addition strain gauge

Keywords: experiment, seismic table, reinforced concrete, brick wall infills, seismic excitation, Vertical Forest, planter, PUFJ, FRPU, basalt rope, resilience, renovation, structural, structural health monitoring, PZT

ΠΕΡΙΛΗΨΗ

Το GREENERGY στοχεύει στην διερεύνηση της Ανακαίνισης Κατασκευών Οπλισμένου Σκυροδέματος με Κάθετα Δάση, σε Περιοχές με Έντονη Σεισμικότητας. Η παρούσα έκθεση εστιάζει στη διαδικασία αναβάθμισης του δοκιμίου 3Δ κατασκευής, με τις επεμβάσεις στα υποστυλώματα και στις τοιχοπληρώσεις, μαζί με τις τροποποιήσεις και προσθήκες που έγιναν ώστε να αναλάβει η κατασκευή τις καινοτόμες ανακαινίσεις με Κάθετα Δάση. Ειδικές κατασκευές-προσαρτήματα προσομοιώνουν οκτώ περιπτώσεις κάθετων ζωντανών τοίχων με διαφορετικές λεπτομέρειες στήριξης, καθώς και πέντε κρίσιμες περιπτώσεις αγκύρωσης γλαστρών με δέντρα σε δώματα και μπαλκόνια. Η μάζα και η δυσκαμψία των κατασκευών κάθετου δάσους και οι διεπιφάνειες παρουσιάζονται με λεπτομέρεια. Η αναφορά παρουσιάζει διεξοδικά τις εφαρμοζόμενες τεχνικές ανακαίνισης.

Επιπρόσθετα της εκτεταμένης ενοργάνωσης που παρουσιάστηκε στις προηγούμενες αναφορές του πακέτου αναφοράς 2, εγκαταστάθηκαν αισθητήρες PZT στους αρμούς PUFJ μεταξύ των υποστυλωμάτων και των τοιχοπληρώσεων, στους μανδύες FRPU καθώς και στα σχοινιά βασάλτη που περιέσφιξαν τα υποστυλώματα. Επιπλέον, αισθητήρες PZT εφαρμόστηκαν στη βάση των χαλύβδινων αγκυρίων των ειδικών κατασκευών κάθετων ζωντανών τοίχων, καθώς και στις αγκυρώσεις με σχοινί βασάλτη στην κορυφή των κατασκευών αυτών. Οι αρμοί PUFJ και τα αγκύρια κορυφής από σχοινί βασάλτη των κάθετων ζωντανών τοίχων διαθέτουν επιπρόσθετα και παραμορφωσιόμετρα.

Λέξεις κλειδιά: πείραμα, σεισμική τράπεζα, οπλισμένο σκυρόδεμα, τοιχοπληρώσεις, τούβλα, σεισμική διέγερση, Κάθετα Δάση, γλάστρα με φύτευση, εύκαμπτοι αρμοί, μανδύας υαλοπλέγματος με πολυουραιθάνη, ανθεκτικότητα, ανανηπτικότητα, ανακαίνιση, δομικός, δομοστατικός, παρακολούθηση δομικής υγείας SHM, PZT

1 THE AS-BUILT TEST SPECIMEN

The following figures show again the detailing of the as built specimen.

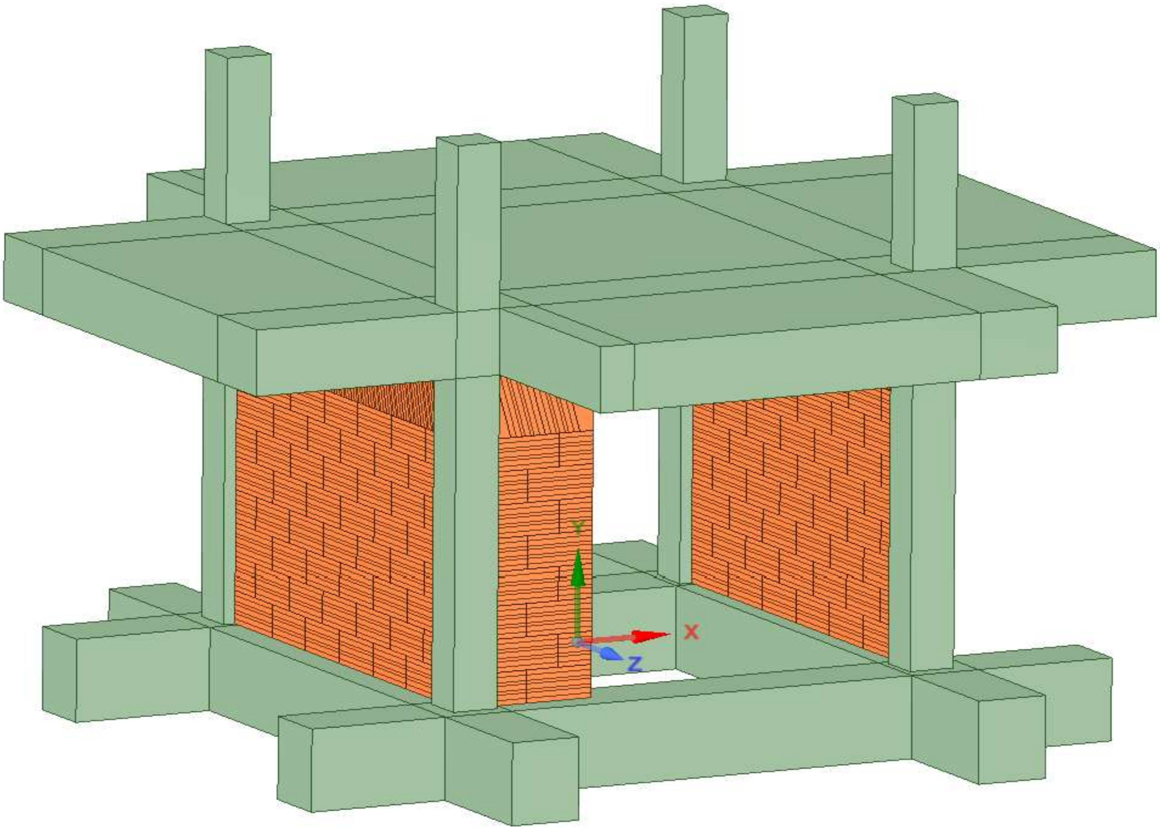

Figure 1.1 3D View of construction

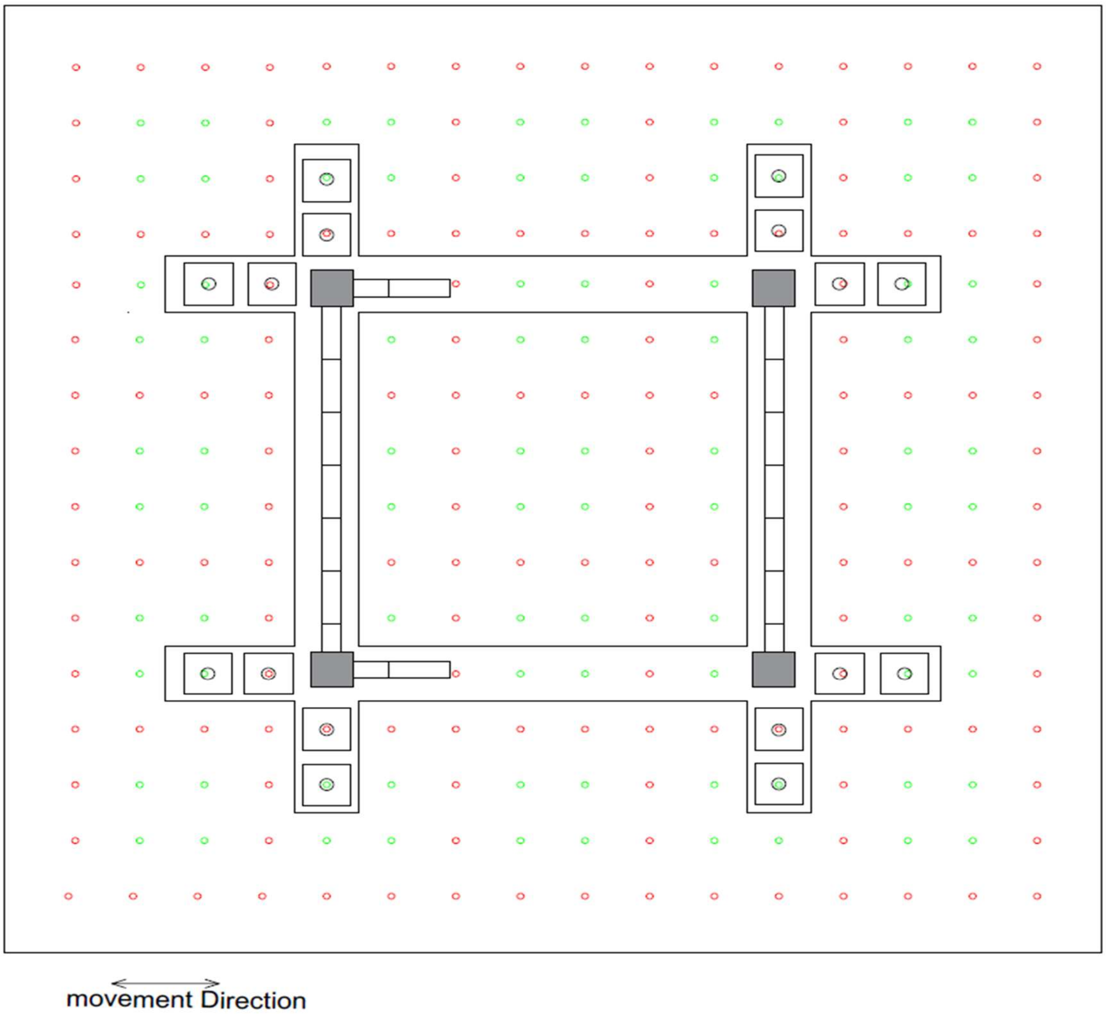

Figure 1.2 Fixing of the specimen on the shake table with steel bolts

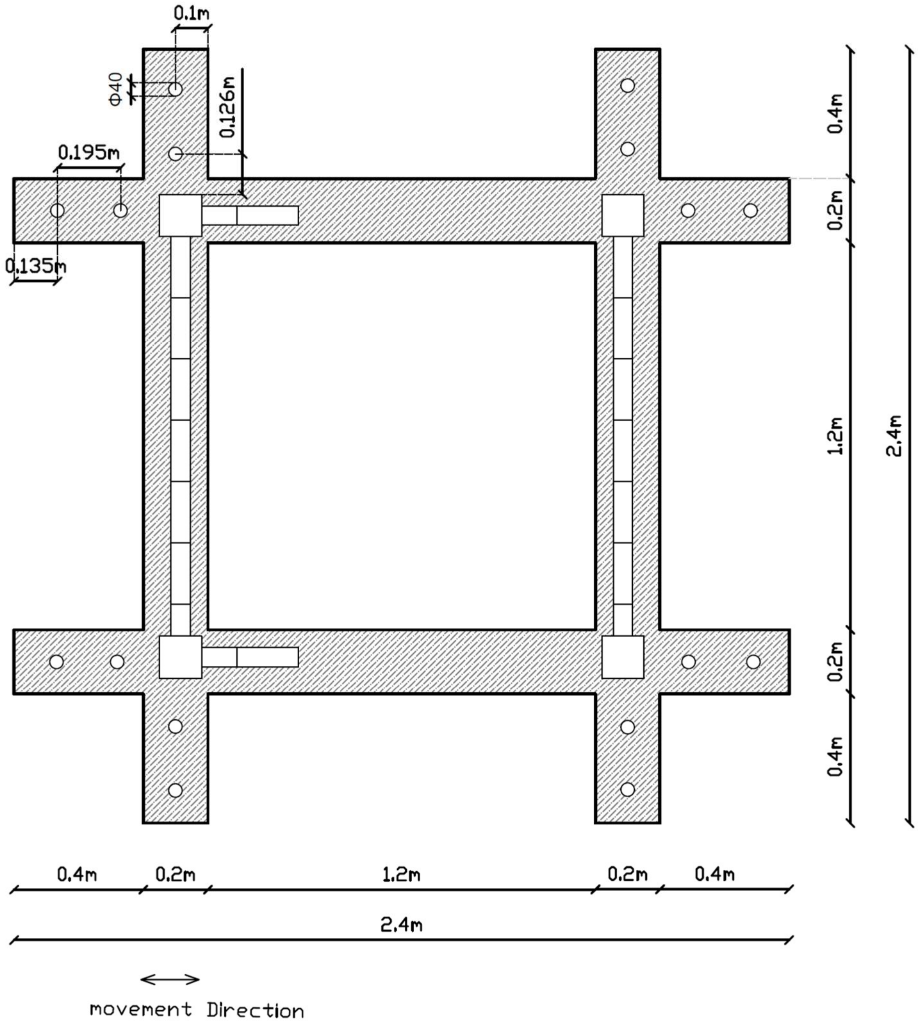

Figure 1.3 Floor plan of foundation

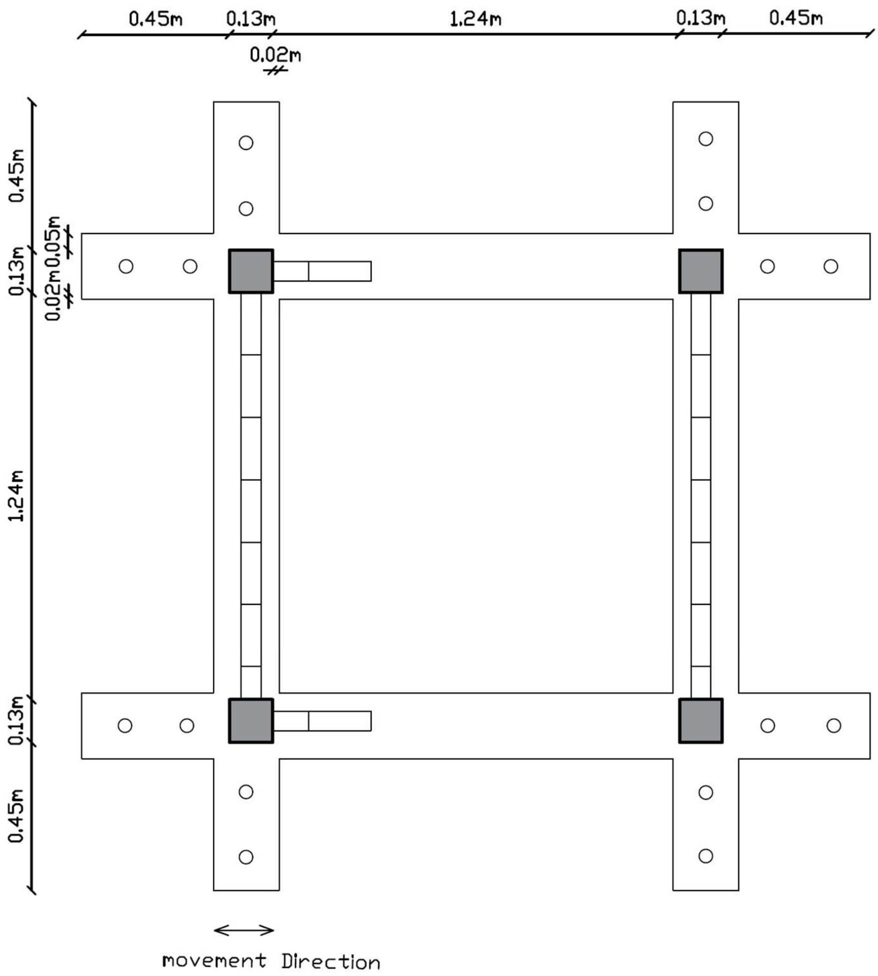

Figure 1.4 Floor plan of columns

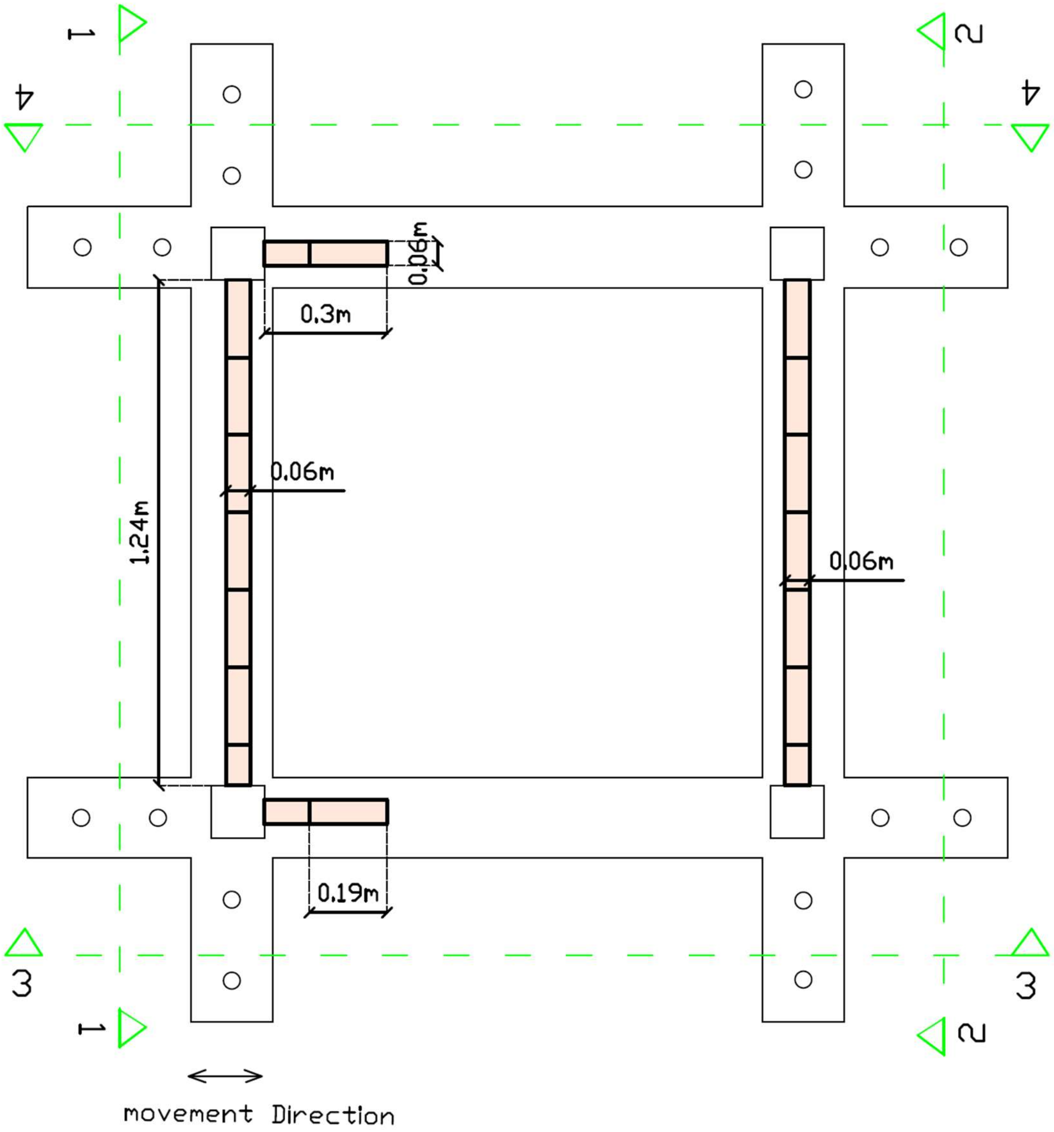

Figure 1.5 Floor plan of brick infill walls

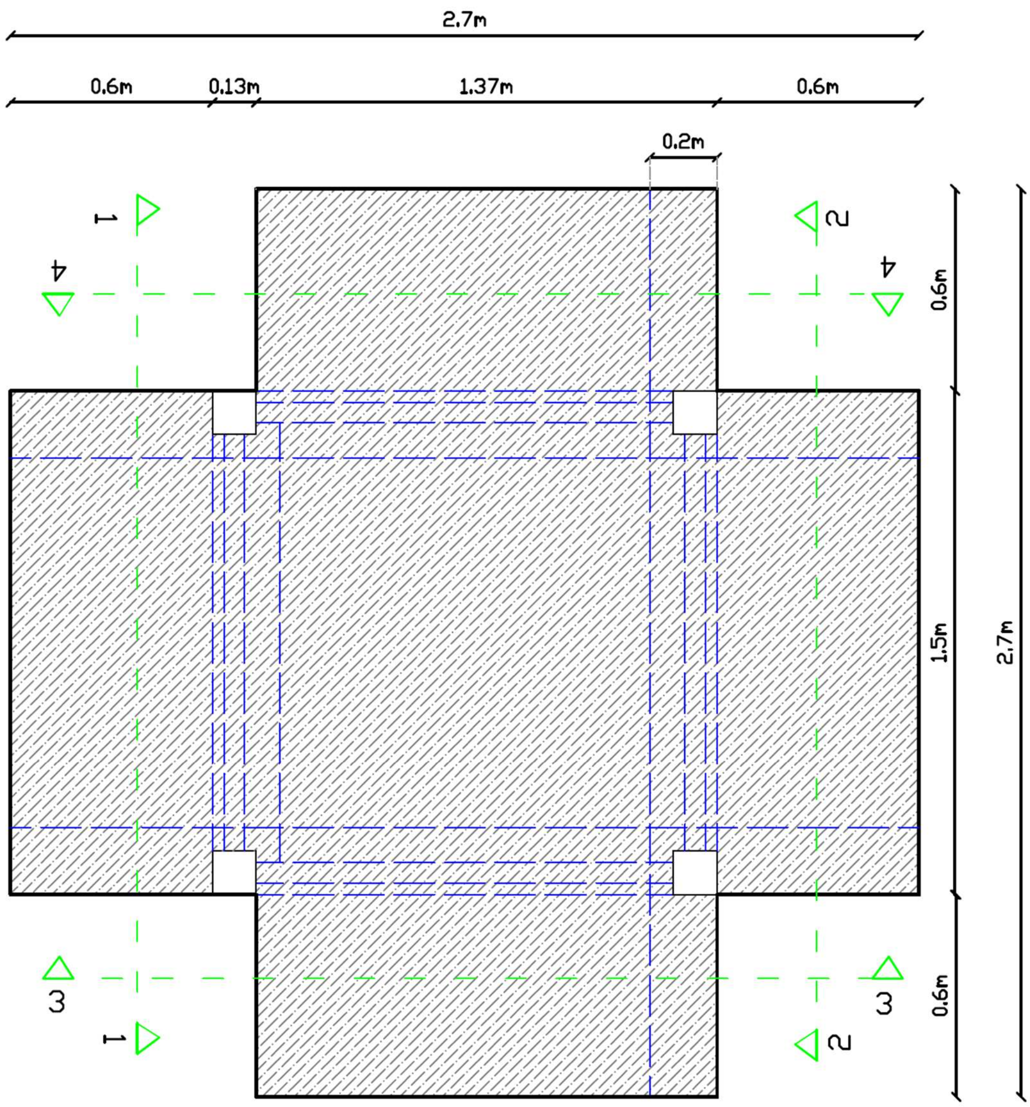

Figure 1.6 Floor plan of top slab

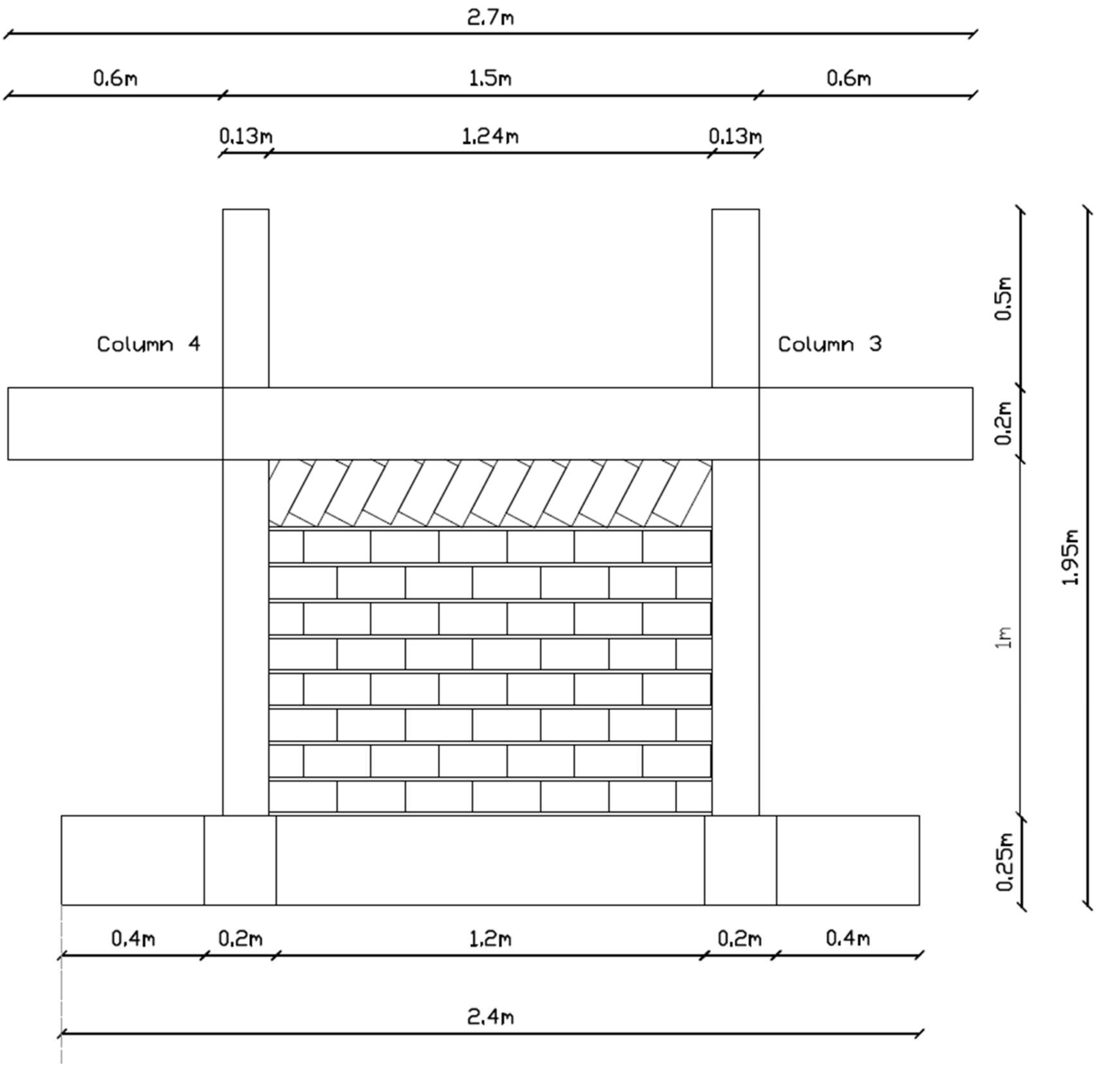

Figure 1.7 View of the structure perpendicular to the direction of loading of the seismic table

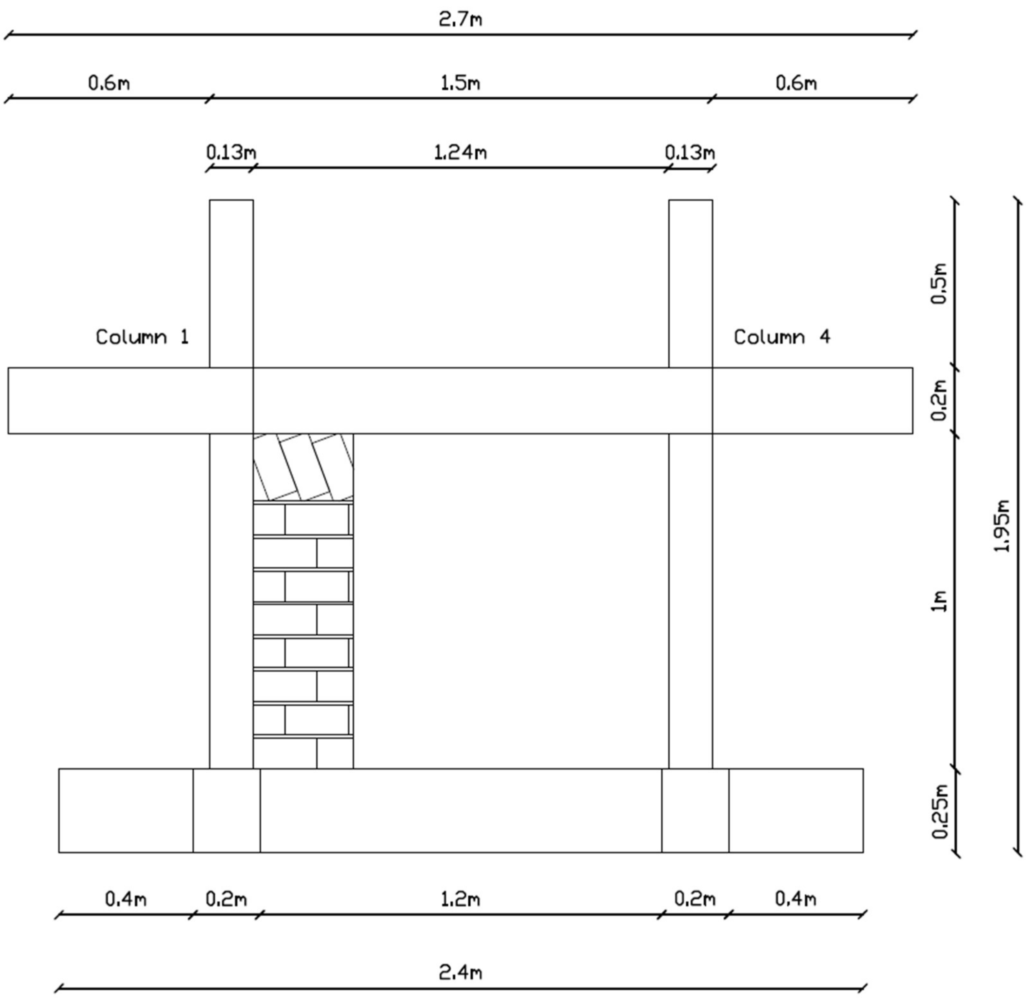

Figure 1.8 View of the structure parallel to the direction of loading of the seismic table

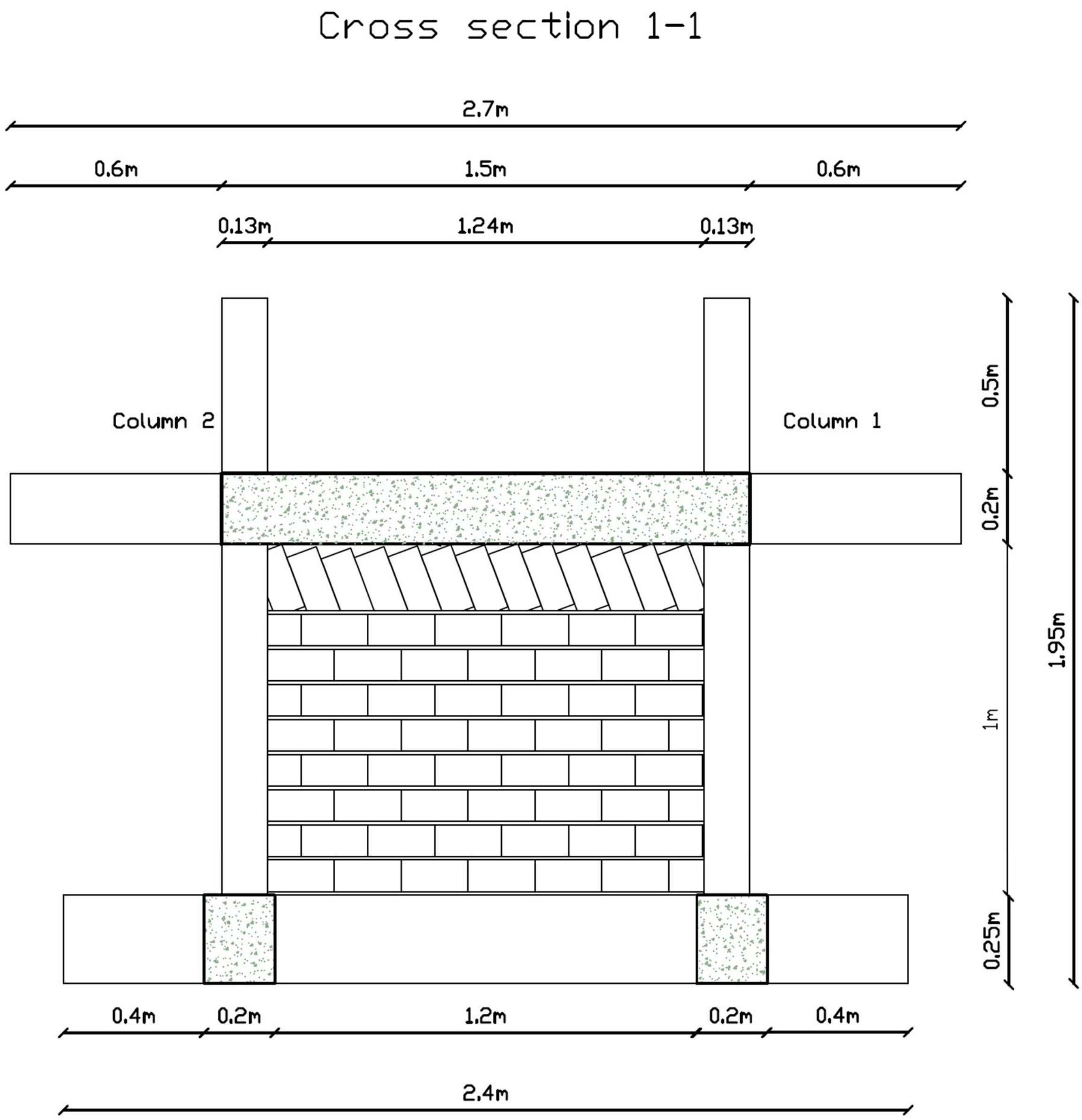

Figure 1.9 Section at the location of the external cantilever, perpendicular to the direction of movement of the seismic table

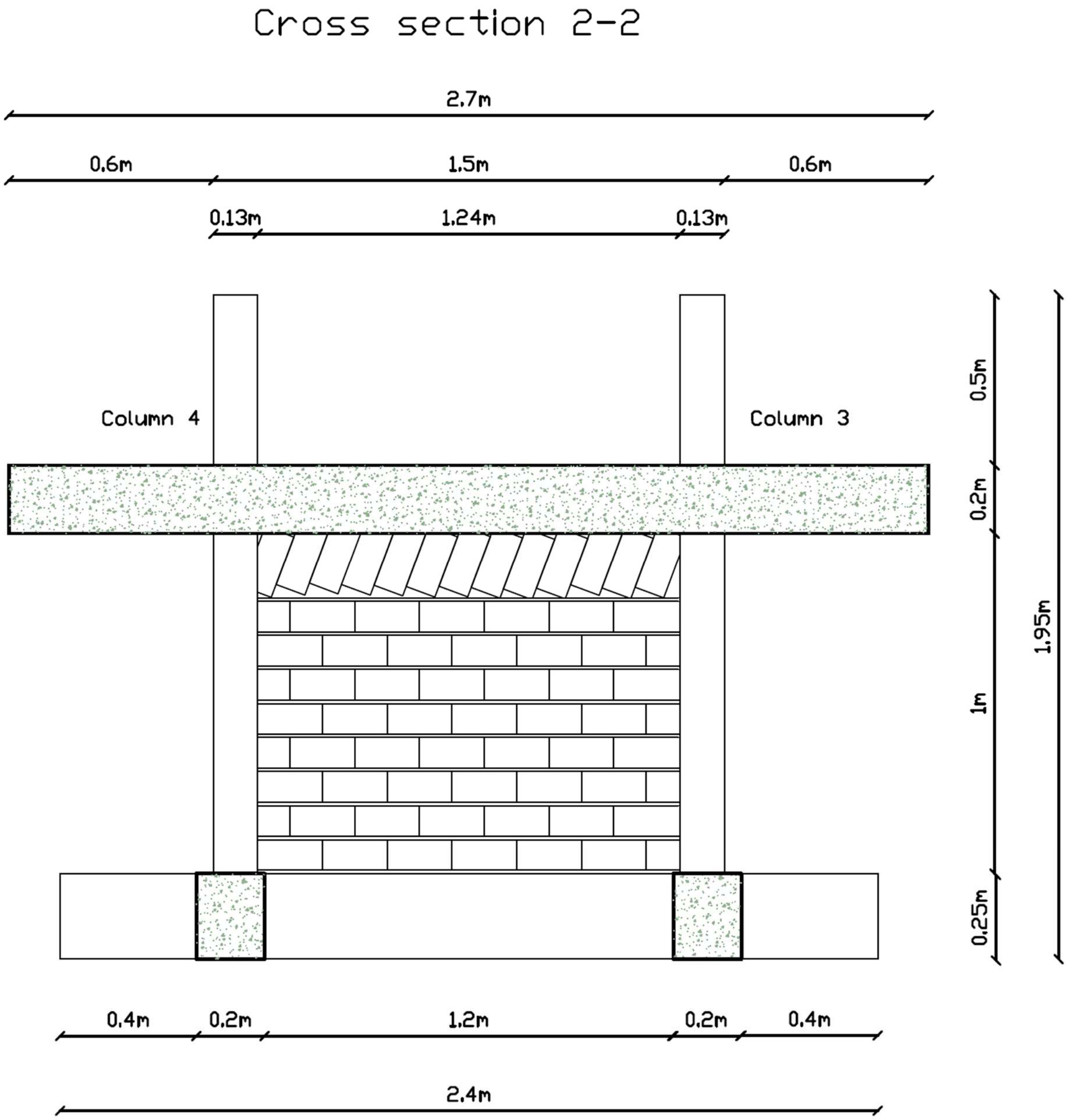

Figure 1.10 Section at the location of the internal slab, perpendicular to the direction of movement of the seismic table

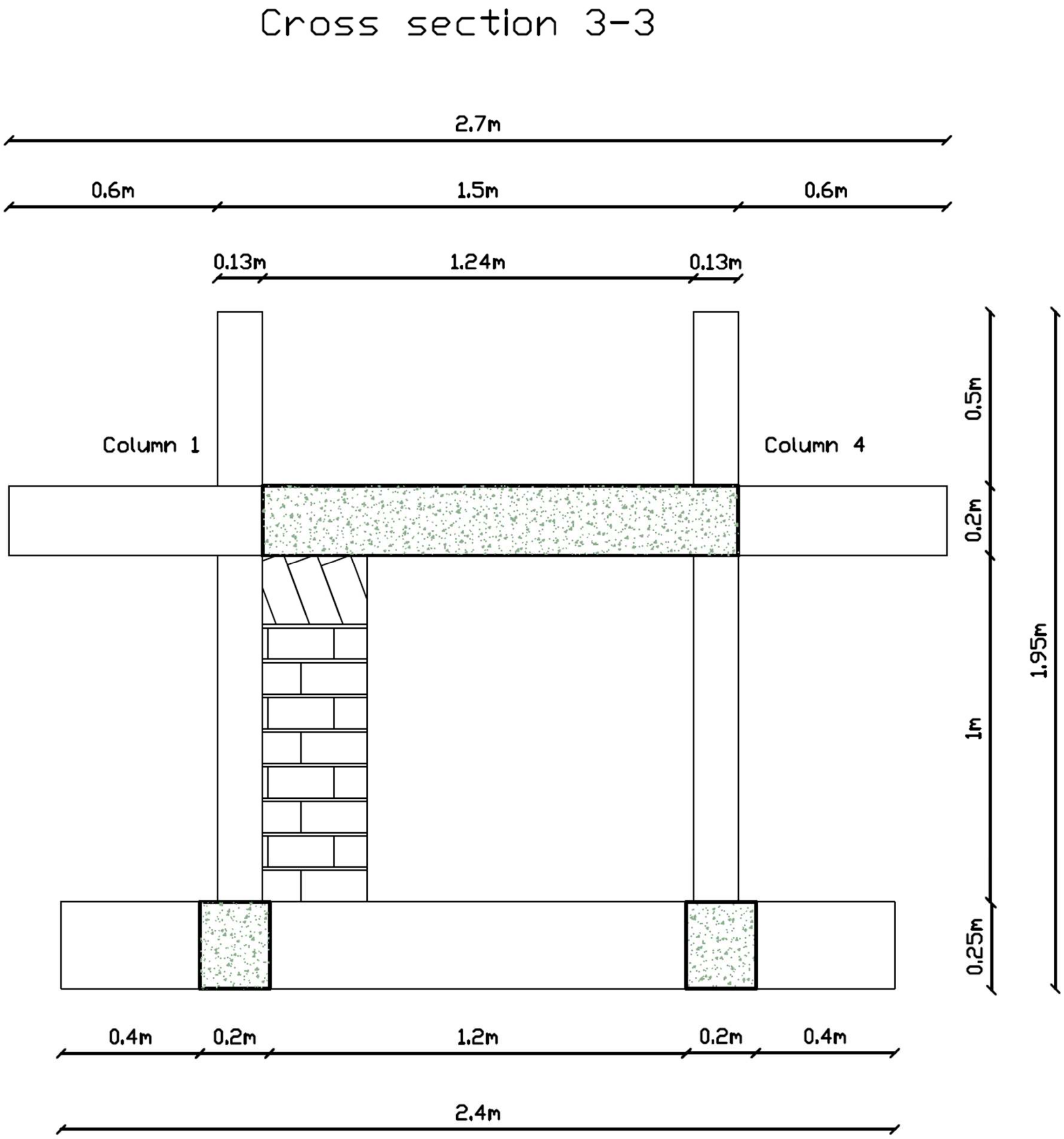

Figure 1.11 Section at the location of the external cantilever, parallel to the direction of movement of the seismic table

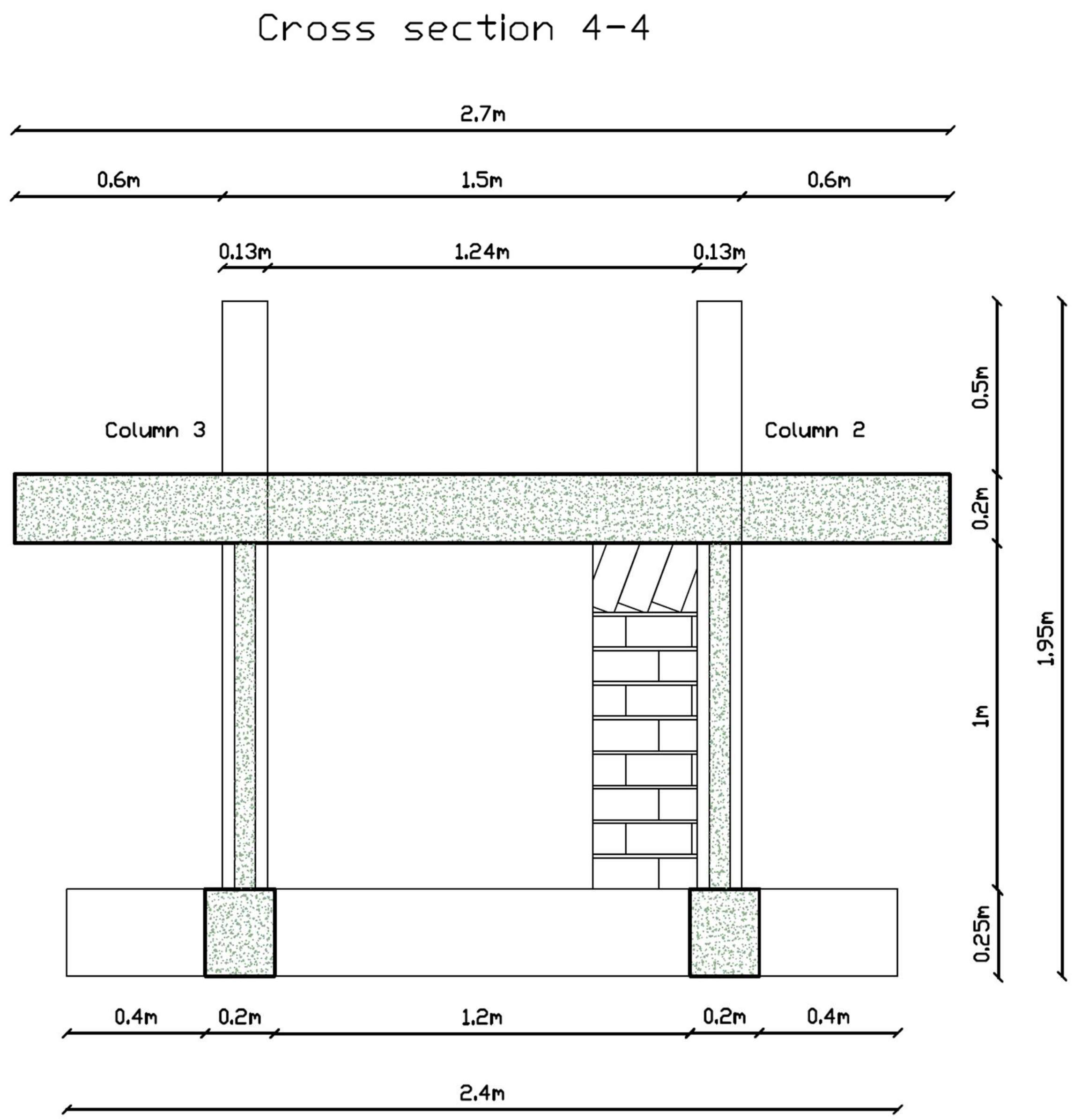

Figure 1.12 Section at the location of the internal slab, parallel to the direction of movement of the seismic table

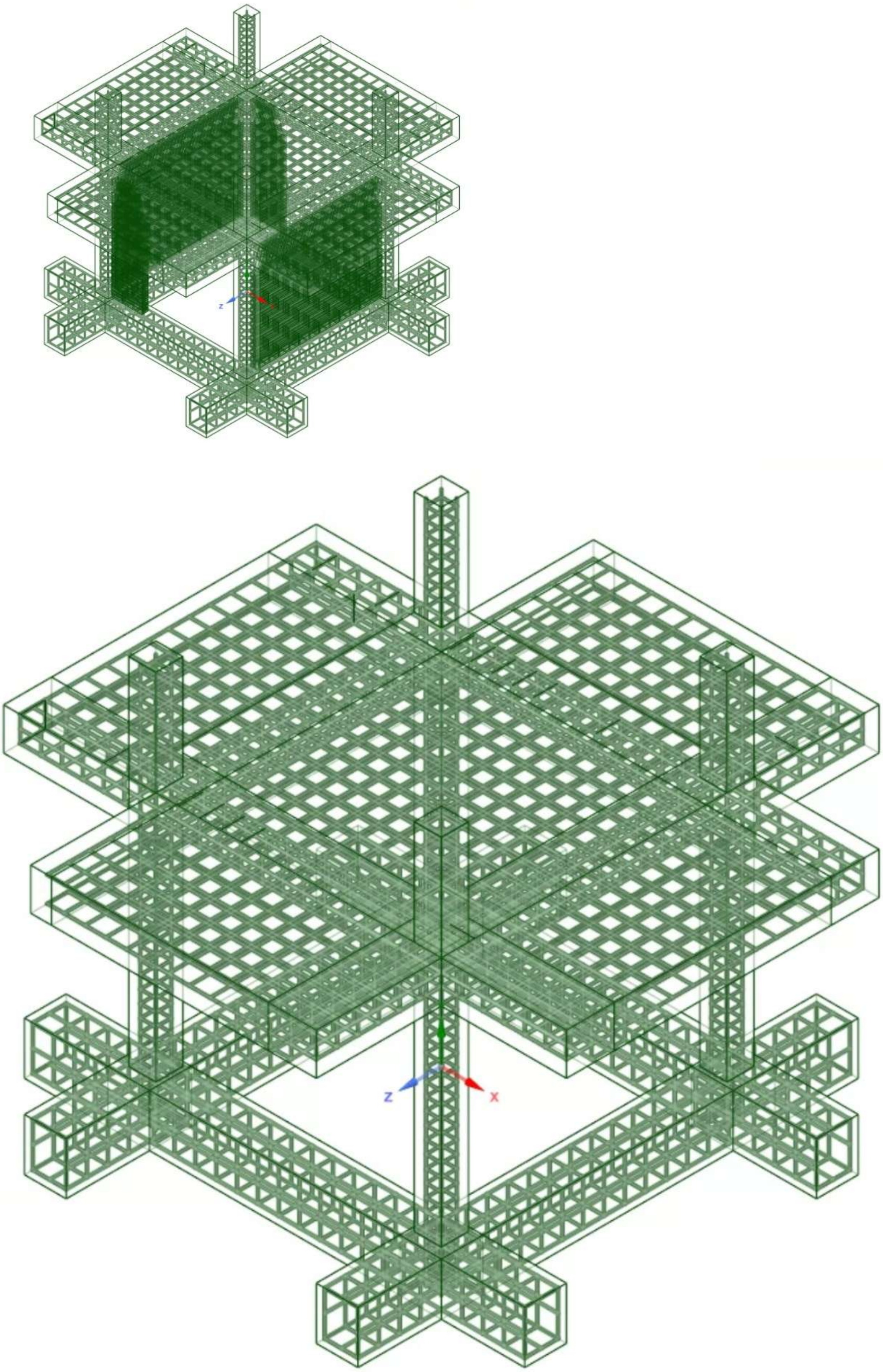

Figure 1.13 3D View of main reinforcement detailing

2. JOINTS OF REINFORCED CONCRETE COLUMNS AND BEAMS HIDDEN INSIDE THE SLAB

During the first phase of testing, there was no obvious damage around the column-beam RC regions or relevant alarming recording by PZT sensor in the region. This section concerns suitable calculations for the shear capacity of the column-slab rc joints in order to assess if there is a need for strengthening before the execution of the second phase of testing.

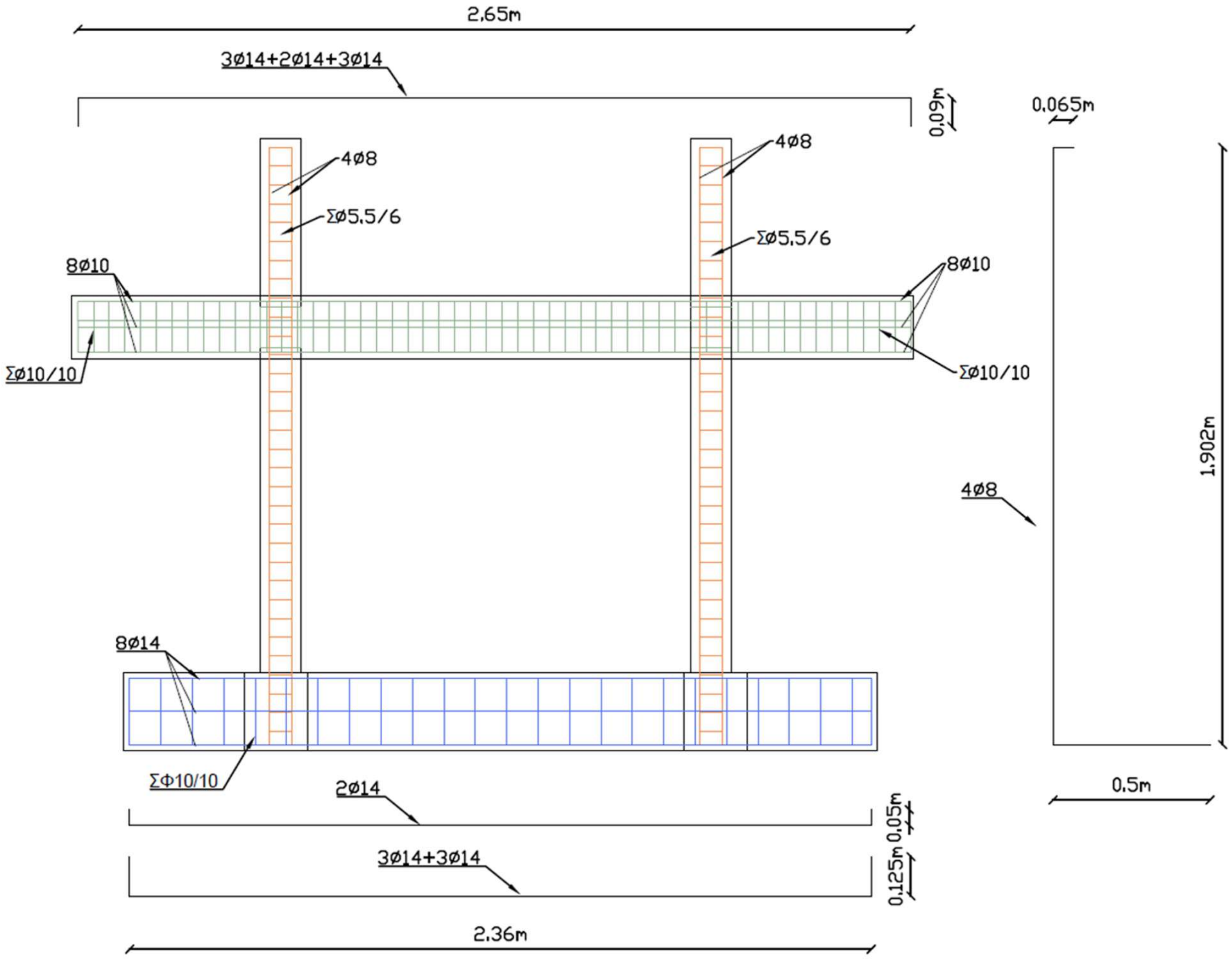

Figure 2.1 Typical frame detailing

Table 2.1 Materials and members

CHARACTERISTICS				
MATERIALS		MEMBERS		
f_{cm} (MPa)	f_y (MPa)	b_w (mm)	b_c (mm)	bj (mm)
25.5	564	200	130	195
f_{ctm} (MPa)	f_u (MPa)	h_b (mm)	h_c (mm)	Aj (mm2)
2.02215	663	200	130	17550
E (MPa)		L_b clear (mm)	L_c (mm)	N (N)
195000		600	1700	8750
		A_{s1} (mm^2)	A_{sc} (mm^2)	
		235.6	100.5	

2.1 THEORETICAL KNOWLEDGE

2.1.1 Interior Joints

The horizontal shear force of an interior RC joint is estimated as:

$$V_{jh} = (A_{s1} + A_{s2})\lambda f_y - V_{col} \quad (1)$$

where, $V_{col} = P_u\,(L_{cl} + \frac{h_c}{2})/H_c$

The total shear capacity of the joint for every direction is equal to the shear forces that the strut and truss mechanisms can transfer:

$$V_{jh} = V_{ch} + V_{sh} \quad (2)$$

The part of shear force that the strut mechanism can transfer (V_{ch} or V_{cv}) is estimated, while the rest of the horizontal shear force (V_{sh}) is used for the calculation of the required transverse reinforcement.

The shear force of the strut mechanism is equal to the horizontal component of the compressive force acting on the joint (Dc) and it consists of (i) the compressive force Cc2 that is developed at the compressive area of the beam, (ii) the force ΔTc the upper reinforcement transfers to the concrete through adhesion, and (iii) the shear force on the column (Vcol)

$$V_{ch} = C_{c2} + \Delta T_c - V_{col} \quad (3)$$

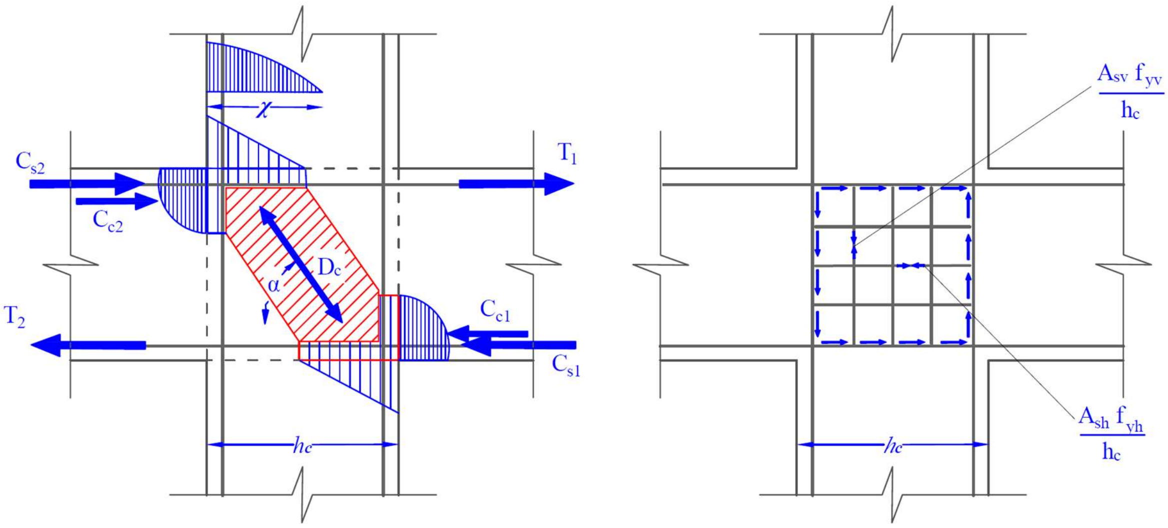

Figure 2.2 Joint forces and resistance mechanism

The force of the reinforcement due to compression is equal to:

$$C_{c2} = \lambda f_y \, A_{s1} = \left(\frac{\gamma}{\lambda}\right) T_1 \quad (4)$$

and also $T_1 = A_{s1} \lambda f_y$ & $T_2 = A_{s2} \lambda f_y$

thus, $T_2 = (A_{s2}/A_{s1}) T_1 = \beta T_1$

From the equilibrium of the beam's cross section

$$C_{c2} = T_2 - C_{s2} = \beta T_1 - \left(\frac{\gamma}{\lambda}\right) T_1 = (\beta - \frac{\gamma}{\lambda}) T_1 \quad (5)$$

Where γ has a maximum value of 0.7.

To continue with,

$$\varDelta T_c = (T_1 + C_{s2}) \left(\frac{x}{hc}\right) = \frac{T_1 \left(1 + \frac{\gamma \beta}{\lambda}\right) x}{hc} \quad (6)$$

Knowing that:

1. γ is not higher than 0.7
2. 1.2< λ < 1.4
3. $\beta = A_{s2}/A_{s1}$ is between 0.5 and 1 for interior joints, and in this case equal to 1:

- $\varDelta T_c = 1.55 \left(\frac{x}{hc}\right) T_1$ (7)

Finally, the part of the horizontal shear force that is taken from the diagonal strut is equal to:

$$V_{ch} = C_{s2} + \varDelta T_c - V_{col} = \left(\beta - \frac{\gamma}{\lambda}\right) T_1 + 1.55 \left(\frac{x}{h_c}\right) T_1 - V_{col}$$

$$V_{ch} = (1.55 \frac{x}{h_c} + \beta - 0.55) T_1 - V_{col} \quad (8)$$

And the part that is taken from the truss mechanism (V_{sh}) is equal to:

$$V_{sh} = V_{jh} - V_{ch} = T_1 + \beta \, T_1 - V_{col} - [\left(1.55 \left(\frac{x}{h_c}\right) + \beta - 0.55\right) T_1 - V_{col}\right] = 1.55 \left(1 - \left(\frac{x}{h_c}\right)\right) T_1 \quad (9)$$

For compression-dominant elements x given as approximately: $x = (0.25+0.85\ N_c/\ f_c\ A_c)\ h_c$

Then,

$V_{sh} = (1.15 - 1.3\ v_c)T_1$ (10)

With

$v_c = N_c/\ f_c A_c$ and $T_1 = \lambda\ f_y\ A_{s1}$

Consequently, the requirement of transverse reinforcement into the joint is estimated to

$A_{sh} = V_{sh}/f_y$ (11)

2.1.2 Exterior Joints

For the case of an **exterior** BC joint, the horizontal shear force is estimated as:

$V_{jh} = A_{s1}\lambda f_y - V_{col}$ (12)

where, $V_{col} = P_u\ (L_{cl} + \frac{h_c}{2})/H_c$

From the equilibrium of moments for the exterior joint, the vertical component of the shear force in accordance with the horizontal component is

$V_{jv} = \left(\frac{h_b}{h_c}\right) V_{jh}$ (13)

The total shear capacity of the joint for every direction is equal to the shear forces that the strut and truss mechanisms can transfer:

$V_{jh} = V_{ch} + V_{sh}$ (14)

where

$V_{ch} = C_c + \Delta T_c - V_{col}$ (15)

with

$C_c = T_1 - \gamma f_y A_{s2} = (1 - \frac{\gamma\beta}{\lambda})T_1$ (16)

For reinforcement in compression γ < 0.7

$\Delta T_c = \frac{\beta}{\lambda}\left(\frac{x}{h_c}\right) T_1$ (17)

and thus,

$V_{ch} = C_c + \Delta T_c - V_{col} = \left(1 - \frac{0.7\beta}{\lambda}\right) T_1 + \frac{\beta}{\lambda}\left(\frac{x}{h_c}\right) T_1 - V_{col}$ (18)

And finally,

$$V_{sh} = V_{jh} - V_{ch} = T_1 - V_{col} - \left[1 - \frac{0.7\beta}{\lambda} + \frac{\beta}{\lambda}\left(\frac{x}{h_c}\right)\right] T_1 + V_{col}$$

$$V_{sh} = \frac{\beta}{\lambda}\left(0.7 - \frac{x}{h_c}\right) T_1 \qquad (19)$$

Consequently, the requirement of transverse reinforcement into the joint is estimated to

$A_{sh} = V_{sh}/f_y$

2.2 GREEK RETROFITTING CODE

For the case where the columns are weaker and consequently yield first, the Greek Retrofitting Code suggest that the yield of the column determines the shear force in the joint, and it is calculated according to

$$V_{jv} = \sum M_{yc}\left(\frac{1}{z_c} - \frac{1}{L_b}\frac{h_{st}}{h_{st,n}}\right) + \frac{1}{2}\left|V_{b,l} - V_{b,r}\right| \qquad (20)$$

Diagonal tensile cracking on the joint occurs when:

$$\tau_j \geq \tau_c = f_{ct}\sqrt{\left(1 + \frac{\rho_{jh} f_{yw}}{f_{ct}}\right)\left(1 + \frac{v_{top} f_c}{f_{ct}}\right)} \qquad (21)$$

where

$\tau_j = V_{jv}/A_j$

and

$\rho_{jh} = A_{sh}/A_j$, i.e. A_{sh} the total area of the transverse reinforcement into the joint, A_j the area of the joint.

Failure of the joint due to compressive strut occurs when

$$\tau_j \geq \tau_{ju} = n f_c \sqrt{1 - \frac{v_{top}}{n}} \qquad (22)$$

where n is calculated according to

$$n = 0.6\left(1 - \frac{f_c}{250}\right) \qquad (23)$$

In the case of $\tau_j \leq \tau_c$ (eq.21), n is taken equal to 1.

Considering the above theoretical knowledge, predictions of the behavior of the joints have been made. The columns as they are the weaker members, are transmitting shear force into the joint area. Thus, assessment according to Greek Retrofitting Code are considered to be more appropriate for this structure.

The yielding moment of the column is calculated based on the column's reinforcement and the characteristic strength of steel and it is equal to

$M_{yc} = A_{sc} * f_y * 0.9d = 5.61kNm$

Using eq. 20 =, V_{jv} is calculated, and it is equal to 13.15kN

Corresponding to a shear stress on the joint equal to

$\tau_j = V_{jv}/A_j = 0.75MPa$ for the case of an interior joint

$\tau_j = V_{jv}/A_j = 1.49MPa$ for the case of an exterior joint

Diagonal tensile cracking on the joint would occur if $\tau_j \geq \tau_c$, where τ_c is calculating according to eq. 21 and it is equal to 3.58MPa.

Finally, eq. 22 is used to estimate if failure due to compression in the diagonal strut is possible to occur.

$$\tau_{ju} = 25.2MPa \geq \tau_j$$

Consequently, $\tau_j \leq \tau_c$ and $\tau_j \leq \tau_{ju}$ for both cases of interior and excterior joints.

3 DESIGNS AND PHOTOS OF DETAILING AND INSTRUMENTATION AND STRUCTURAL, ENERGY, FORESTRY RETROFIT OF RENOVATED 3D VF STRUCTURE.

The building, after being subjected to a sequence of seismic loads, developed SLS related damages. The following procedures were followed to retrofit the building:

3.1 RETROFIT MATERIALS.

Polymer for PUFJ (PolyUrethane Flexible Joints) was of type Sika **PM**. The elastic modulus, strength and ultimate elongation of the polymer were 4 MPa, 1.4 MPa and 110%, respectively in a tensile test.

Polymer for FRPU (Fibre Reinforced PolyUrethane) was of type Sika **PS**. The elastic modulus, strength and ultimate elongation of the polymer were 16 MPa, 2.5 MPa and 40%, respectively.

Glass fiber mesh of type Sika Wrap 350G Grid, made of glass fibre reinforced polymer mesh, was used for the repair of the walls. The mesh of a real weight 360 g/m^2 has the elastic modulus , strength and ultimate elongation of the glass mesh were 80 000 MPa, 2 600 MPa and 4%, respectively in a tensile test. This mesh was impregnated and glued with resin PS.

Braided basalt fiber rope, with a tensile modulus of elasticity of 69.3 GPa, an ultimate stress of 1282 MPa and 1.85% elongation at failure was applied (as provided by the manufacturer) with no use of impregnating or gluing resin.

Quantities of retrofit materials that were used:

FRPU (PS) , GFRP

1) 2 Full masonry walls

Dimensions of grid: 1,10 (height) * 0,33 (width) = 0,36 m^2

1,10 (height)* 0,24 (width) = 0,26 m^2

3 * 0,36 = 1,08 m^2

Sum: 1,08 + 0,26 = 1,34 m^2

2 * 1,34 = 2,68 m^2

2) 2 Partial masonry walls

Dimensions of grid: 1,10 (height) x 0,30m (width) = 0,33m^2

2 x 0,33 = 0,66m^2

Sum: 2,68 + 0,66 = 3,52 m^2 of glass mesh, of primer and of PS

PUFJ (PM) Construction joint

Joint thickness 0,019 m

0,06 m (width of wall) x 0,019 m (joint thickness) x 0,1 m (height) = 0,00011 m^3 (PM volume per joint length)

Joint thickness 0,02 m

0,06 m (width of wall) x 0,02 m (joint thickness) x 0,1 m (height) = 0,00012 m^3 (PM volume per joint length)

Joint thickness 0,021 m

0,06 m (width of wall) x 0,021 m (joint thickness) x 0,1 m (height) = 0,00013 m^3 (PM volume per joint length)

Joint thickness 0,022 m

0,06 m (width of wall) x 0,022 m (joint thickness) x 0,1 m (height) = 0,00013 m^3 (PM volume per joint length)

Joint thickness 0,023 m

0,06 m (width of wall) x 0,023 m (joint thickness) x 0,1 m (height) = 0,00014 m^3 (PM volume per joint length)

Joint thickness 0,024 m

0,06 m (width of wall) x 0,024 m (joint thickness) x 0,1 m (height) = 0,00014 m^3 (PM volume per joint length)

Joint thickness 0,025 m

0,06 m (width of wall) x 0,025 m (joint thickness) x 0,1 m (height) = 0,00015 m^3 (PM volume per joint length)

Joint thickness 0,026 m

0,06 m (width of wall) x 0,026 m (joint thickness) x 0,1 m (height) = 0,00016 m^3 (PM volume per joint length)

Joint thickness 0,027 m

0,06 m (width of wall) x 0,027 m (joint thickness) x 0,1 m (height) = 0,00016 m^3 (PM volume per joint length)

Joint thickness 0,028 m

0,06 m (width of wall) x 0,028 m (joint thickness) x 0,1 m (height) = 0,00017 m^3 (PM volume per joint length)

Joint thickness 0,029 m

0,06 m (width of wall) x 0,029 m (joint thickness) x 0,1 m (height) = 0,00017 m^3 (PM volume per joint length)

Joint thickness 0,022 m

0,06 m (width of wall) x 0,022 m (joint thickness) x 0,2 m (height) = 0,00026 m^3 (PM volume per joint length)

Joint thickness 0,023 m

0,06 m (width of wall) x 0,023 m (joint thickness) x 0,2 m (height) = 0,00027 m^3 (PM volume per joint length)

Joint thickness 0,024 m

0,06 m (width of wall) x 0,024 m (joint thickness) x 0,2 m (height) = 0,00029 m^3 (PM volume per joint length)

Joint thickness 0,027 m

0,06 m (width of wall) x 0,027 m (joint thickness) x 0,2 m (height) = 0,00032 m^3 (PM volume per joint length)

6 m (total length for six vertical interfaces)

(a) $0{,}00012 + 0{,}00015 + 0{,}00014 + 3 * 0{,}00013 + 0{,}00013 + 0{,}00014 + 0{,}00027 =$ **$0{,}0011 m^3$**

(b) $0{,}00012 + 0{,}00013 + 0{,}00012 + 2 * 0{,}00011 + 0{,}00014 + 2 * 0{,}00013 + 0{,}00026 =$ **$0{,}0013\ m^3$**

(a) $2 * 0{,}00014 + 0{,}00017 + 0{,}00014 + 2 * 0{,}00017 + 2 * 0{,}00016 + 0{,}00029 =$ **$0{,}0041\ m^3$**

$2 * 0{,}00014 + 0{,}00013 + 0{,}00013 + 2\ 0{,}00013 + 0{,}00013 + 0{,}00015 + 0{,}00027 =$ **$0{,}0014\ m^3$**

(b) $3 * 0{,}00013 + 0{,}00013 + 0{,}00012 + 0{,}00011 + 0{,}00013 + 0{,}00016 + 0{,}00027 =$ **$0{,}0013\ m^3$**

$3 * 0{,}00012 + 0{,}00017 + 0{,}00016 + 0{,}00017 + 0{,}00016 + 0{,}00016 + 0{,}00032 =$ **$0{,}0015\ m^3$**

Sum: $= 0{,}0011 + 0{,}0013 + 0{,}0041 + 0{,}0014 + 0{,}0013 + 0{,}0015 = 0{,}0106\ m^3$ = 10,6 litr. of PM

3.2 PREPARATION OF CONCRETE SUBSTRATE AND JOINT GAPS

The corners of the columns were rounded with a radius of curvature ranging from 1.6cm – 2.2cm. The resulting plan view of the columns is shown in Figure 3.1(a) and the column 2 in Figure 3.2(b).

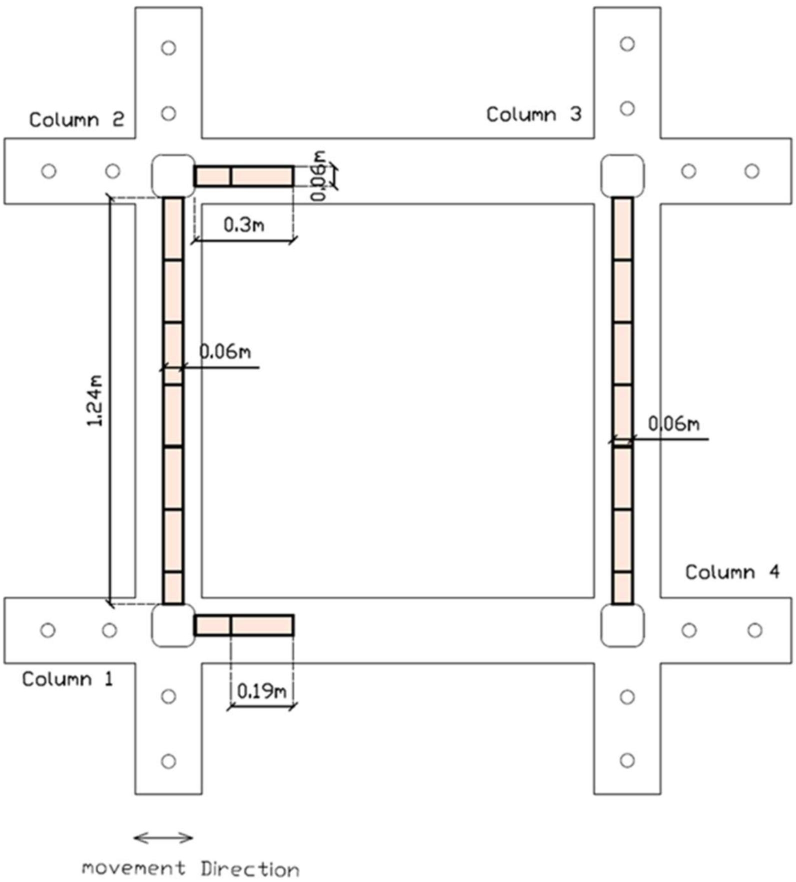

(a)

(b)

Figure 3.1 (a) Floor plan and (b) column with rounded corners of section

Table 3.1 Columns perimeter bottom – top

Perimeter (cm)	Column 1	Column 2	Column 3	Column 4
Bottom	48,8	48,6	48,6	48,4
Top	47,4	48	48,6	47,6
Corner radius	1.6 cm to 2.2 cm			

Column 1

Bottom perimeter: 48,8 cm

Top perimeter: 47,4 cm

Column 2

Bottom perimeter: 48,6 cm

Top perimeter: 48 cm

Column 3

Bottom perimeter: 48,6 cm

Top perimeter: 48,6 cm

Column 4

Bottom perimeter: 48,4 cm

Top perimeter: 47,6 cm

Corner radius from 1.6cm to 2.2cm.

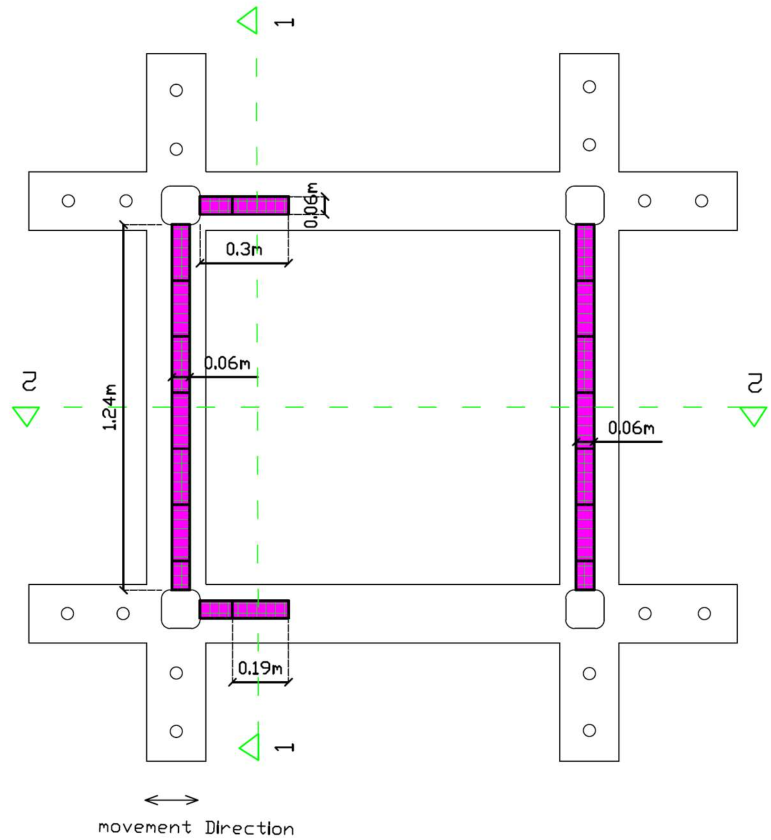
1
0.06m
0.3m
0.06m
2
1.24m
0.06m
0.19m
movement Direction

(a)

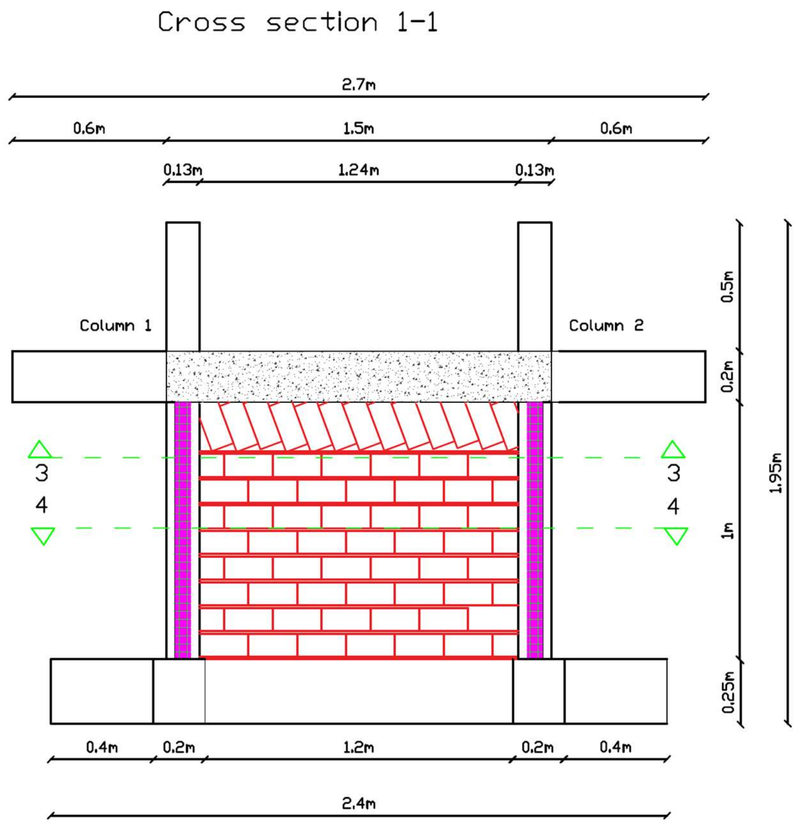
Cross section 1-1
2.7m
0.6m
1.5m
0.6m
0.13m
1.24m
0.13m
Column 1
Column 2
3
4
0.5m
0.2m
1m
0.25m
1.95m
0.4m
0.2m
1.2m
0.2m
0.4m
2.4m

(b)

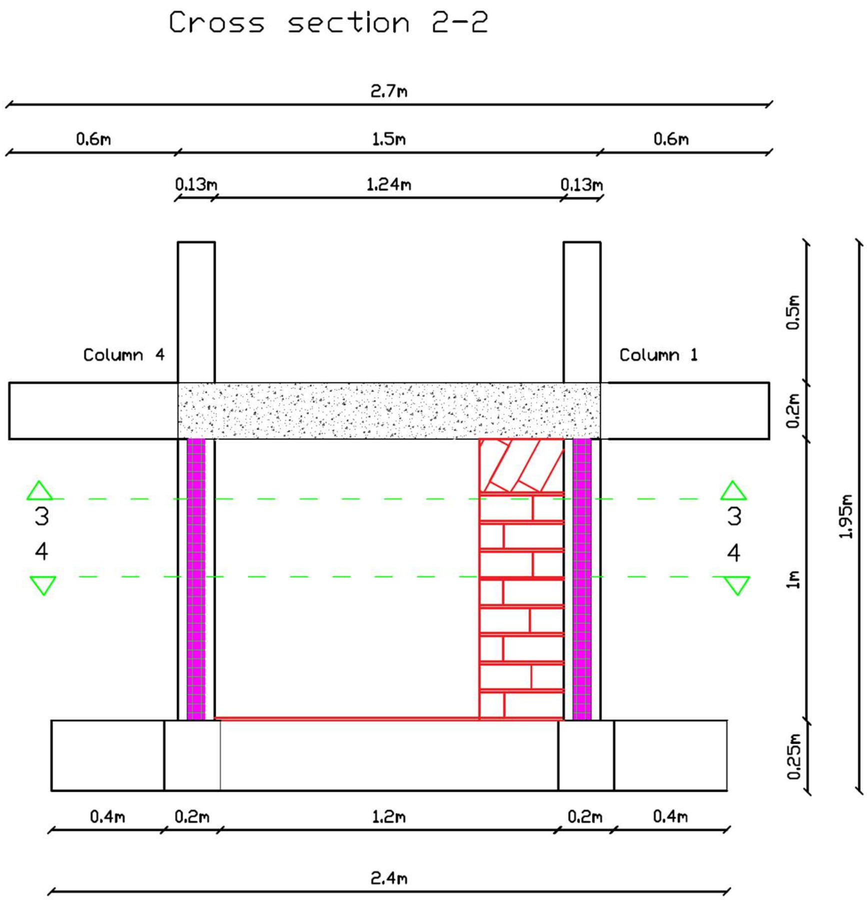

(c)

Figure 3.2 (a) Floor plan (b,c) cross section 1-1, 2-2

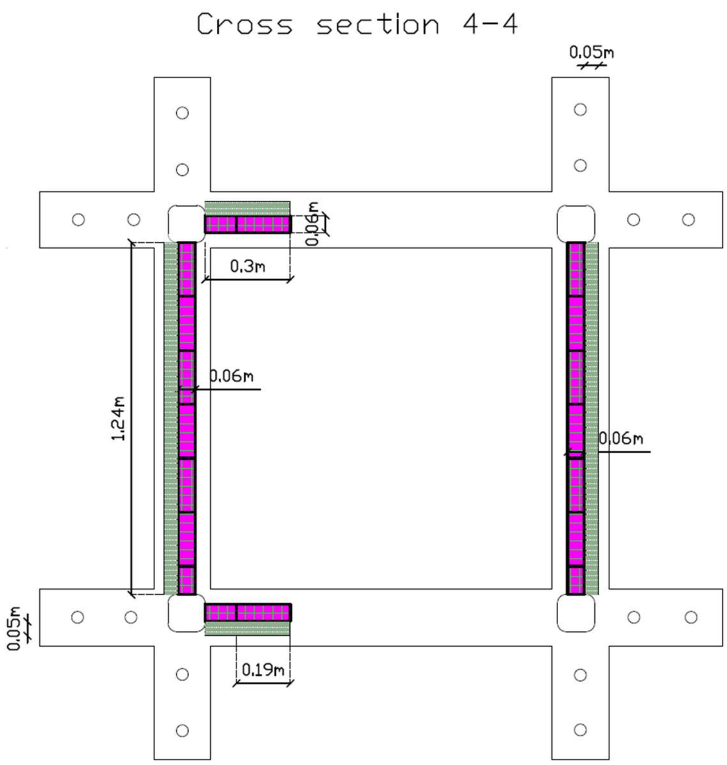

(a)

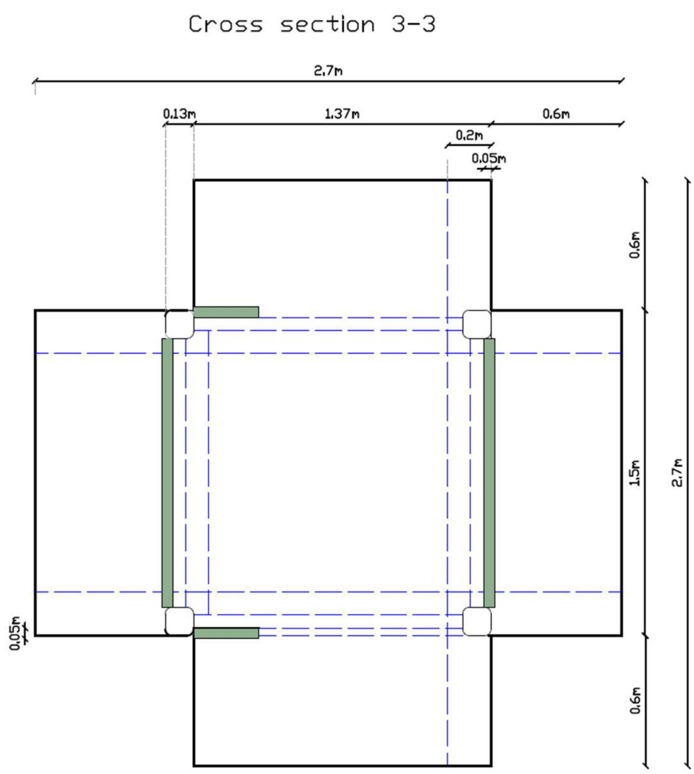

(b)

Figure 3.3 (a) Cross section 4-4, grinding surfaces on the foundation (b) Cross section 3-3, grinding surfaces on the top slab

3.3 LIGHTWEIGHT RETROFITS

The lightweight green retrofits applied herein, follow the design and implementation as reported in previous experimental campaigns of the research team (Hojdys et al., Rousakis et al. 2021, Rousakis et al. 2021a, Rousakis et al. 2021b, Hojdys et al. 2023, Rousakis and Tourtouras 2014, Golias et al. 2021, Karayannis et al. 2022, Karabini et al. 2023 & Karayannis et al. 2022, Rousakis and Macha 2023 Rousakis 2016, Rousakis et al. 2019, Kwiecień et al., 2017, Rousakis et al. 2020, Kwiecien et al. 2016, Tedeschi et al. 2014) .

At first a structural joint (gap) was created in both the partial and full masonry. The joint was constructed between the columns and the masonry. The width of the joint varies along the length of the columns. In the partial masonry it ranges from 0.09 m - 0.025 m, as shown in Figure 3.4. In the full masonry it ranges from 0.019 m - 0.025 m, as shown in Figure 3.5. The minimum joint width was 1.9% of the clear height of the columns.

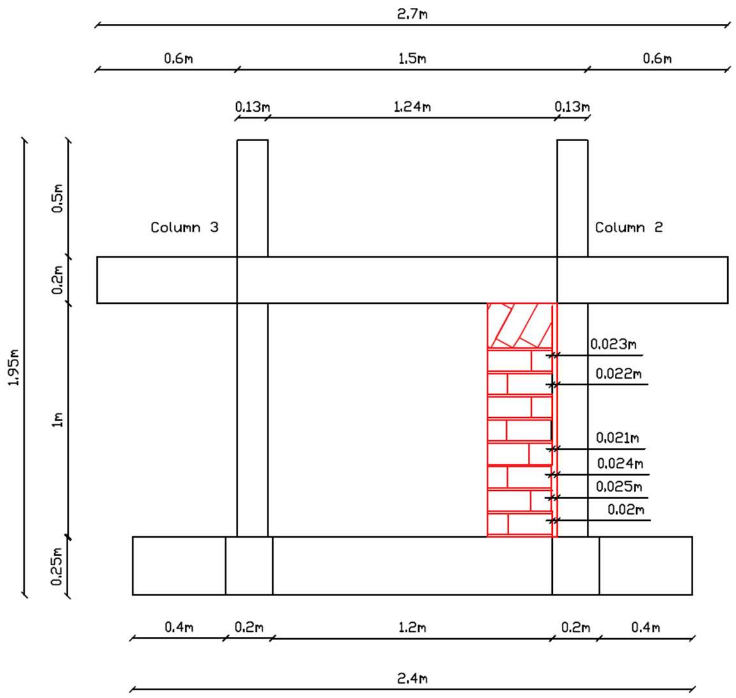

(a)

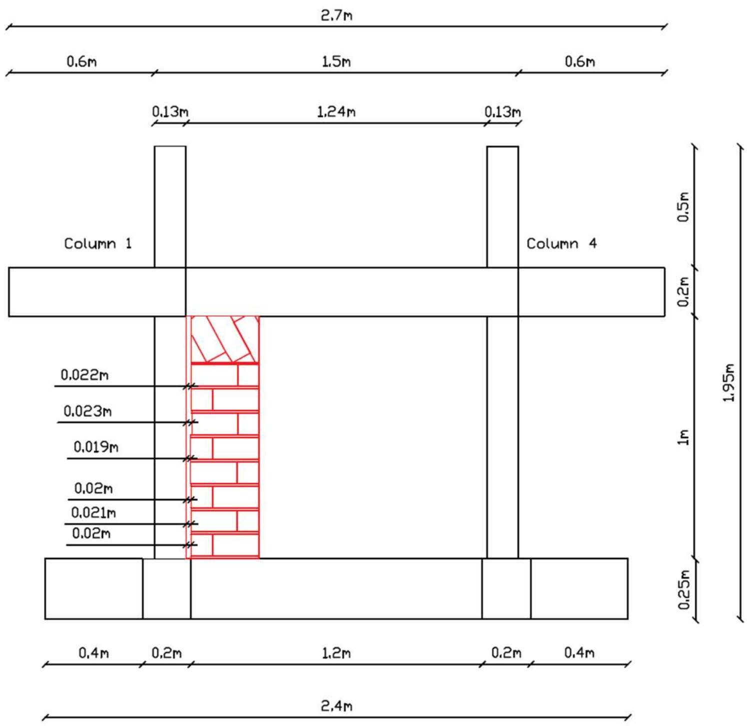

(b)

Figure 3.4 Construction of gap of joint in partial infill (a) between columns 3-2, and (b) 1-3

H.F.R.I. Hellenic Foundation for Research & Innovation
Greece 2.0 NATIONAL RECOVERY AND RESILIENCE PLAN
Funded by the European Union NextGenerationEU
GREENERGY

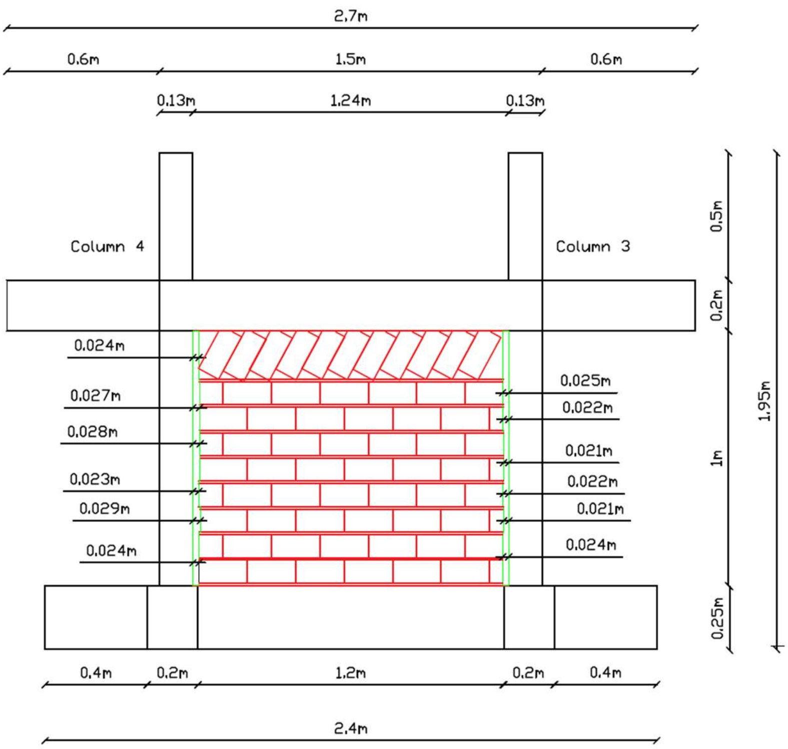

(a)

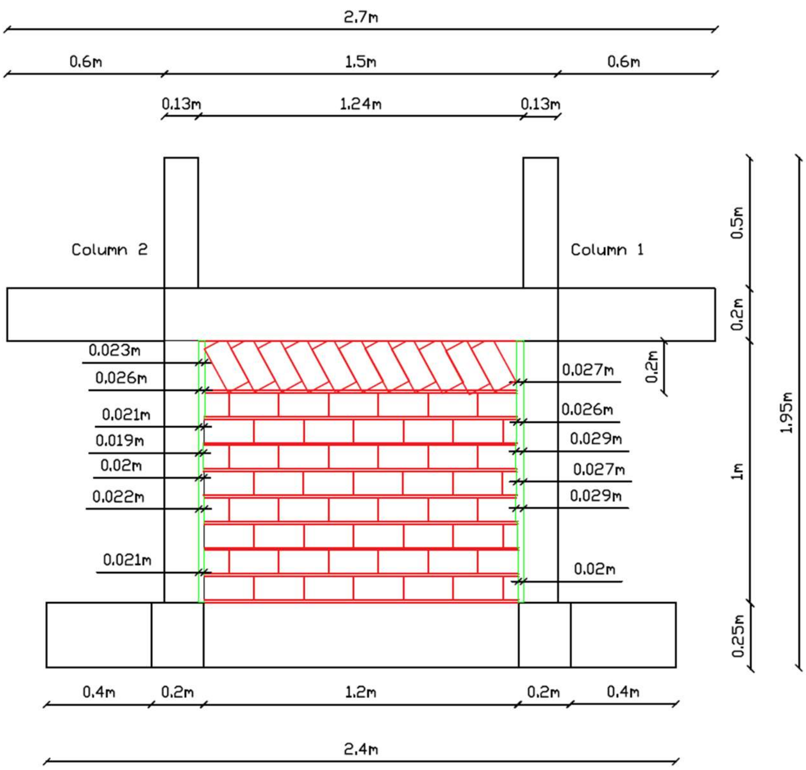

(b)

Figure 3.5 Construction of gap of joint in full infill (a) between columns 4-3 (b) between columns 2-1

Continuous basalt rope was wrapped around the column sections to provide additional confinement of concrete. The 1 layer of rope covered 20 cm at the bottom and top regions of the column. The second layer served only the self anchorage of the columns. The rope coils in each layer are given below. In Figure 3.6 and Figure 3.7, the reinforced concrete columns for the partial and full masonry are shown respectively.

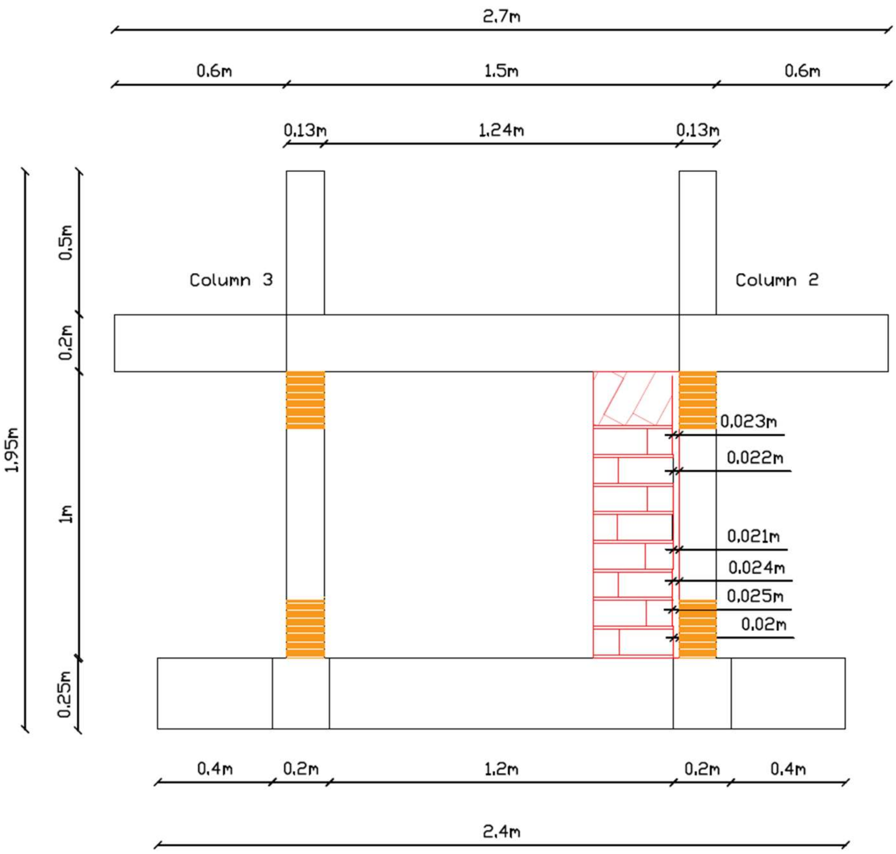

(a)

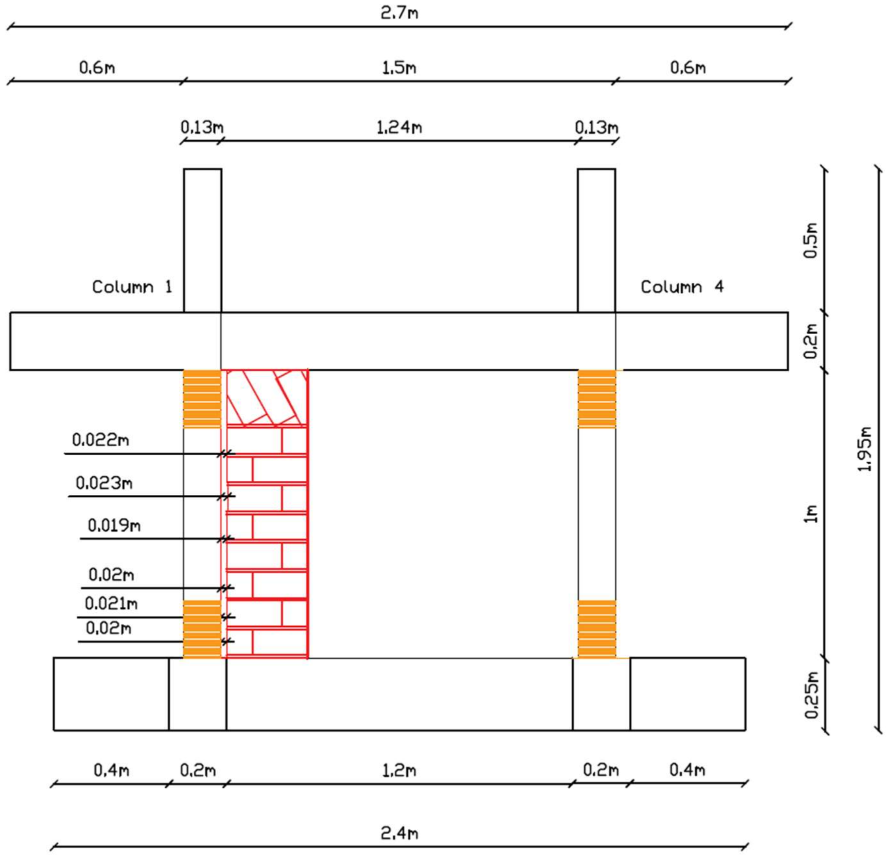

(b)

Figure 3.6 Application of basalt rope (a) on column 2 and gap dimension with partial infill 3-2 and (b) on column 1, partial infill 1-4

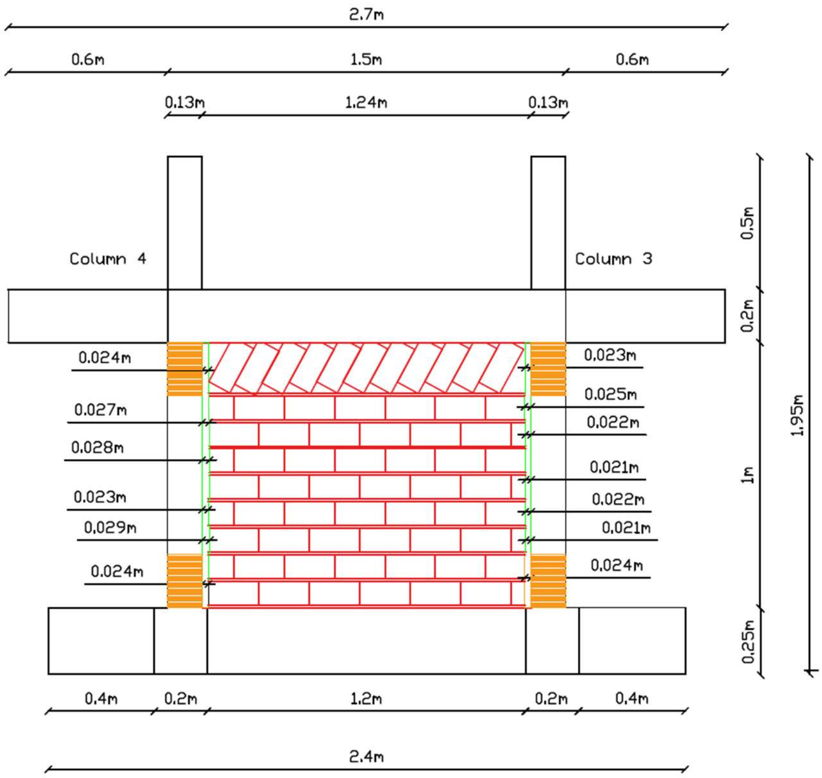
2.7m
0.6m
1.5m
0.6m
0.13m
1.24m
0.13m
Column 4
Column 3
0.5m
0.2m
1.95m
1m
0.25m
0.024m
0.027m
0.028m
0.023m
0.029m
0.024m
0.023m
0.025m
0.022m
0.021m
0.022m
0.021m
0.024m
0.4m
0.2m
1.2m
0.2m
0.4m
2.4m

(a)

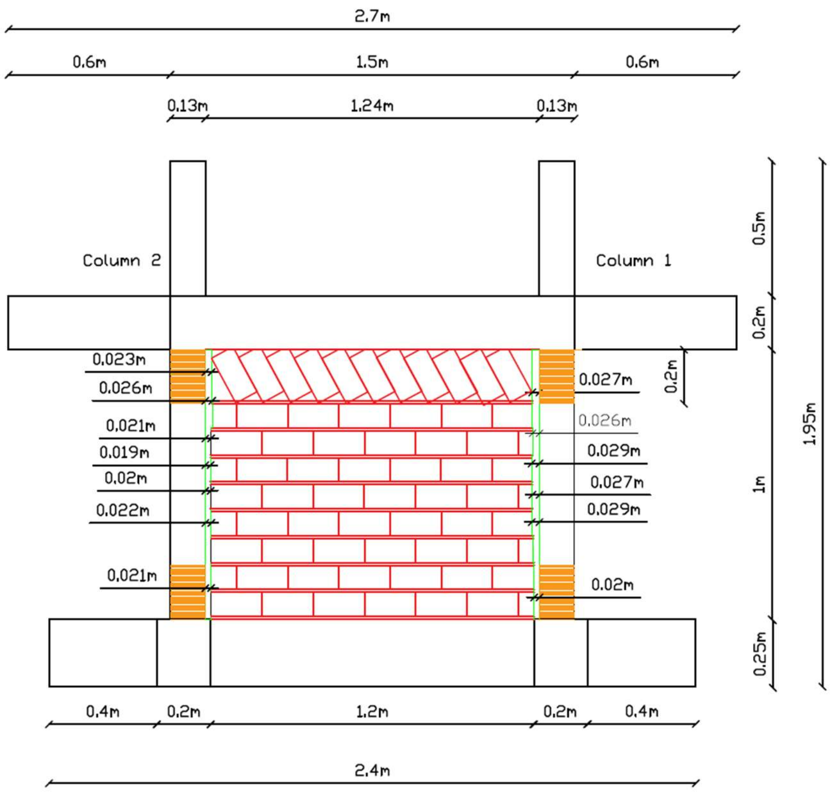
2.7m
0.6m
1.5m
0.6m
0.13m
1.24m
0.13m
Column 2
Column 1
0.5m
0.2m
0.2m
1.95m
1m
0.25m
0.023m
0.026m
0.021m
0.019m
0.02m
0.022m
0.021m
0.027m
0.026m
0.029m
0.027m
0.029m
0.02m
0.4m
0.2m
1.2m
0.2m
0.4m
2.4m

(b)

(c)

Figure 3.7 Columns wrapped with basalt rope (20cm on the top side and 20 cm at the bottom) (a) 4-3 (b) 2-1, (c) retrofitted column & joint gap with the infill wall

Basalt rope

rope thickness of 3 rows = 1,2 cm

20 cm (column height of retrofit) /1,2 cm = 16,67 = 17 triads

17 x 3 = 51

13 x 4 = 52 cm = 0,52 m

0,52 x 51 = 26,52 m of rope per 20 cm height

Column 1

Bottom side

Inside layer: 53 spirals

Outside layer (self anchorage): 11spirals

Top side

Inside layer: 50 spirals

Outside layer: 13 spirals

Column 2

Bottom side

Inside layer: 48 spirals

Outside layer: 15 spirals

Top side

Inside layer: 50 spirals

Outside layer: 11 spirals

Column 3

Bottom side

Inside layer: 48 spirals

Outside layer: 18 spirals

Top side

Inside layer: 49 spirals

Outside layer: 20 spirals

Column 4

Bottom side

Inside layer: 45 spirals

Outside layer: 30 spirals

Top side

Inside layer: 48 spirals

Outside layer: 20 spirals

Polyurethane PM poured into the joint

Primer was applied on the surfaces that would receive the PM joint. The PM resin was poured into the joint with the help of ewooden molds of 20cm height. Therefore, each joint was completed after 5 sequential castings. The polyurethane hardens within half an hour, so it needs to be applied quickly before it cures.

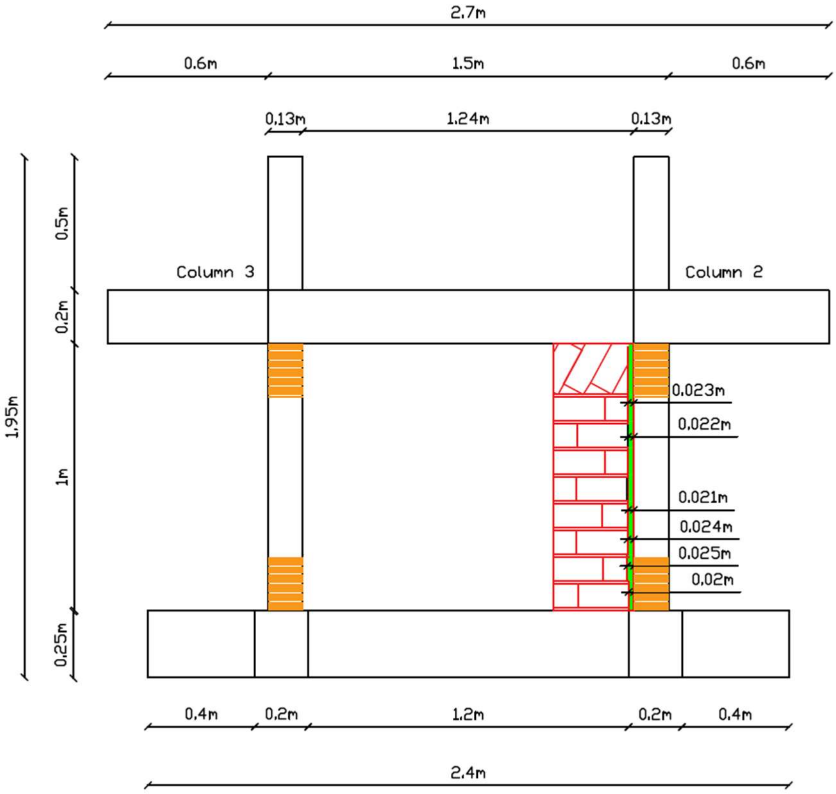
2.7m
0.6m
1.5m
0.6m
0.13m
1.24m
0.13m
Column 3
Column 2
1.95m
0.5m
0.2m
1m
0.25m
0.023m
0.022m
0.021m
0.024m
0.025m
0.02m
0.4m
0.2m
1.2m
0.2m
0.4m
2.4m

(a)

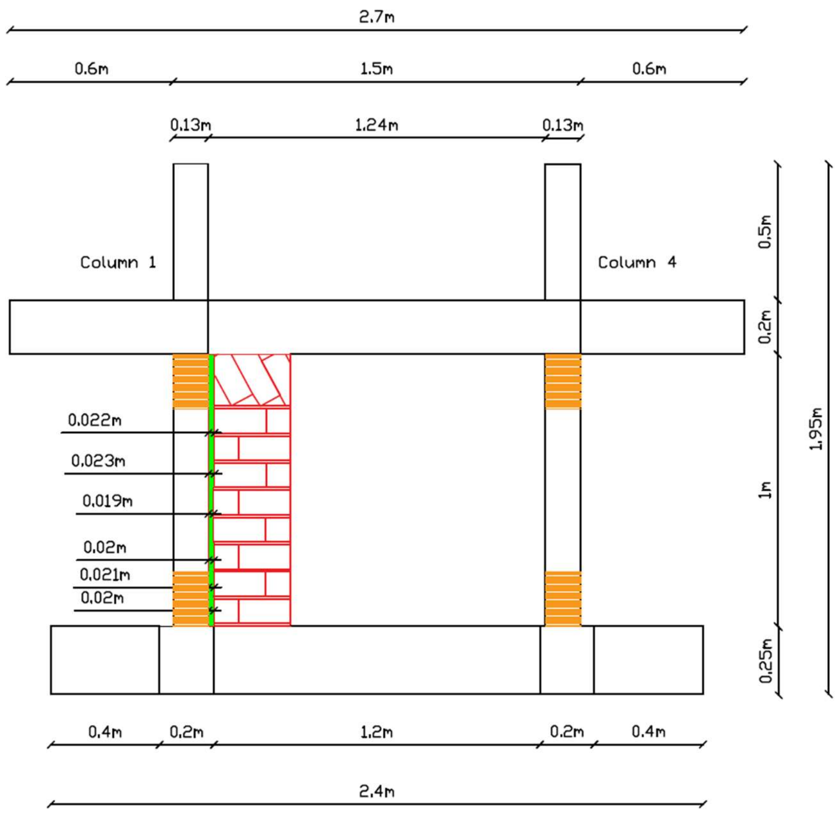
2.7m
0.6m
1.5m
0.6m
0.13m
1.24m
0.13m
Column 1
Column 4
0.022m
0.023m
0.019m
0.02m
0.021m
0.02m
0.5m
0.2m
1m
0.25m
1.95m
0.4m
0.2m
1.2m
0.2m
0.4m
2.4m

(b)

(c)

Figure 3.8 Cured PUFJ (polyurethane flexible joint) (a), (b) in the partial infill and application of the primer resin for the bonding of the glass grid (c)

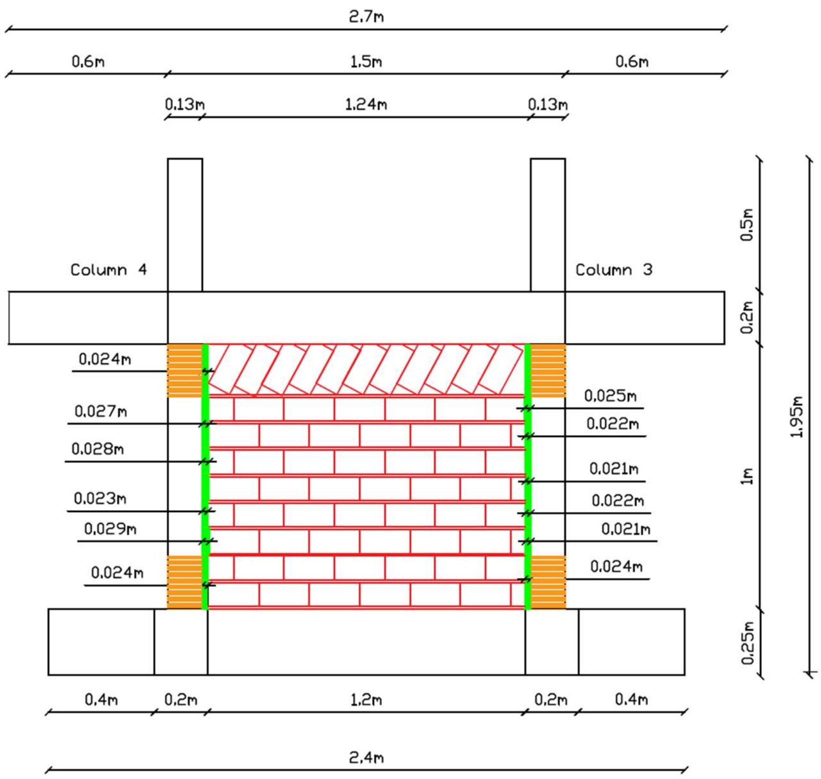
2.7m
0.6m
1.5m
0.6m
0.13m
1.24m
0.13m
Column 4
Column 3
0.5m
0.2m
1.95m
1m
0.25m
0.024m
0.027m
0.028m
0.023m
0.029m
0.024m
0.025m
0.022m
0.021m
0.022m
0.021m
0.024m
0.4m
0.2m
1.2m
0.2m
0.4m
2.4m

(a)

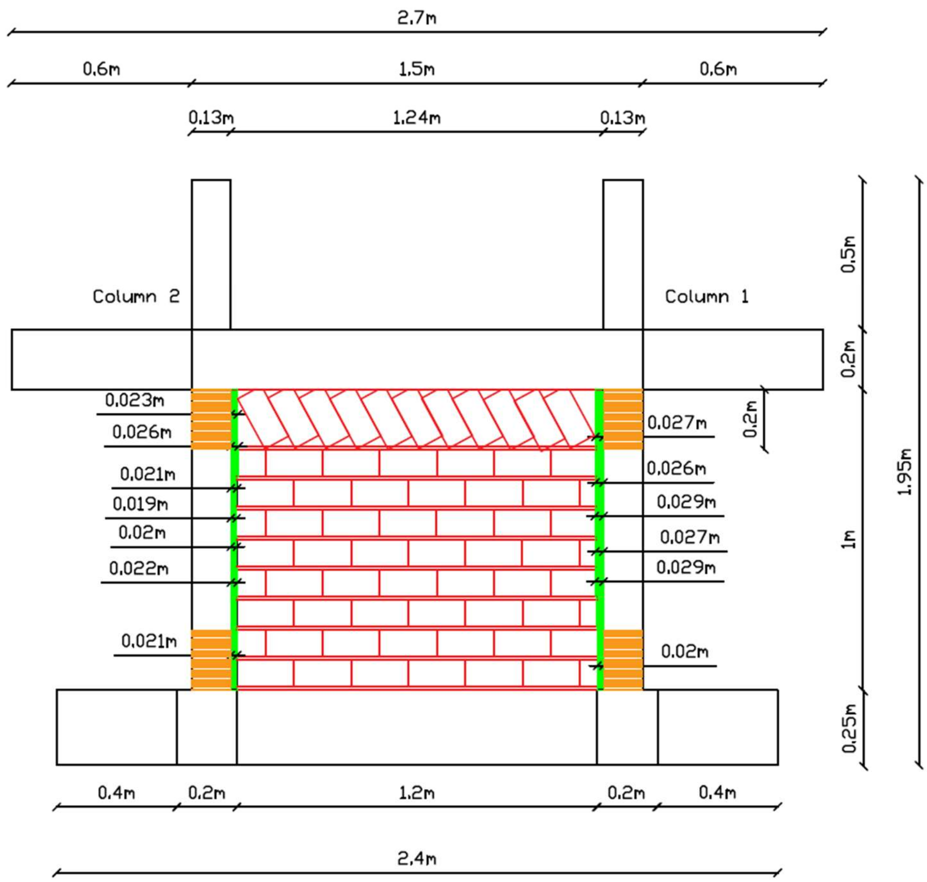

(b)

(c)

Figure 3.9 Dimensions of constructed PUFJ joint for the full infill brick walls (a), (b), (c)

Application of glass fiber grid on partial and full masonry

The grid was cut into two different dimensions, one piece of 1.10*0.24m^2 and three pieces of 1.10*0.33m^2 for the full masonry (without vertical overlapping), and one piece of 1.10*0.30 m^2 for the partial masonry (Figure 3.10). The grid was placed on the partial masonry as shown in Figure 3.11 and on the full masonry Figure 3.12.

To apply the grid, first, the masonry was cleaned. Then, a layer of primer was applied before the application of the PS polyurethane layer. The grid was placed on the PS layer and then the voids of the grid were covered with a final layer of the same PS polyurethane.

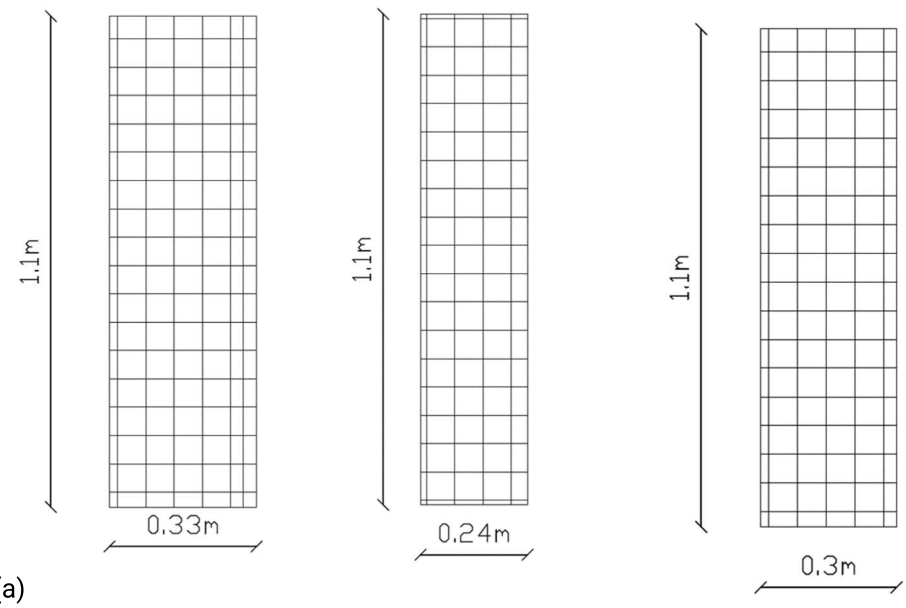

(a)

(b)

Figure 3.10 Dimensions of grid

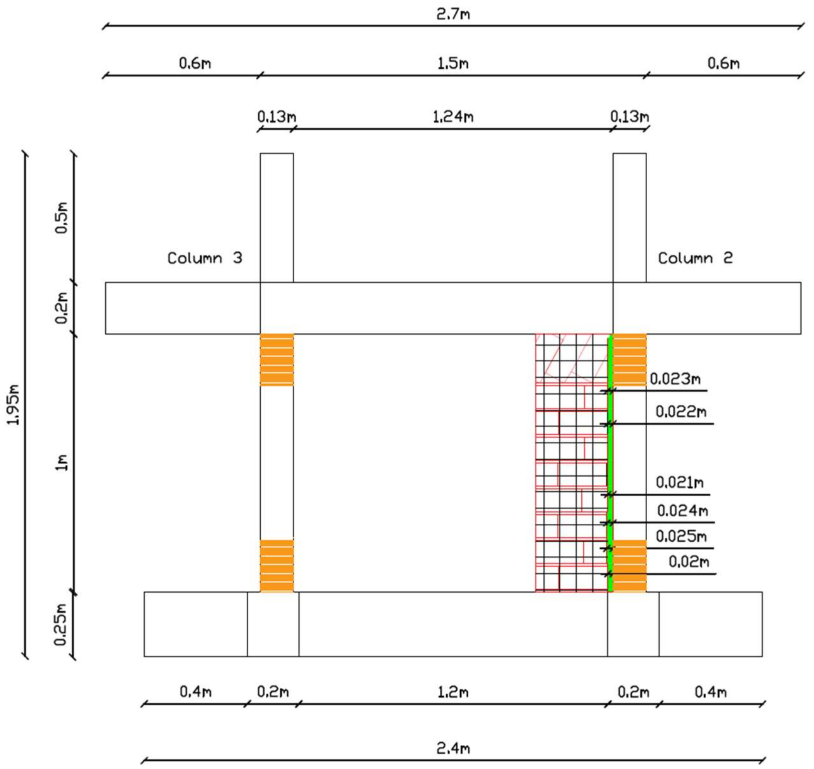

(a)

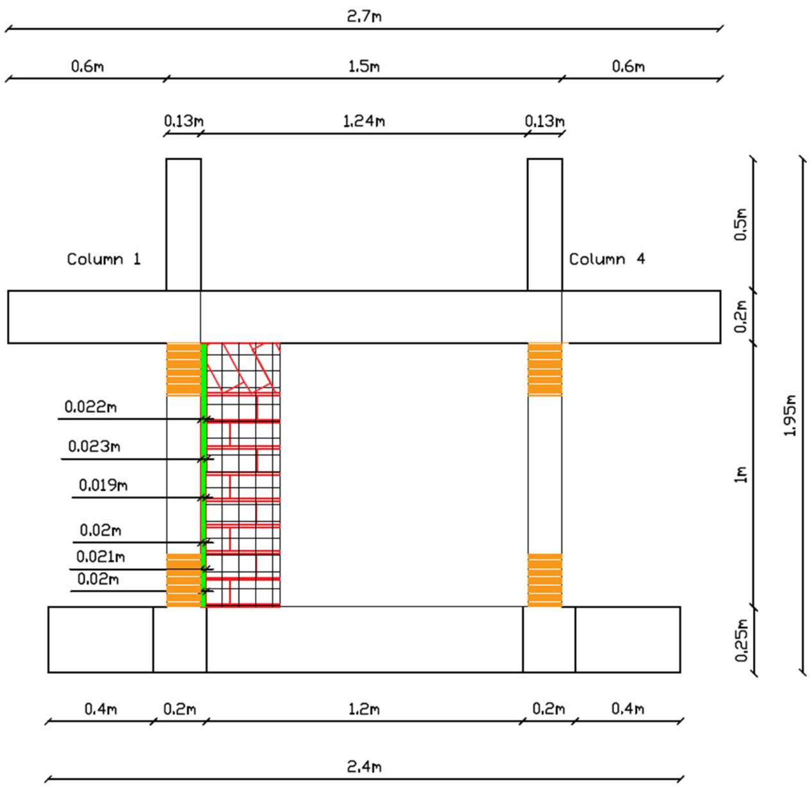

(b)

Figure 3.11 (a), (b) Application of grid

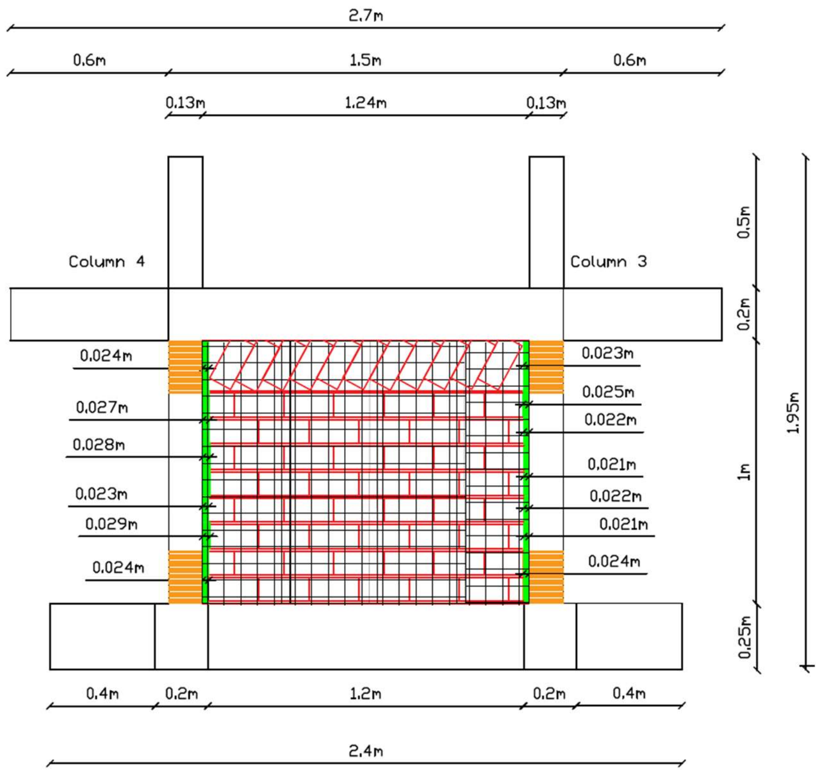
2.7m
0.6m
1.5m
0.6m
0.13m
1.24m
0.13m
Column 4
Column 3
0.5m
0.2m
1.95m
1m
0.25m
0.024m
0.027m
0.028m
0.023m
0.029m
0.024m
0.023m
0.025m
0.022m
0.021m
0.022m
0.021m
0.024m
0.4m
0.2m
1.2m
0.2m
0.4m
2.4m

(a)

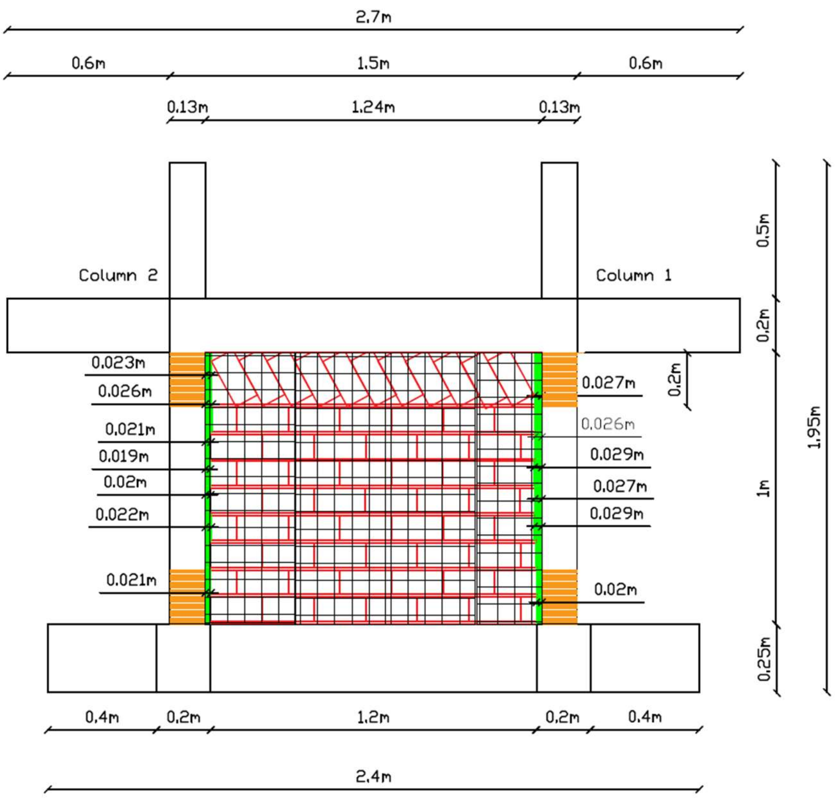
2.7m
0.6m
1.5m
0.6m
0.13m
1.24m
0.13m
Column 2
Column 1
0.5m
0.2m
1.95m
1m
0.25m
0.2m
0.023m
0.026m
0.021m
0.019m
0.02m
0.022m
0.021m
0.027m
0.026m
0.029m
0.027m
0.029m
0.02m
0.4m
0.2m
1.2m
0.2m
0.4m
2.4m

(b)

(c)

Figure 3.12 Constructed FRPU (glass grid & PS polyurethane) one-sided jacket on the full infill (a), (b), (c)

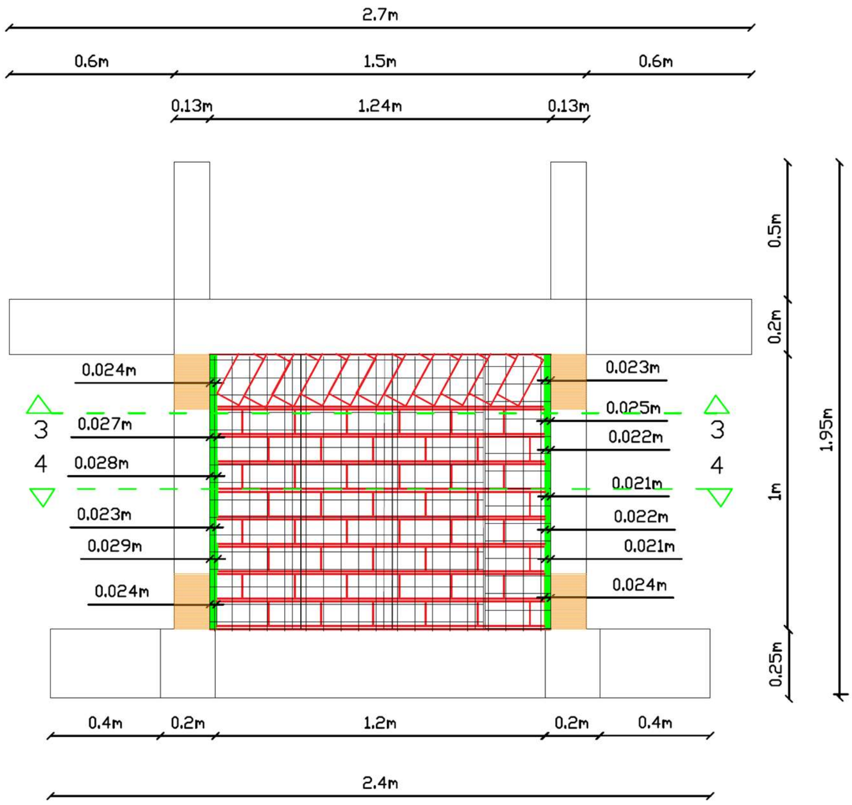

Figure 3.13 Designation of plan sections 3-3, 4-4

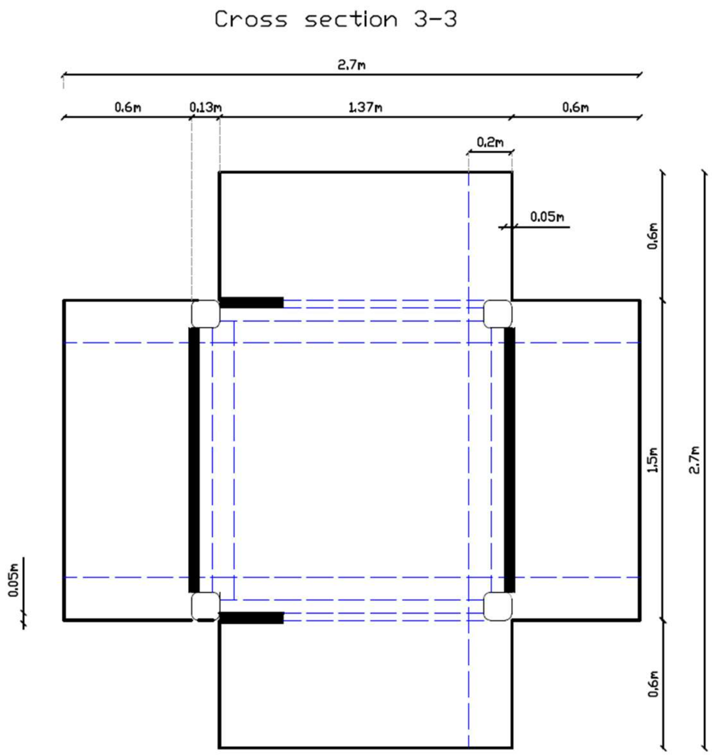

(a)

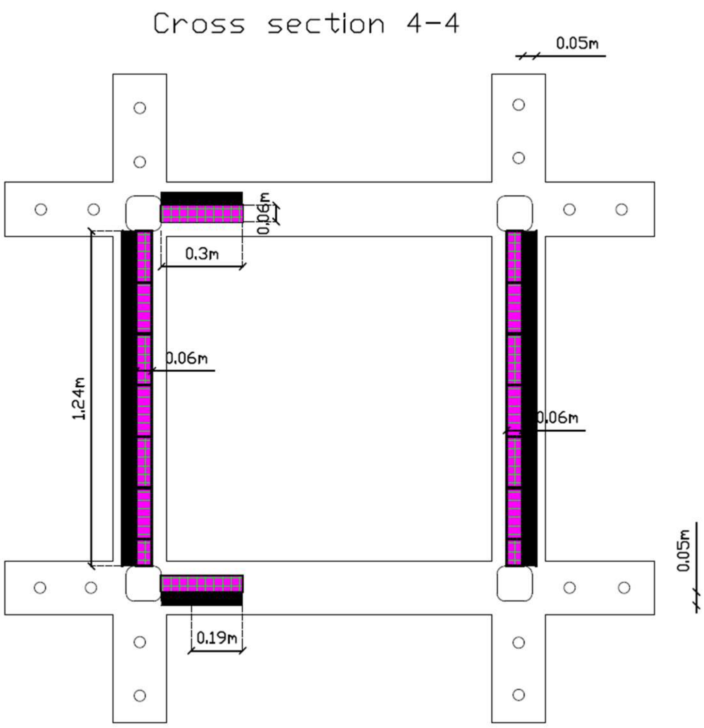

(b)

Figure 3.14 Concrete surfaces on the slab (a) and on the foundation (b) with bonded glass grid FRPU

3.4 VERTICAL LIVING WALLS AND PLANTERS (VF) RENOVATION

In the building, special constructions to simulate vertical living walls were placed on the frames with full and partial masonry respectively. More specifically, steel structures were constructed with steel bars of diameter of 20mm (Φ20) and additional spacers from the concrete structure of diameter of 10mm (Φ10) to simulate the mass and stiffness of vertical living walls construction (LW) together with greenery (Figure 3.15). The weight of each steel structure was 40 kg/m^2, that is 12kg, and a total of 96kgs for the eight vertical living walls. The constructions were attached on the foundation beam and top slab as shown in the images. Also, five concrete planters, were placed on the roof slab (Figure 3.17) to simulate a greenery mass of 600kg/m^2, that is 153kg on an area of 0.35m x 0.7m for each planter (Figure 3.16). The height of the planter is 0.7m and the distribution of concrete mass simulates a demanding case that is vulnerable to overturning because of rocking effects during severe earthquake excitation. In addition, wooden sticks were attached on the planters to simulate common trees (Figure 3.17). The positions of the concrete planters are shown in Figure 3.17. The total extra mass added to the structure is 59+153x5+ 12x8+ 30 = 950 kg.

Figure 3.15 Constructions to simulate vertical living walls (LW)

Figure 3.16 Concrete planters

Figure 3.17 Placement of construction simulating planters with trees and Vertical living walls on the structure

Detailing of supports of constructions to simulate vertical living walls

During the retrofit phase, eight (8) steel structures were attached on the specimen to simulate the additional mass and stiffness of vertical living walls (Fig 3.15). Of the eight, four (4) constructions were placed parallel to the loading direction (two (2) per side – in-plane loading) and four (4) respectively perpendicular to the loading direction (out-of-plane loading).

The bottom connection (anchoring) of the construction on the foundation beam was realized with the common approach through two steel screw connectors in all cases. The eight different cases of top connection of the constructions on the slab are cited below:

Out of plane – vertical to the loading direction (4 different cases):

1. Common approach with one steel screw connector on the top slab.

2. Top attachment of the steel construction with two Basalt ropes, anchored through the slab depth. Initially, suitable through holes were drilled, pre-tensioning was applied to the ropes with a special metal structure from the upper part of the slab and the holes were filled with epoxy resin (Sikadur®-52 Injection LP). After the resin developed its strength, the tensioning device was removed.

3. Top attachment of the steel construction with two Basalt ropes, anchored through the slab depth. Initially, suitable through holes were drilled and then pre-tensioning was applied to the cords with a special metal structure from the upper part of the plate. The tensioning device will remain in place throughout the series of testing and will function as an active anchoring device.

4. Top attachment of the steel construction with one Basalt rope, anchored through the slab depth. The application stages are similar to case 3.

In-plane - parallel to the loading direction (4 different cases):

1. Top attachment of the steel construction with one Basalt ropes, anchored through the slab depth. Initially, a suitable through hole was drilled and then a tension was applied to the rope with a special metal structure from the upper part of the slab and the hole was filled with polyurethane resin (Polyurethane PM). After the polyurethane has developed its strength, the tensioning device was removed.

2. Top attachment of the steel construction with one Basalt ropes, anchored through the slab depth. Initially, a suitable through hole was drilled and then a pre-tension was applied to the rope with a special metal structure from the upper part of the slab and it was filled with epoxy resin (Sikadur®-52 Injection LP). After the resin has developed its strength, the tensioning device was removed.

3. Top attachment of the steel construction with two Basalt ropes, anchored through the slab depth. The application steps are the same as in case 1.

4. Top attachment of the steel construction with two Basalt ropes, anchored through the slab depth. The application steps are the same as in case 2.

All eight constructions had top polyurethane PM pads of dimension 40mmX40mmX5 mm (one or two pieces, based on the gap of the steel construction from the slab (figure 3.19, 3.21, 3.25, 3.36).

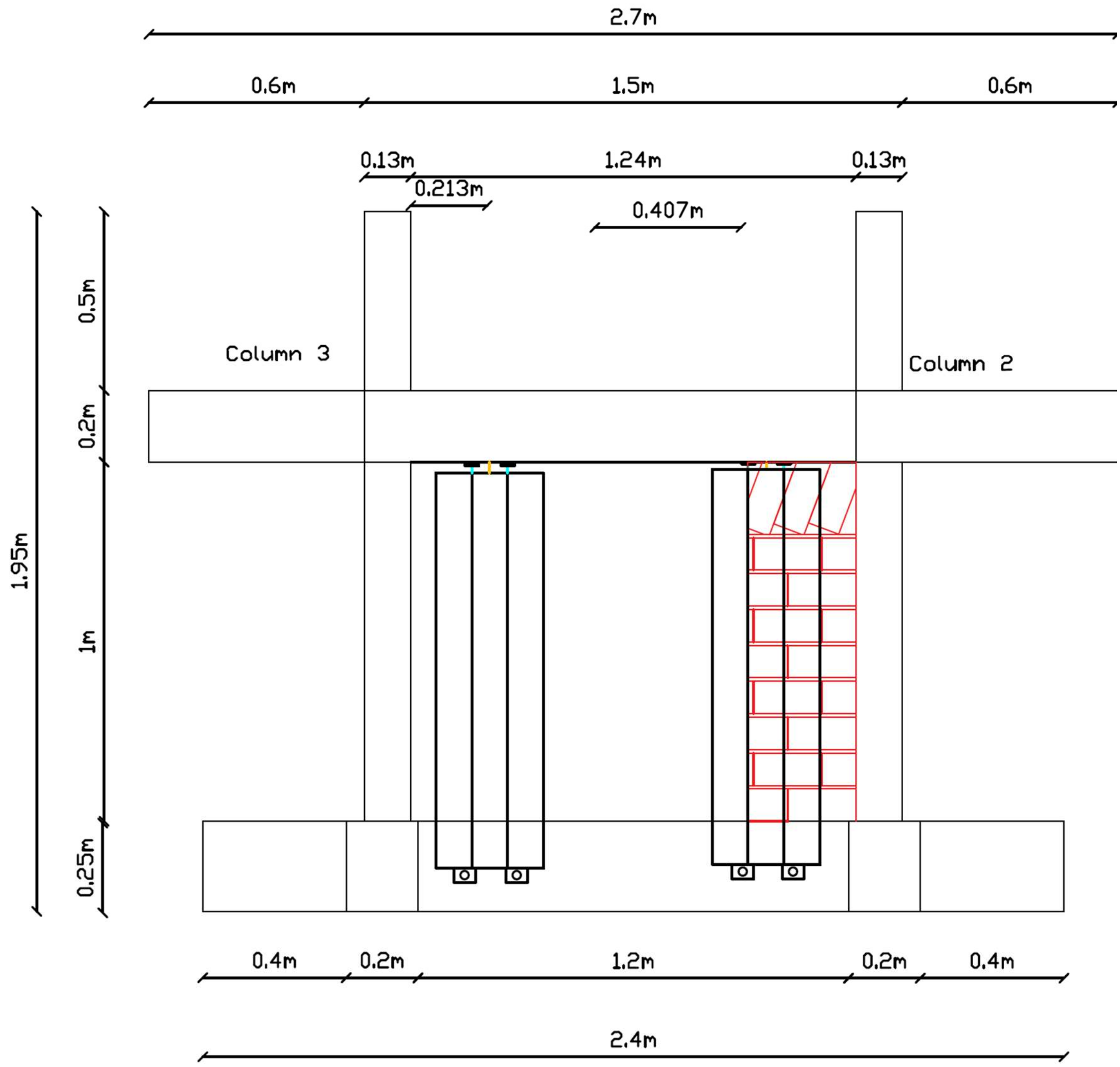

(a)

Figure 3.18 View of vertical living wall 3-2 (LW3-2L, LW3-2R)

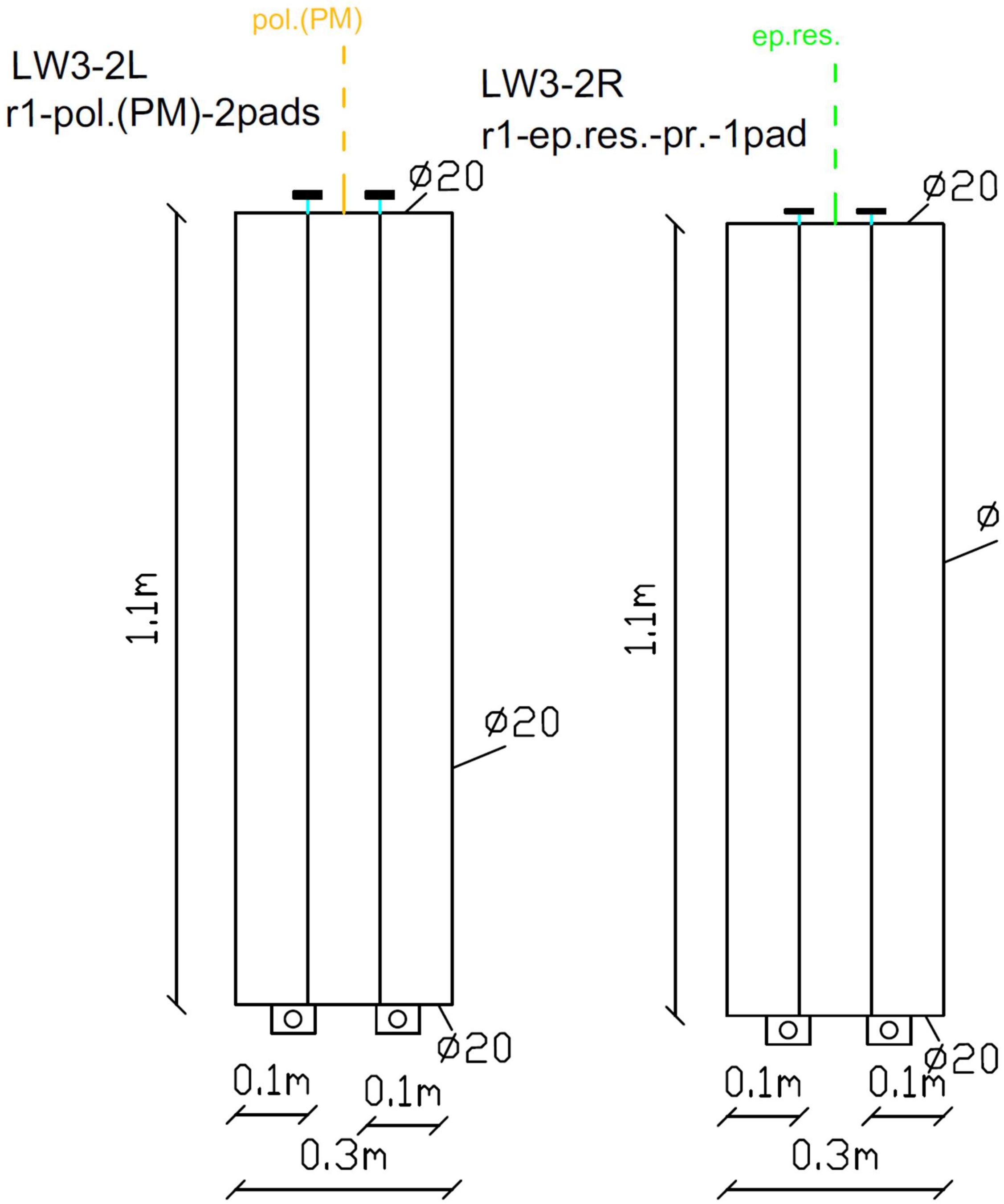

Figure 3.19 Living wall 3-2 (left side of frame between columns 3-2 LW3-2L) and living wall 3-2 (right side LW3-2R)

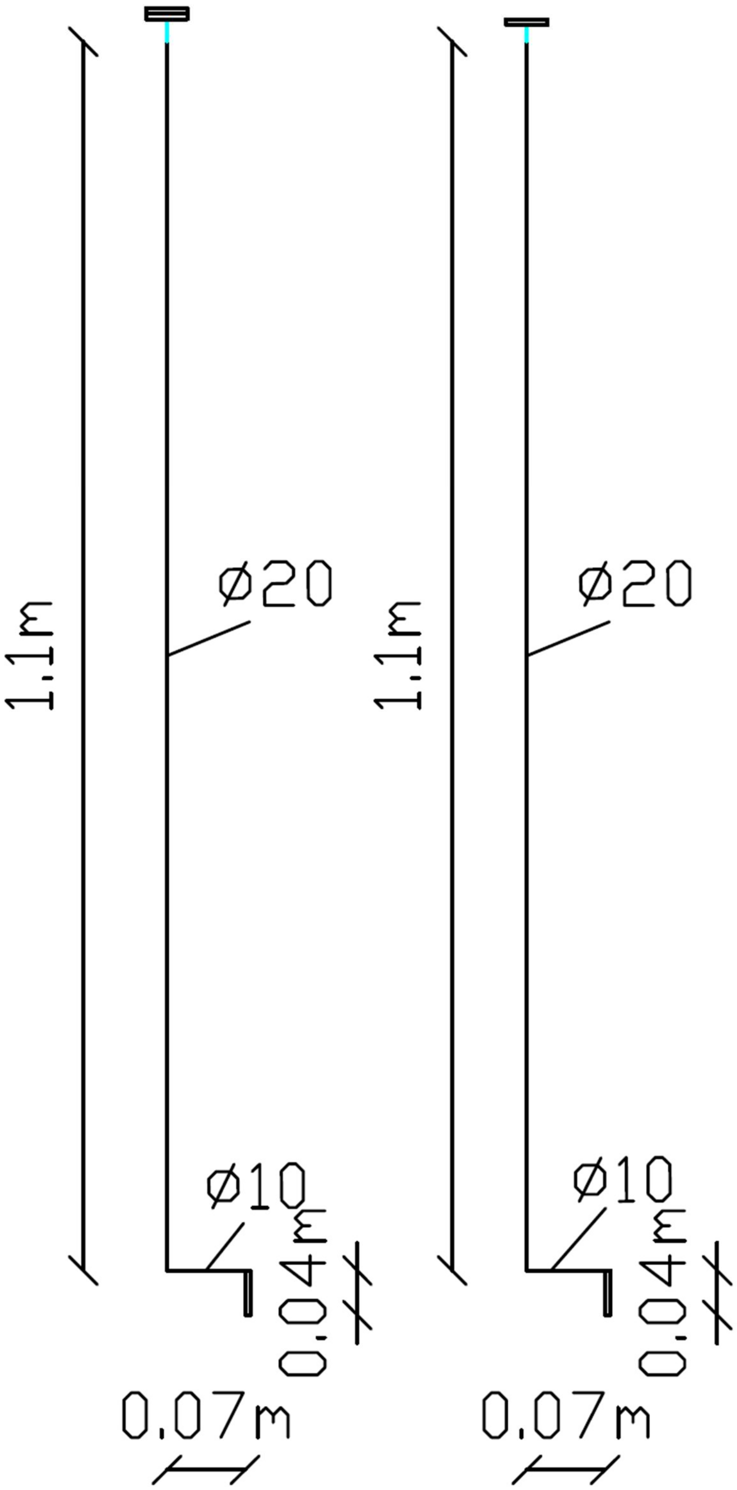

Figure 3.20 Cross section of living wall 3-2 left, 3-2 right

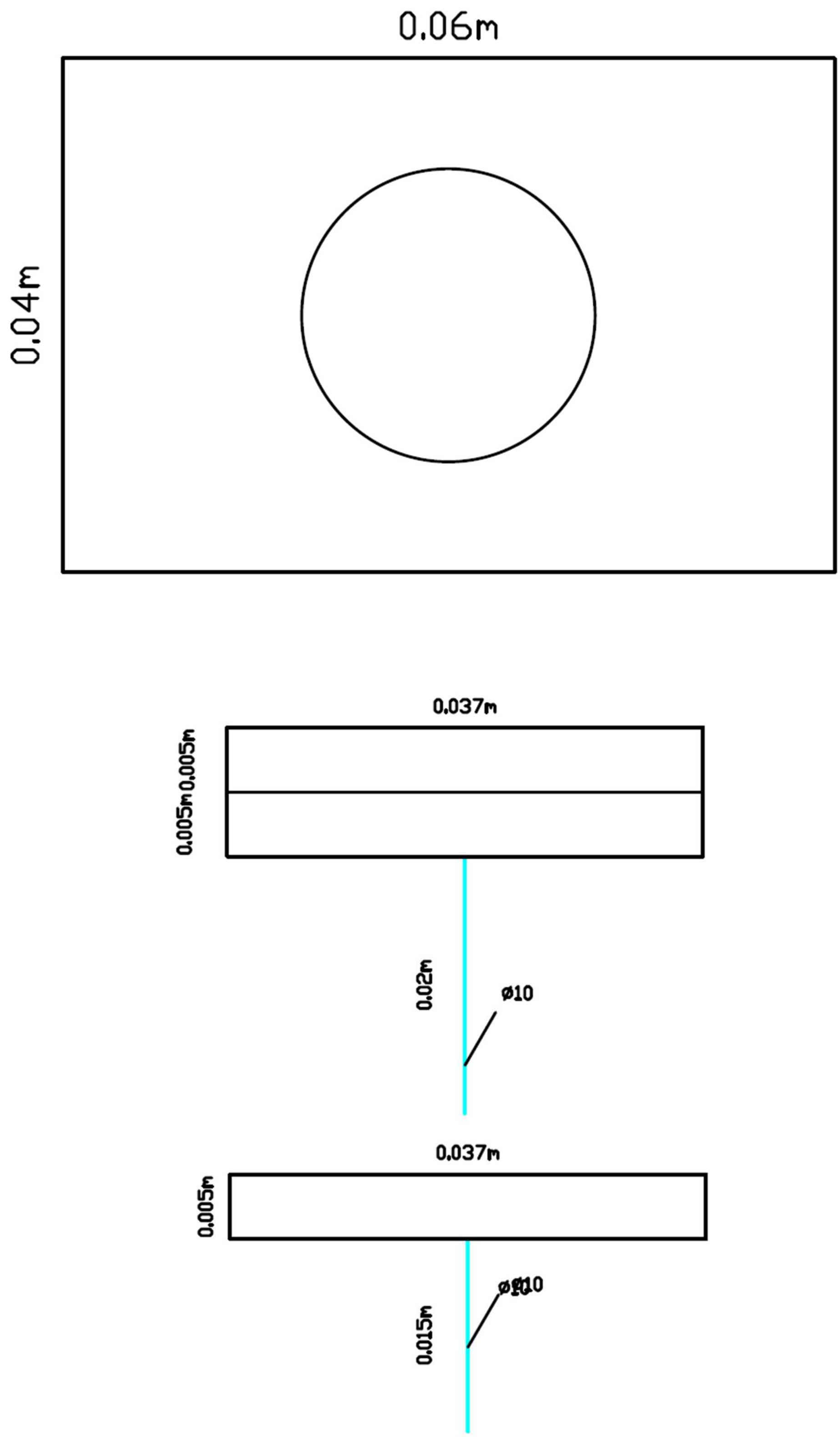

Figure 3.21 Anchoring details and PU pads dimensions (under the top slab)

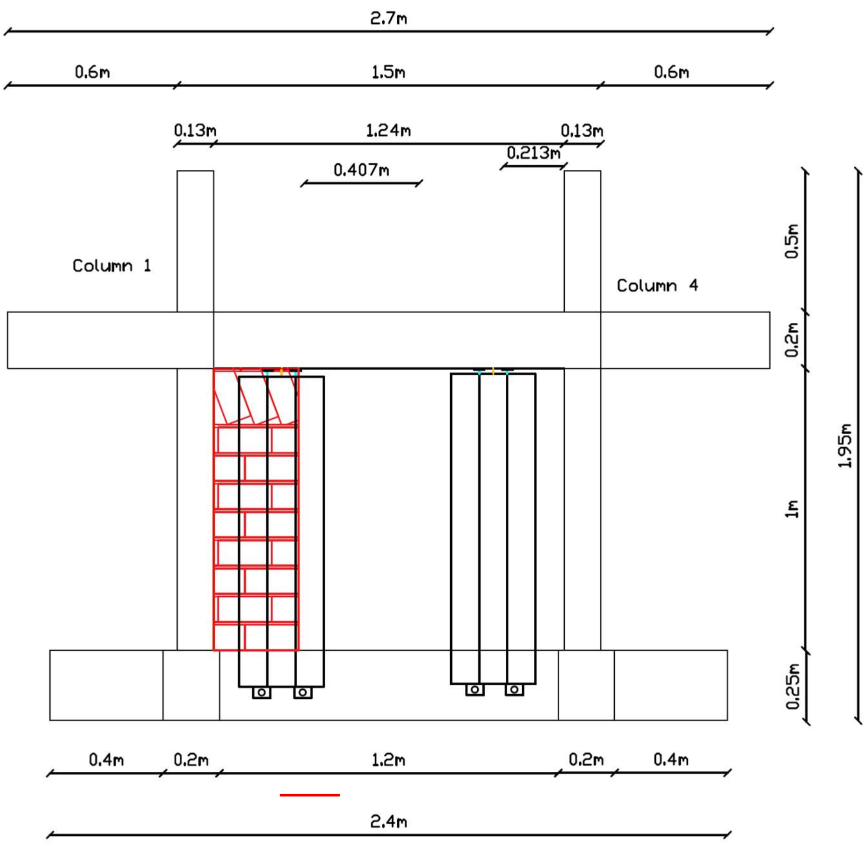

Figure 3.22 View of living wall 1-4

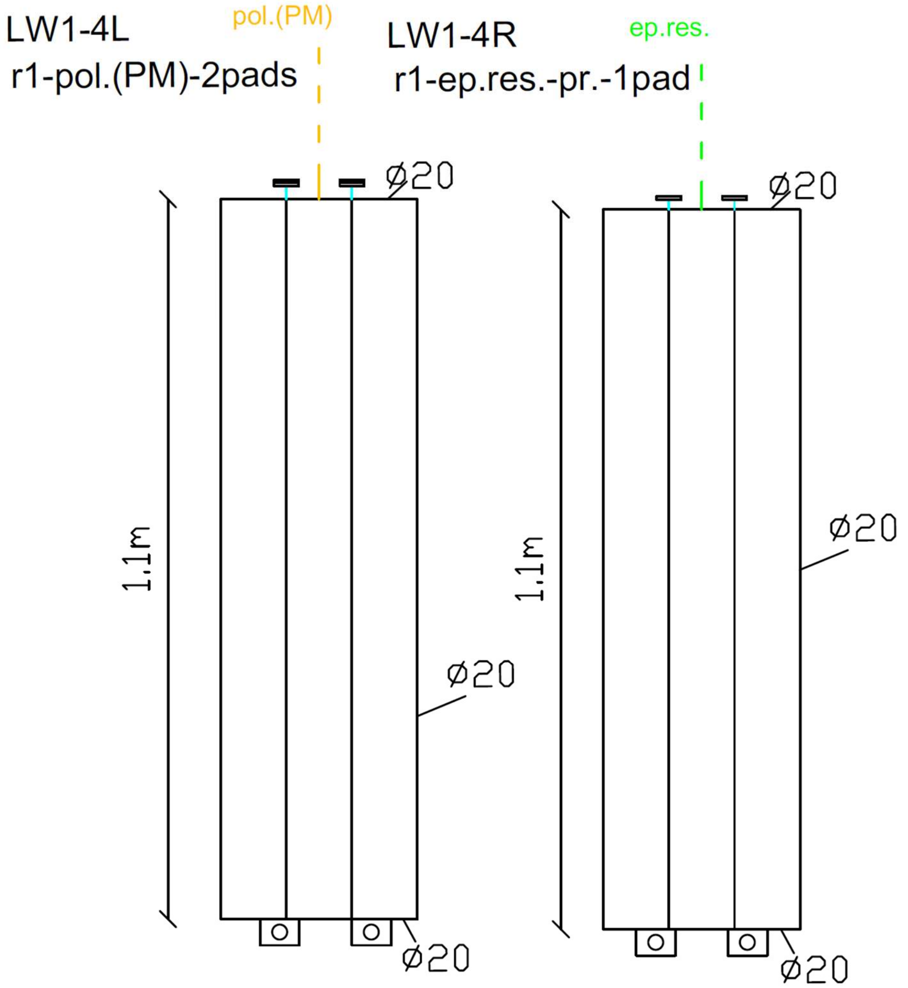

Figure 3.23 Living wall 1-4 left side and living wall 1-4 right side.

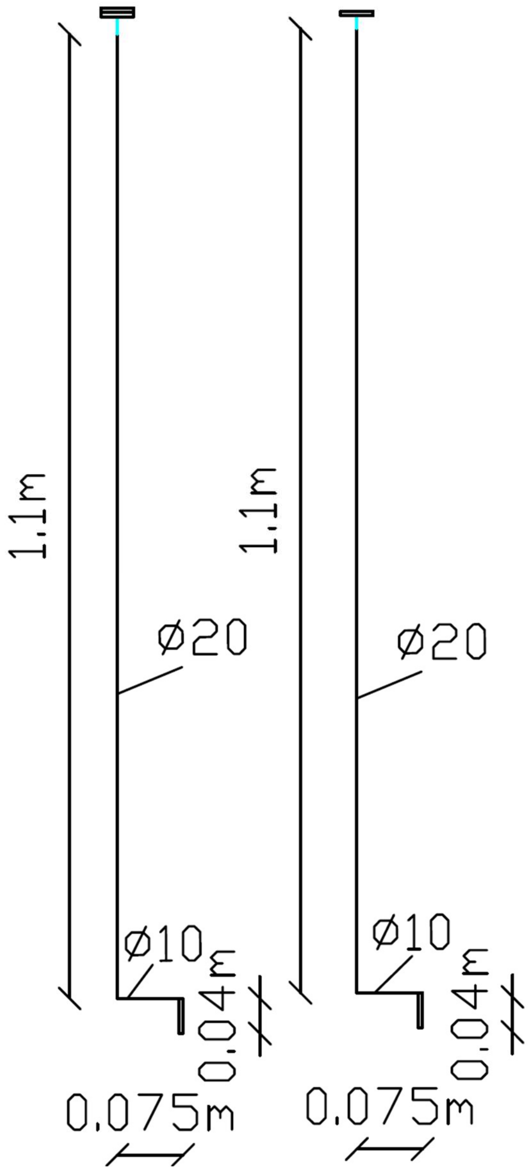

Figure 3.24 Cross section of living wall 1-4 left, 1-4 right

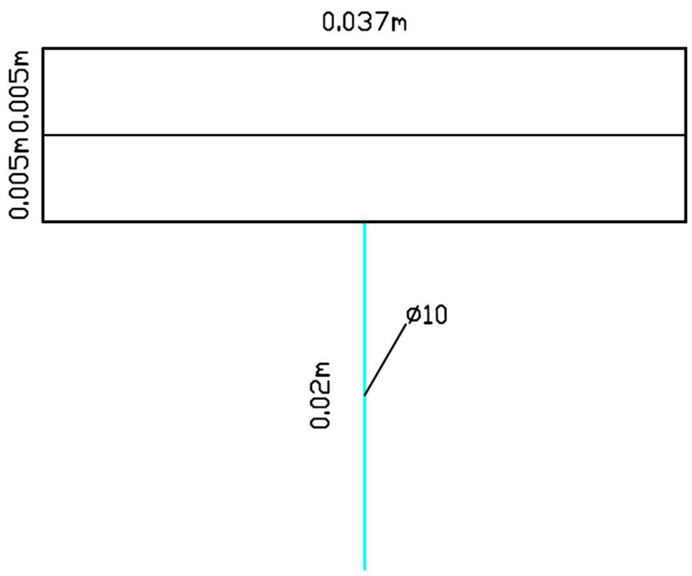

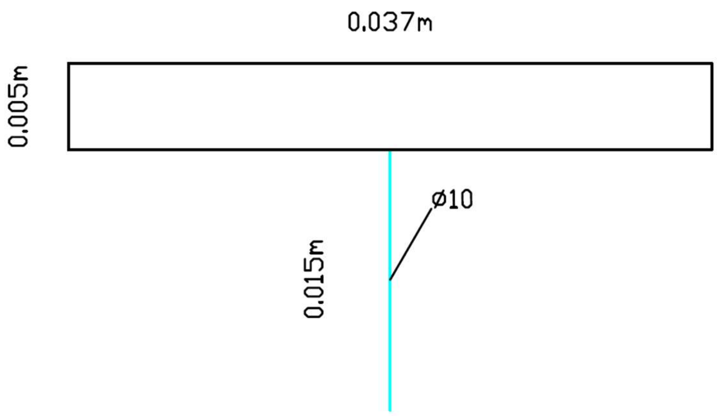

Figure 3.25 Anchoring details of LW1-4, under the top slab

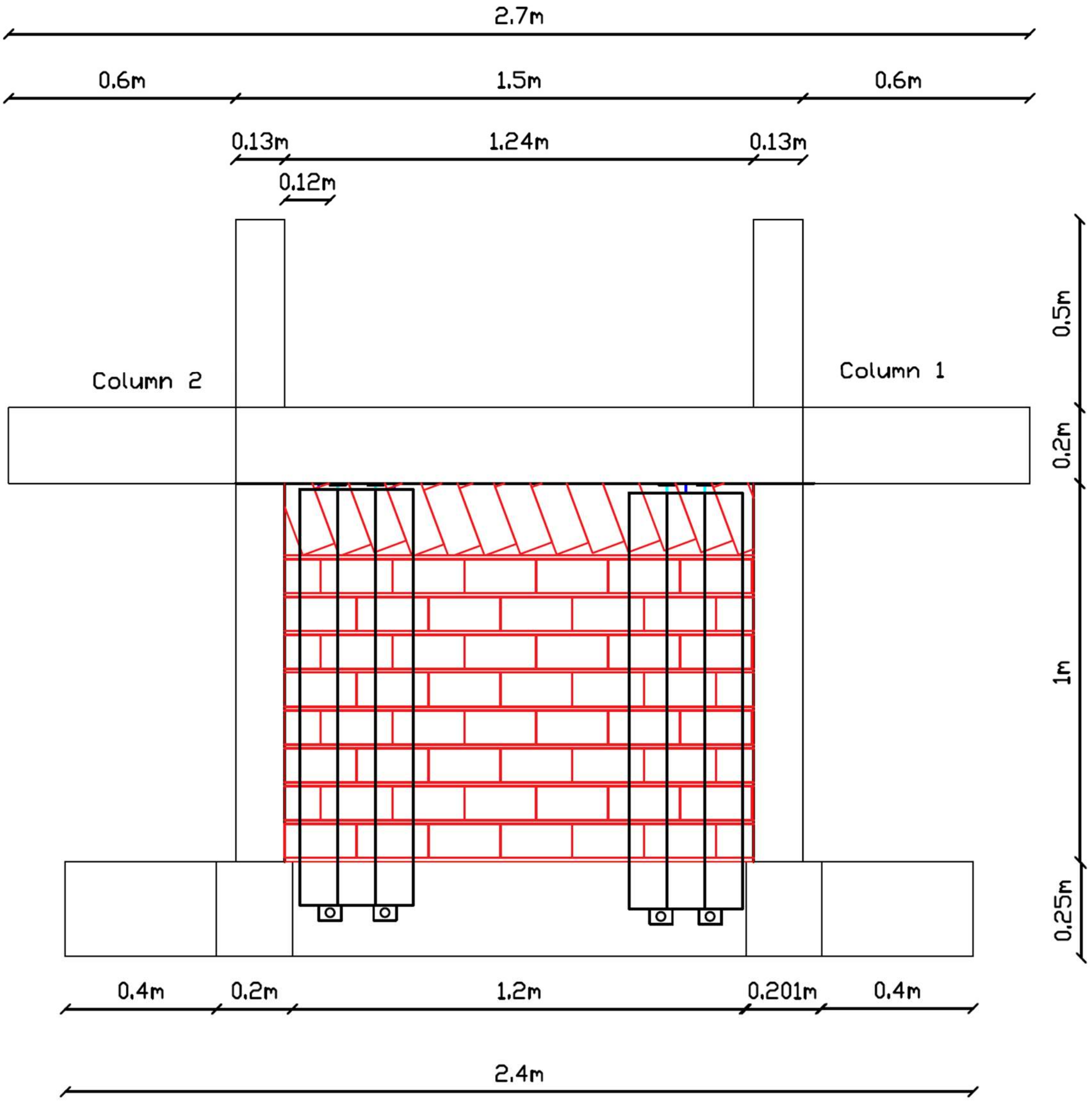

Figure 3.26 view of living wall 2-1

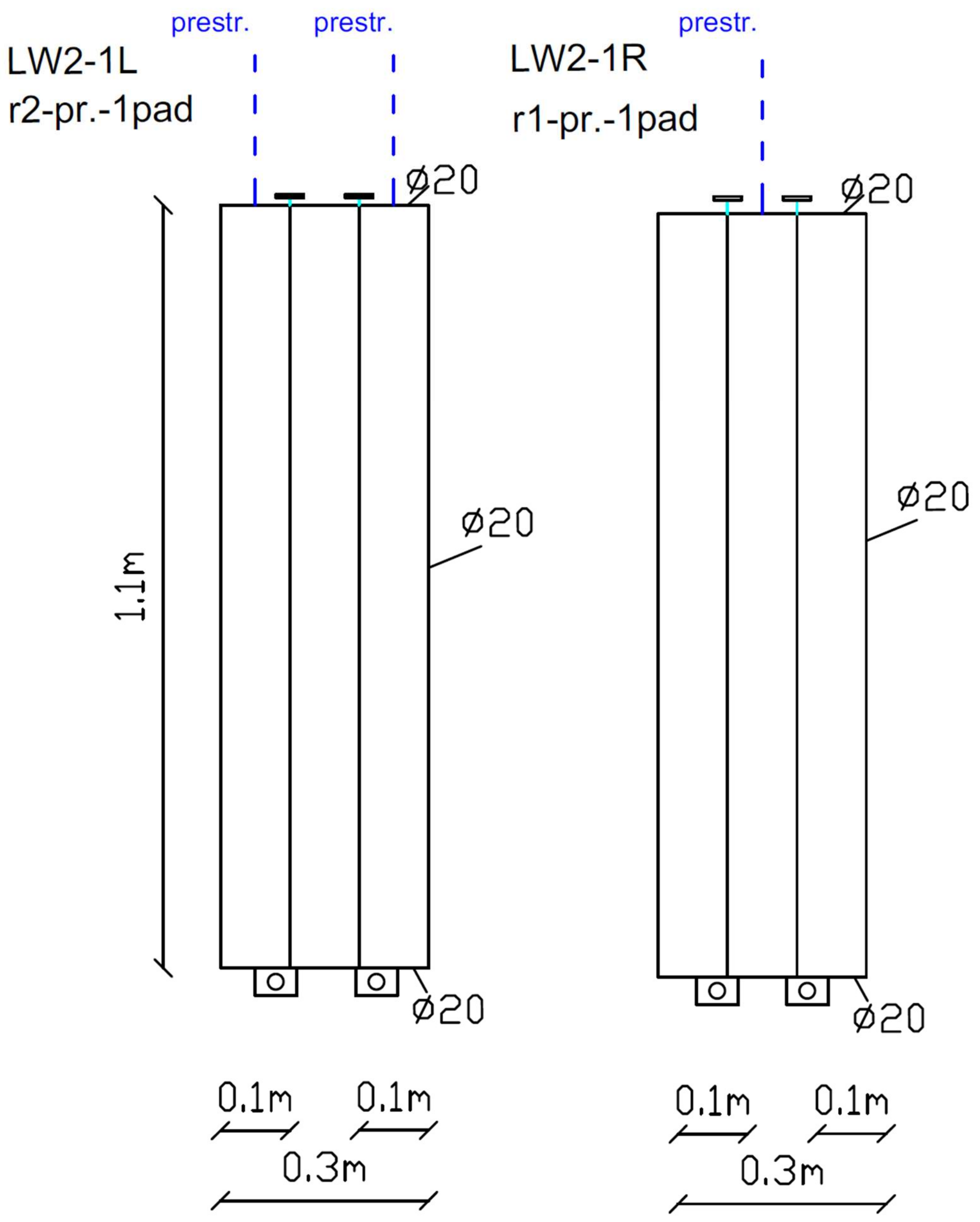

Figure 3.27 Living wall 2-1 left side and living wall 2-1 right side

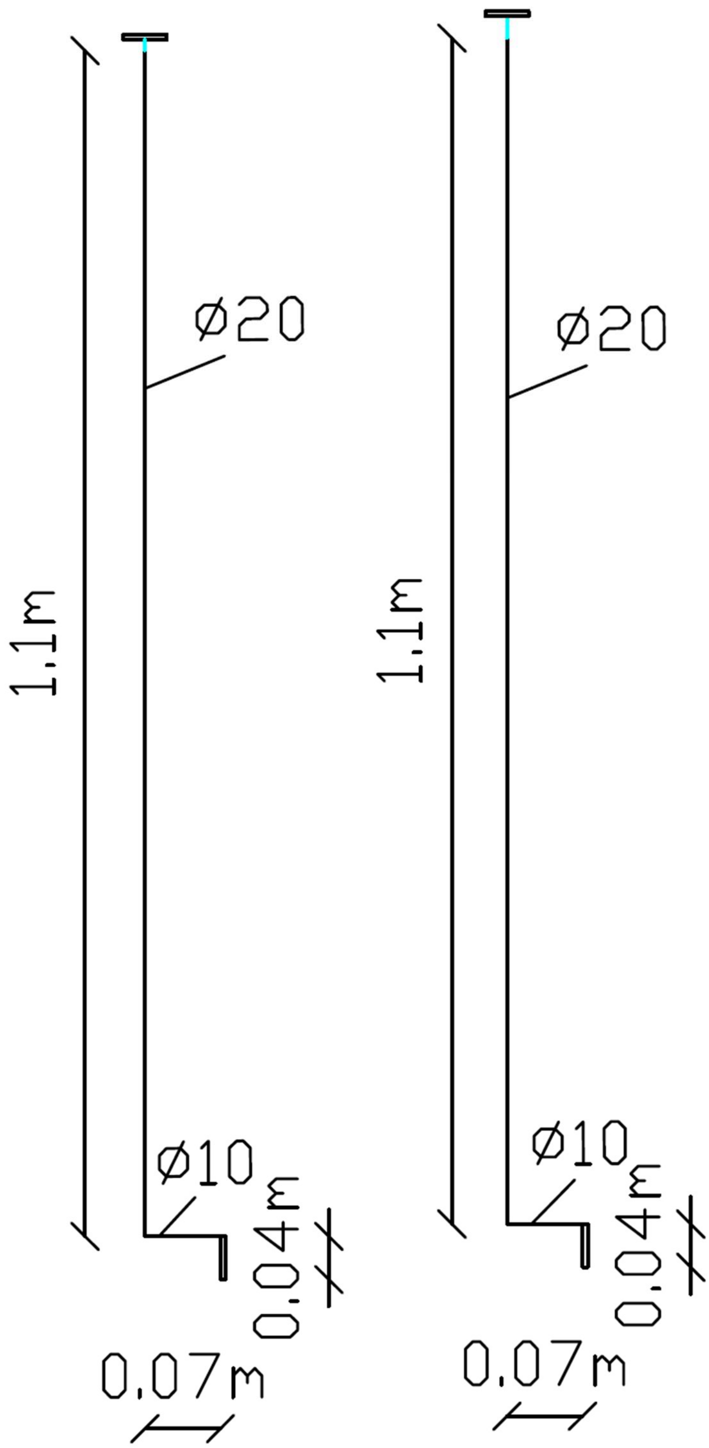

Figure 3.28 Cross section of living wall 2-1 left, 2-1 right

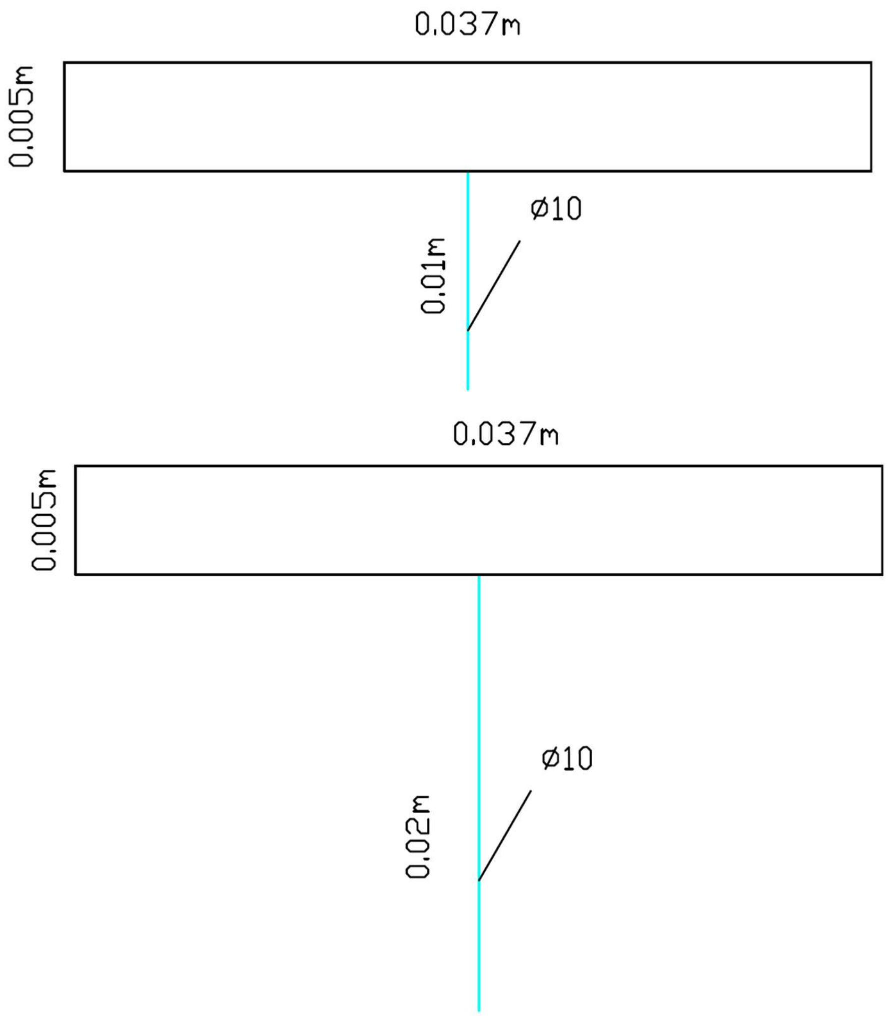

Figure 3.29 Anchoring details for LW2-1 under the top slab

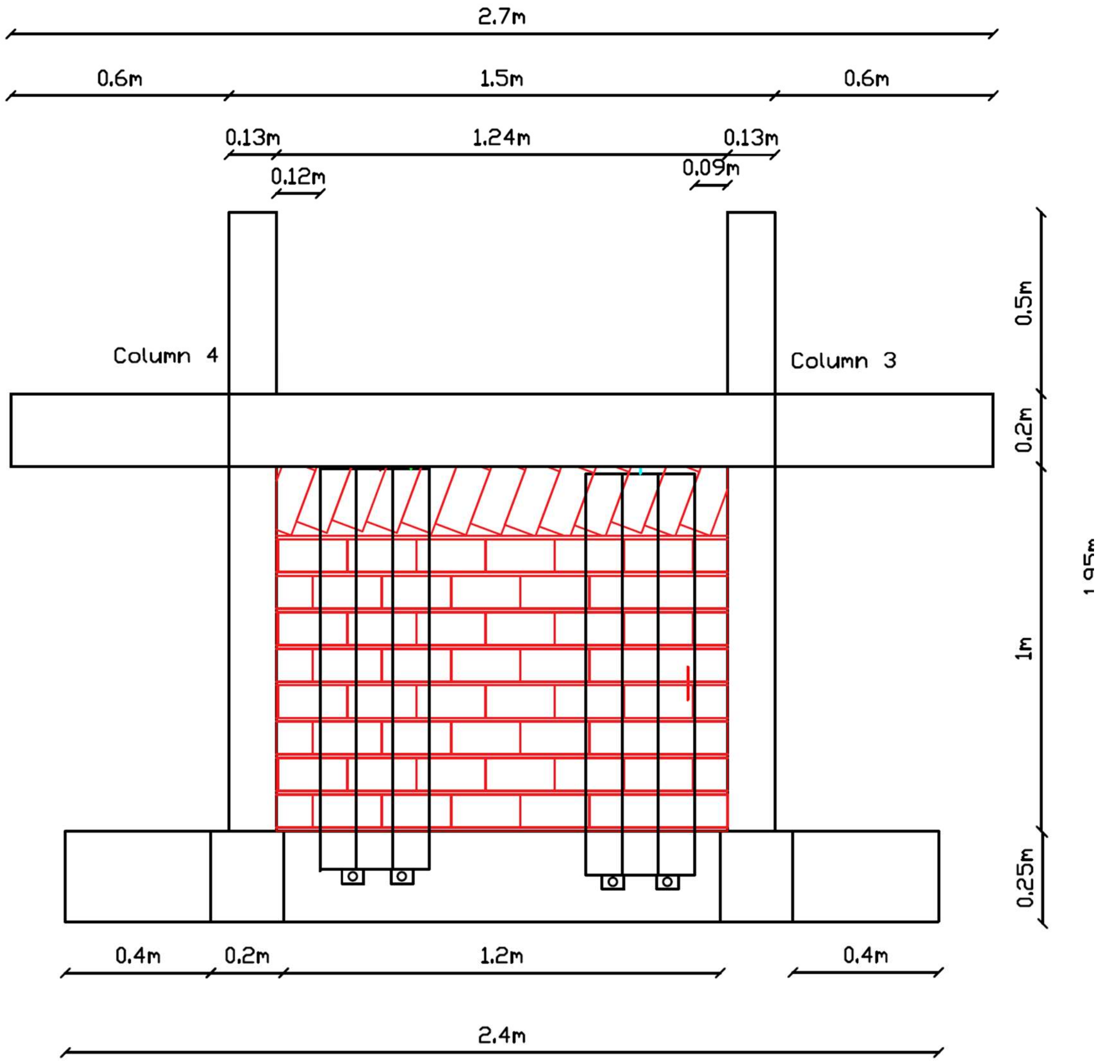

Figure 3.30 View of living wall 4-3

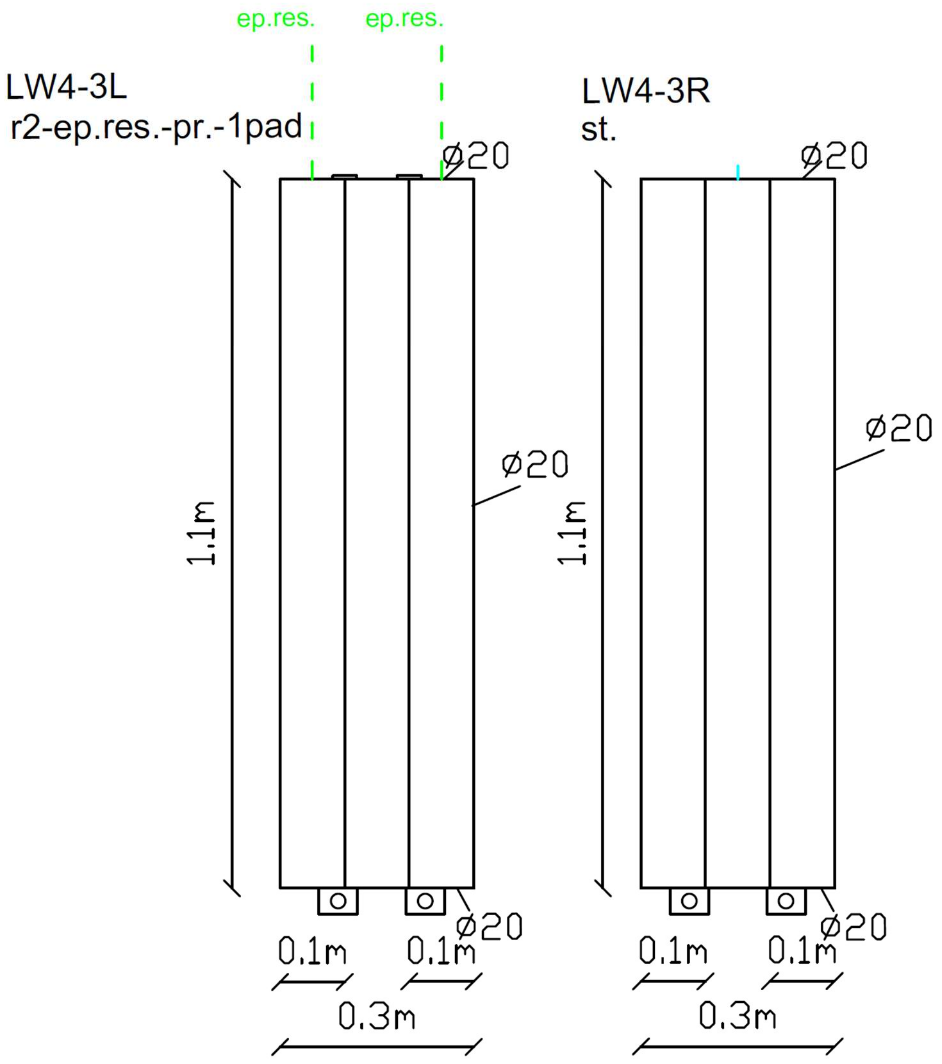

Figure 3.31 Living wall 4-3 left side and living wall 4-3 right side

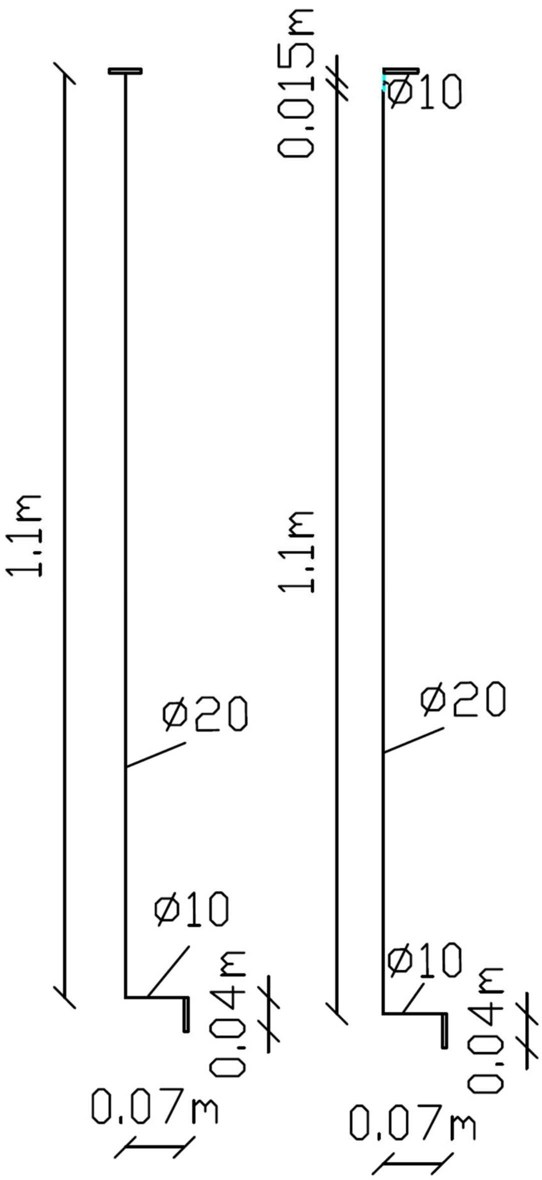

Figure 3.32 Cross section of living wall 4-3 left, 4-3 right

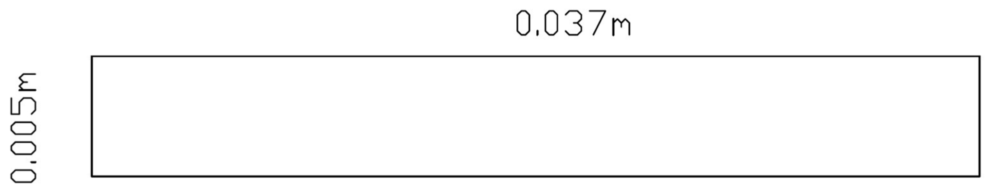

Figure 3.33 Anchoring details of LW4-3, under the top slab

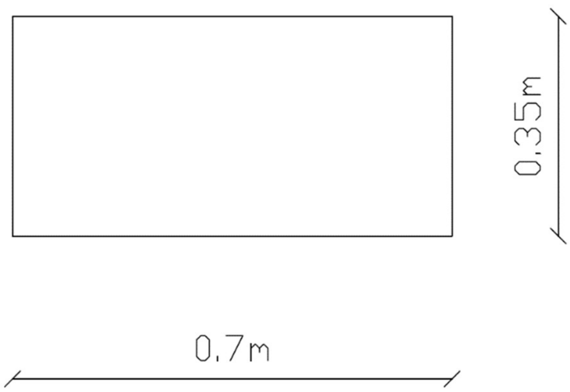

(a)

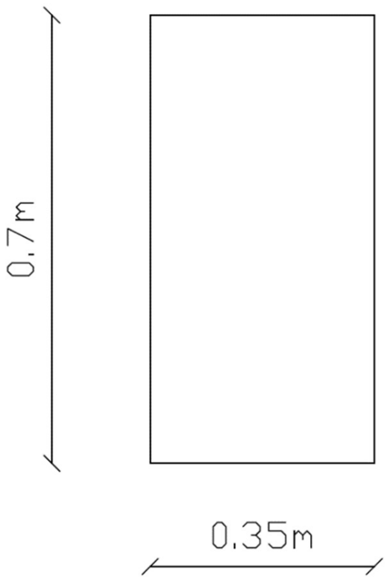

(b)

Figure 3.34 (a) View of tree planters, (b) Floor plan of planters

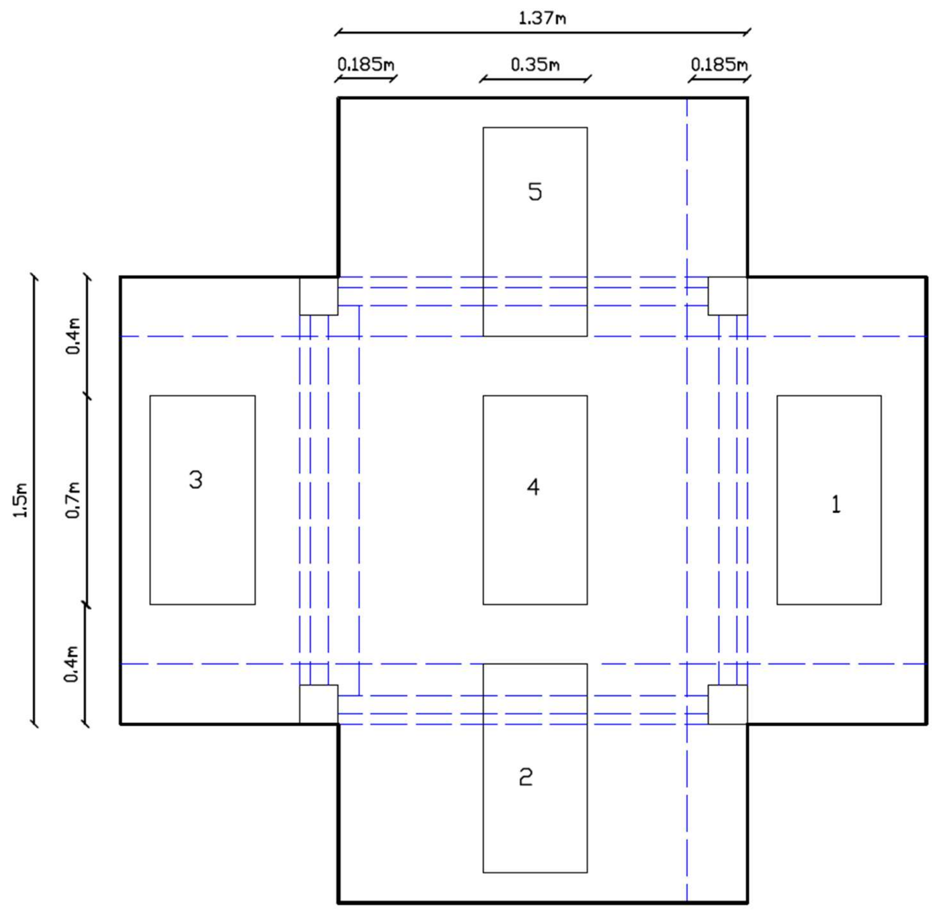

(a)

Figure 3.35 Floor plan of top slab with planters

Detailing of planter anchoring on the top slab

Planter 1

Drilling through the slab. Steel rod that passes through the slab, the planter, and is tightened with a nut at the bottom of the slab (downside) and at the top of the planter (simulating of anchoring of both tree rooting system and planter.

Planter 2

Drilling through the slab. Two basalt ropes used as tendons passing through the hole made in the slab. One rope (double) has been fully post-tensioned, while the second rope (double) was partially tensioned to serve as safety rope.

Planter 3

Two basalt ropes used as tendons pass through the hole made in the slab. One has been fully post-tensioned, while the second partially.

Planter 4

No basalt anchors have been used. The planter is just simply supported on two opposite PM pads with dimensions 400mmX40mmX5mm.

Planter 5

Two basalt ropes used as tendons that have been fully post-tensioned.

(a)

(b)

Figure 3.36 Living wall 3-2 anchoring details under the top slab (a) LW3-2L, (b) LW3-2R


(a)


(b)

Figure 3.37 Living wall 1-4 anchoring details under the top slab (a) LW1-4L, (b) LW1-4R

(a)

(b)

Figure 3.38 Living wall 2-1 anchoring details under the top slab (a) LW2-1L, (b) LW1-1R

(a)

(b)

Figure 3.39 Living wall 4-3 anchoring details under the top slab (a) LW4-3L, (b) LW4-3R

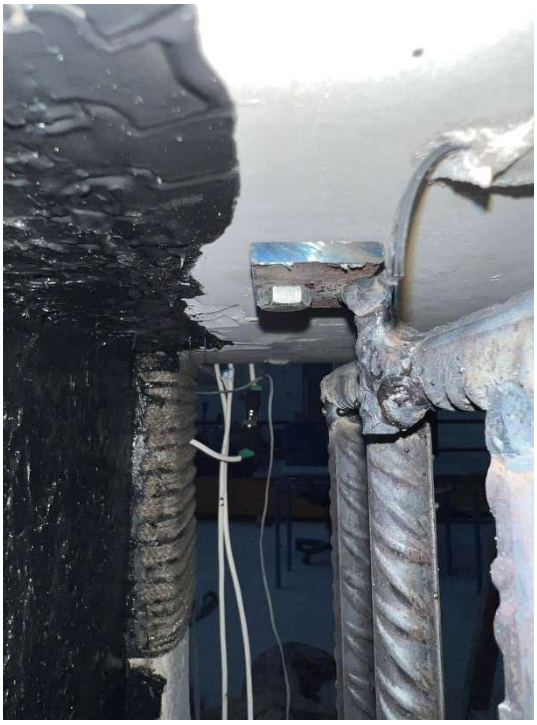

(a)

(b)

Figure 3.40 Steel bolt (a) and Wall plug/ screw anchor used for the anchorage (b)

3.5 MASS OF THE STRUCTURE

The total mass of concrete and reinforcement at each structural level is as follows: the foundation beams weigh 1,139.6 kg, the columns below the slab weigh 172.6 kg, and the four brick infill walls have a combined mass of 200 kg. The slab and hidden beams together weigh 2,691.7 kg, while the columns above the slab weigh 84.1 kg. This results in a total structural mass of 4,288 kg. Additionally, the mass attributed to the slab level—including the slab itself, the columns above the slab, and half the mass of both the columns below the slab and the infill walls—is calculated as 2,962.1 kg.

Eight steel structures of 12kg each represented the vertical living walls. Five concrete planters of 153kg have an area of action of 0.35x0.70m for each planter. Wooden sticks of total weight of 30kg were attached to the planters to simulate common trees.

The total extra mass added to the structure is 59+153x5+ 12x8+ 30 = 950 kg

Table 3.2 Calculation of the total mass of the structure

Element	mass (kg)
Mass of as built structure	4,288
Panters (5)	5 x 153
Steel structures-LW (8)	12 x 8
Wooden sticks	30
Retrofits	59
Total	5,238

4 INSTRUMENTATION

The instrumentation includes 12 uniaxial accelerometers (ACC) positioned at four locations as shown in Figure 4.1 (identical to the instrumentation of as-built specimen). At each location, three accelerometers capture the acceleration components in three directions, covering both in-plane and out-of-plane motions at the center of the full infill walls, as well as accelerations of the top slab and the bottom foundation beam. Additionally, eight in total draw wire sensors (W) monitor the horizontal displacements of the foundation beams and of the top slab, as illustrated in Figure 4.2 and presented in Table 4.1. These sensors measure linear displacement through a highly flexible yet tensioned steel wire connected to a cable drum, which provides an output signal proportional to displacement.

Except for the already installed 20 strain gauges in the as-built structure, two more strain gauges were placed on the polyurethane PM at the PUFJ joint. The joint is located between column 1 and the partial brick infill while the 2 strain gauges are placed on the PUFJ surface (opposite to each other: internal-external), 5cm under the slab along direction x, totaling them to 22.

Additionally, PZTs are installed as patches at specific locations to monitor the health of the retrofits and the connection (anchoring) of the structures created by the presence of the vertical forest. More specifically, 11 extra PZTs were placed on the strengthened structure:

- 2 on basalt rope at the top and the bottom of column 2,

- 1 at the surface of the infill connected to column 2, inside the polyurethane

- 1 on basalt rope at the top of column 1

-1 at the surface on the infill connected to column 1

- 1 on the basalt rope at the bottom of column 3

- 1 on the basalt rope at the bottom of column 4

- 2 on the surface of the roof

- 2 on the anchoring metal structures, 1 at the planter’s and 1 at the living wall’s.

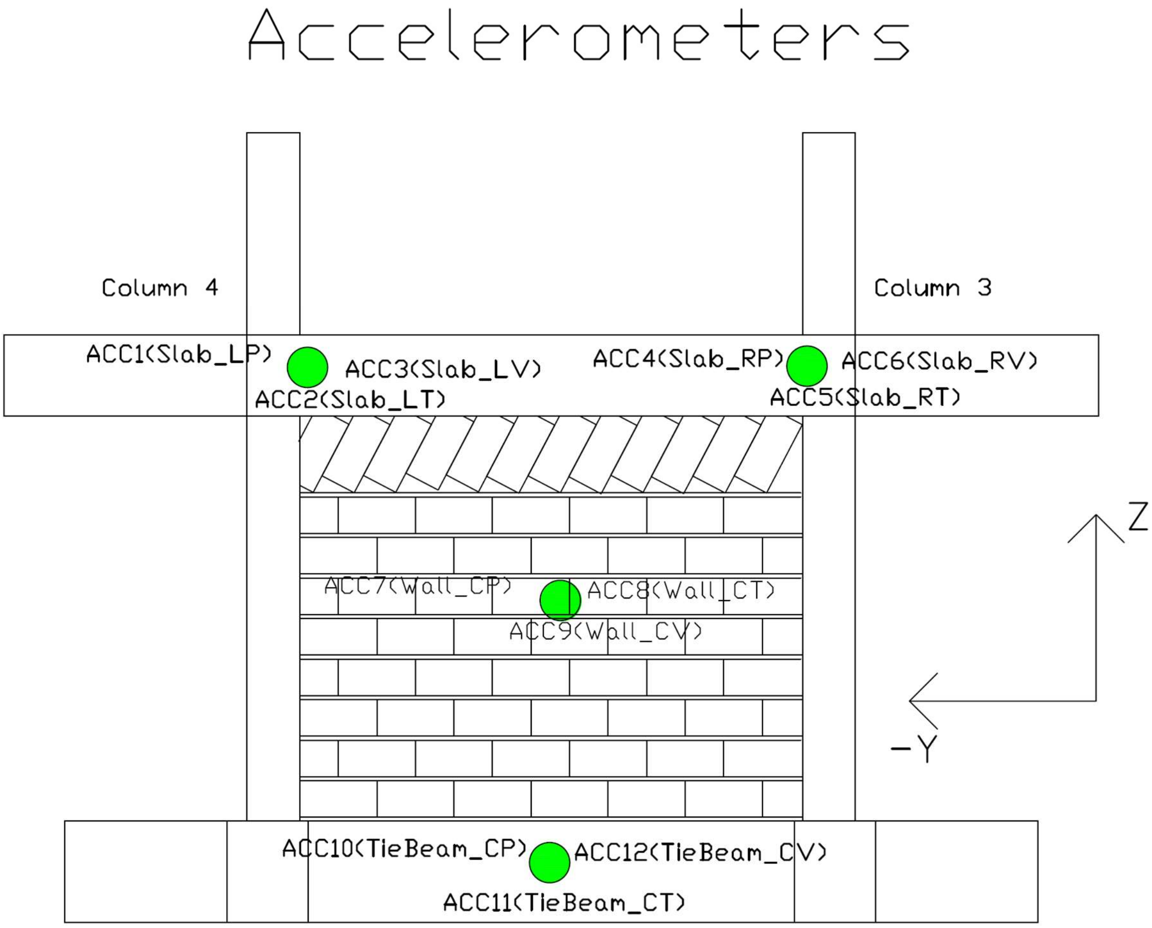

Figure 4.1 Position of accelerometers (specimen's view perpendicular to the direction of the seismic table movement)

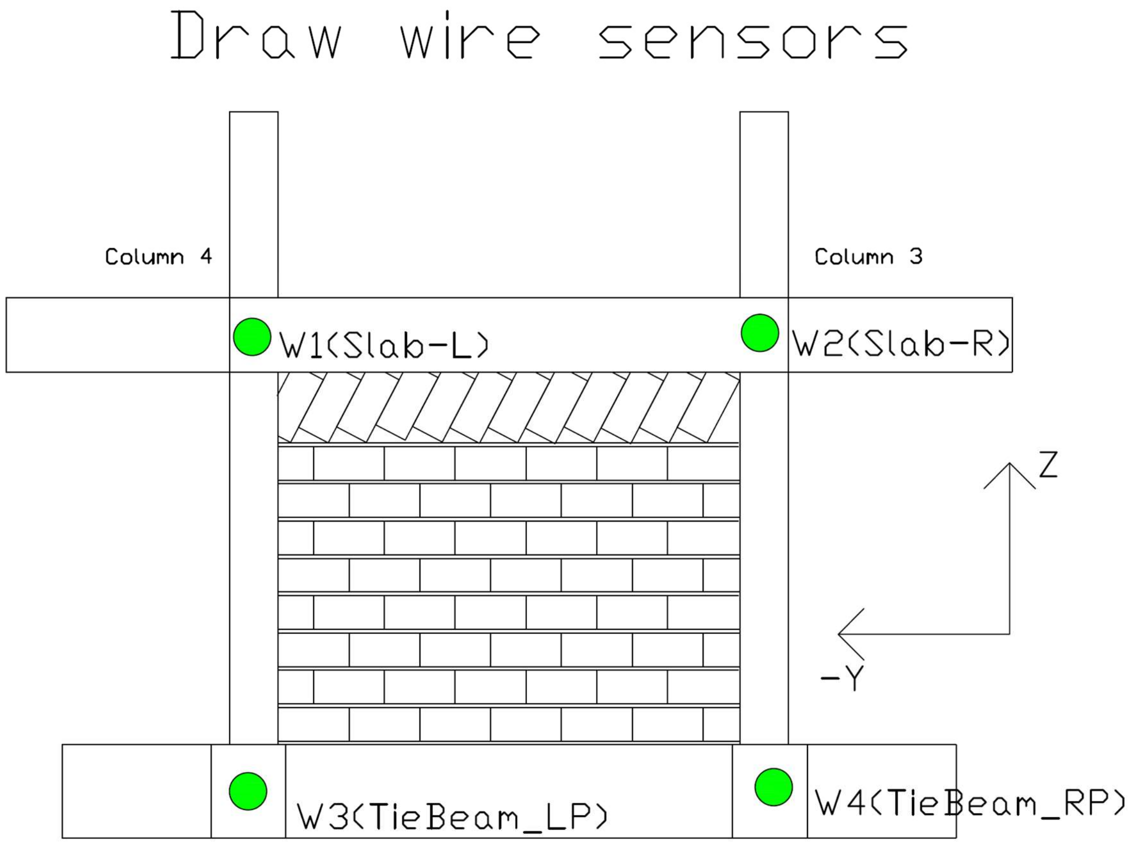

Figure 4.2 Position of the draw wire sensors on the concrete structure slab and foundation beams (specimen's view parallel to the direction of the seismic table movement)

Table 4.1 List of accelerometers, draw wire meters and strain gauges placed inside and on the structure

Ch No.	Channel name	Type of instrument	Measured quantity (units)	Position
1	ACC 1	Accelerometer	Acceleration (g)	On the slab, on the left corner, dir. (x)
2	ACC 2			On the slab, on the left corner, dir. (y)
3	ACC 3			On the slab, on the left corner, dir. (z)
4	ACC 4			On the slab, on the right corner, dir. (x)
5	ACC 5			On the slab, on the right corner, dir. (y)
6	ACC 6			On the slab, on the right corner, dir. (z)
7	ACC 7			On the infill, on the center, dir (x)
8	ACC 8			On the infill, on the center, dir (y)
9	ACC 9			On the infill, on the center, dir (x)
10	ACC 10			On the foundation, on the center, dir (x)
11	ACC 11			On the foundation, on the center, dir (y)
12	ACC 12			On the foundation, on the center, dir (z)
13	W 1	Draw wire sensors	Length (mm)	On the slab, on the left side
14	W 2			On the slab, on the right side
15	W 3			On the foundation, on the left side
16	W 4			On the foundation, on the right side
17	W 5			along the partial masonry infill diagonal
18	W 6			along the partial masonry infill diagonal
19	W 7			along the partial masonry infill diagonal
20	W 8			along the partial masonry infill diagonal
21	S1	Strain gauges	Strain	In the longitudinal reinforcement, on the underside
22	S2			
23	S3			
24	S4			
25	S5			
26	S6			
27	S7			
28	S8			
29	S9			In the longitudinal reinforcement, on the upper side
30	S10			
31	S11			

32	S12			
33	S13			
34	S14			
35	S15			
36	S16			
37	S17	Strain gauges	Strain	On the centre of partial masonry 1 along direction x
38	S18			On the centre of partial masonry 1 along direction z
39	S19			On the centre of partial masonry 2 along direction x
40	S20			On the centre of partial masonry 2 along direction z
41	S21			On the polyurethane (PM) at the joint between column and the partial masonry, 5cm under the slab along direction x
42	S22			On the polyurethane (PM) at the joint between column and the partial masonry, 5 cm under the slab along direction x

4.1 EXPANDING THE SMART PZT MONITORING SYSTEM FOR THE RENOVATED 3D VF STRUCTURE

Structural health monitoring for real-time condition assessment and damage detection in the tested VF concrete structure is performed using PZTs. Prompt damage diagnosis of seismically deficient VF buildings requires, in addition to the other common testing measurements, the monitoring and evaluation in a real-time system based on piezoelectric sensors or piezoelectric transducers (PZTs) Fig.4.3.

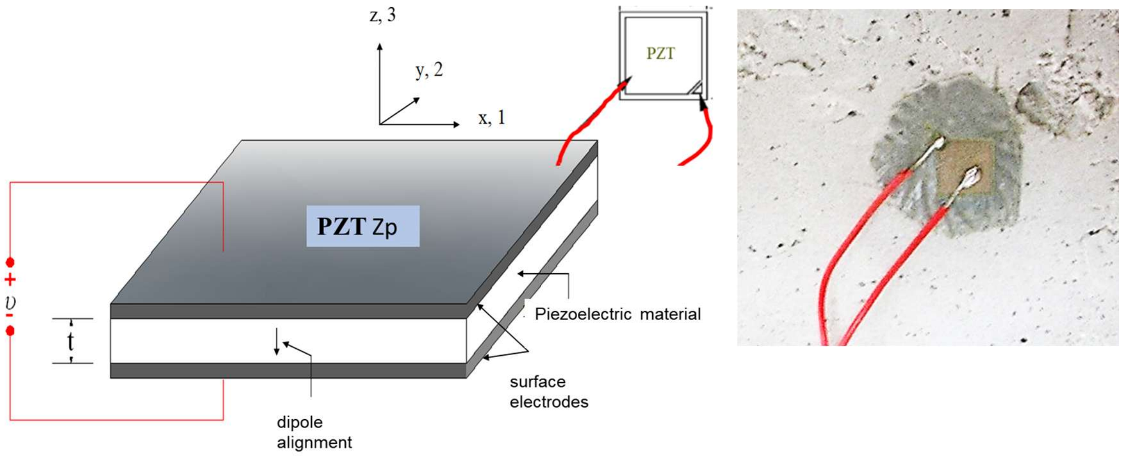

Figure 4.3 PZT connected using wires

This innovative Structural Health Monitoring (SHM) system in this phase uses the sensors that have already been installed as patches or embedded-in "smart aggregate" (SAs) featuring smart properties or implements a network of piezoelectric patches to monitor the condition of the reinforced VF concrete structure. Additionally, PZTs are installed as patches at specific locations to monitor the health of the retrofits and the connection (anchoring) of the structures created by the presence of the vertical forest.

The Electromechanical Impedance (EMI) method has demonstrated significant potential as a reliable technique for continuous inspection and damage assessment in both new and existing in-service infrastructure, including retrofitted structures. One of its primary advantages lies in its sensitivity to local damage detection, even in complex structural systems. This includes monitoring damage in retrofitted concrete frames and evaluating the performance of strengthened reinforced concrete elements (Na et al., 2018; Sam-Daliri Na et al., 2018, 2021; Haq et al., 2022; Naoum et al., 2024), as well as in composite materials (Voutetaki et al., 2022; Naoum et al., 2023). Moreover, extensive research has been conducted on the application of EMI-based Structural Health Monitoring (SHM) in full-scale structural members, such as shear-critical RC beams (Chalioris et al., 2016; Voutetaki et al., 2016), RC frames (Chalioris et al., 2020), and RC joints (Karayannis et al., 2022), under both monotonic and cyclic loading conditions.

In this case, the PZT patches are positioned at several locations to receive results for the structural health of the renovated 3d VF structure. Basalt rope reinforcement was applied in two layers around the top and bottom to improve structural performance. Throughout the wrapping process, special care was taken to keep the pre-installed PZT wires safe and intact. The basalt rope was tightly coiled with consistent tension to ensure full contact without affecting the PZT functionality. This method provides effective reinforcement while preserving the integrity of the PZT wiring. The following figure illustrates the basalt ropes wrapped around the top and bottom sections of the column, showing how the reinforcement is applied carefully to protect the PZT patches and their wires.

Figure 4.4 Application of the basalt ropes concerning the PZT patches that were already installed in the as-built structure.

The following figures depict the placement and installation of PZT patches on designated areas of the renovated 3D Vertical Forest structure, with a focus on evaluating the effectiveness of the retrofits and the structural impact of the vertical forest structure attached to the RC structure.

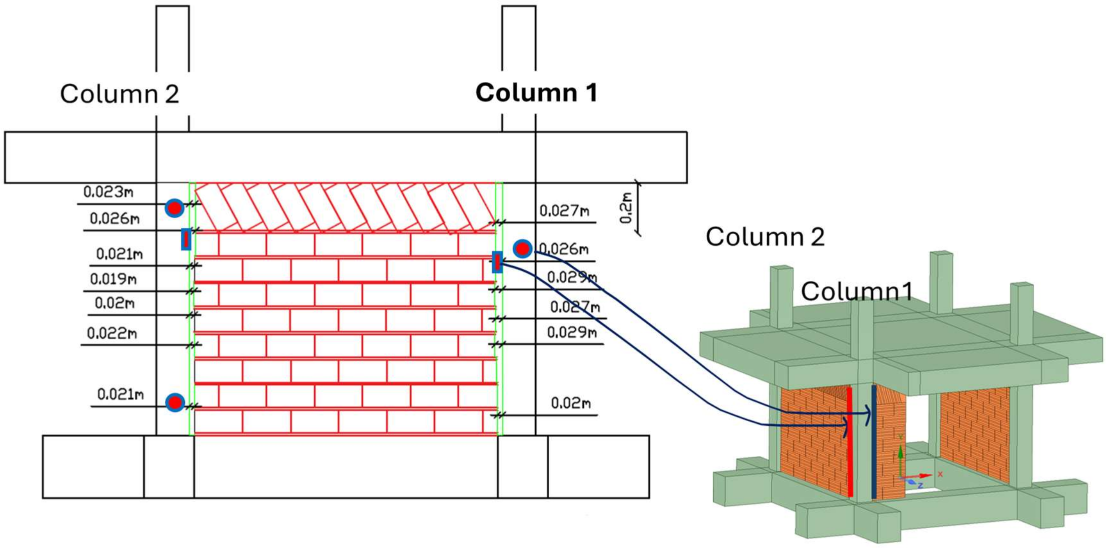

Figure 4.5 Location of the PZT patches installed at the surface of column 1

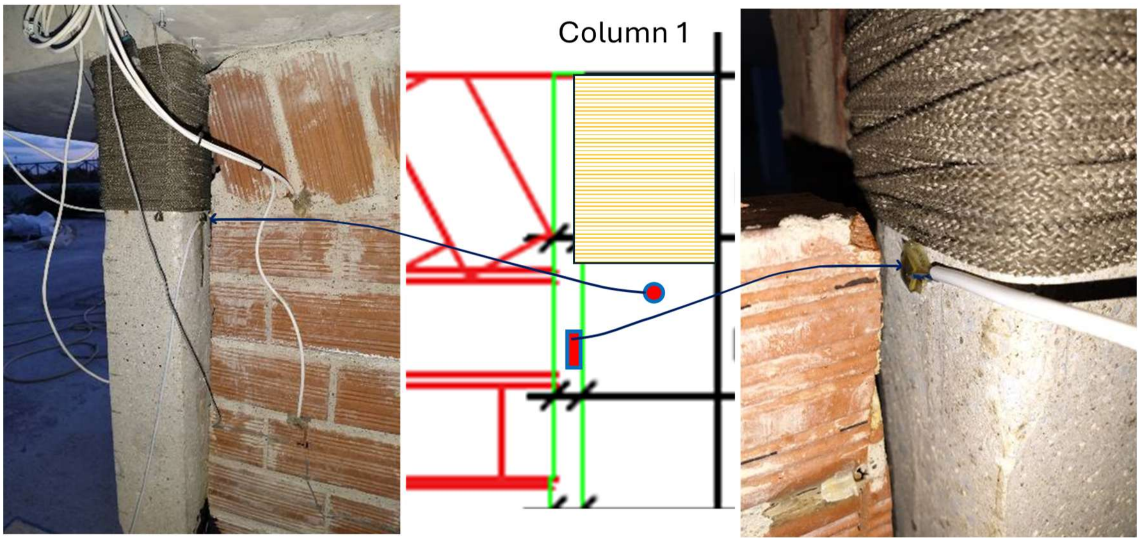

Figure 4.6 Details of the PZT patches installed at the surface of RC column 1

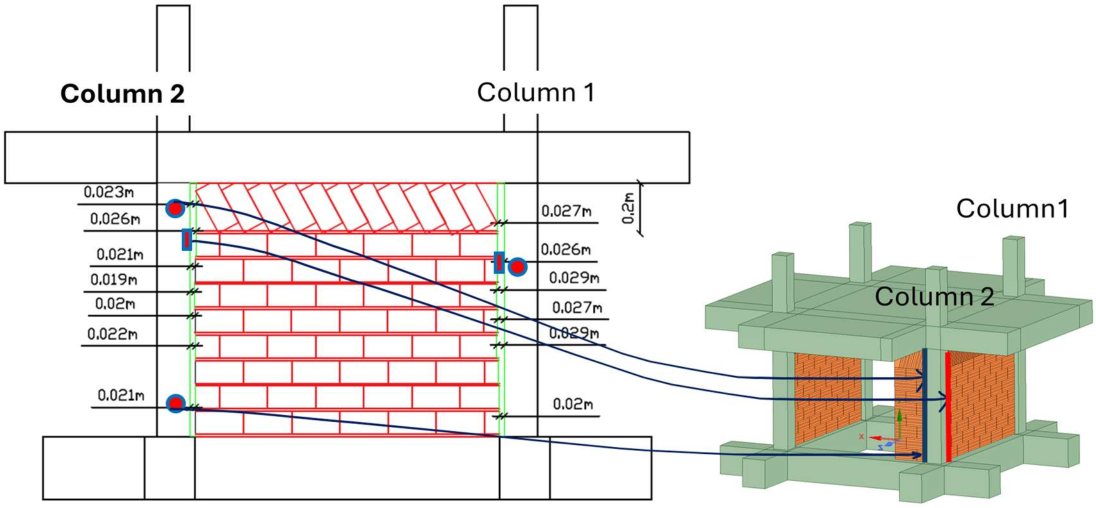

Figure 4.7 Location of the PZT patches installed at the surface of column 2

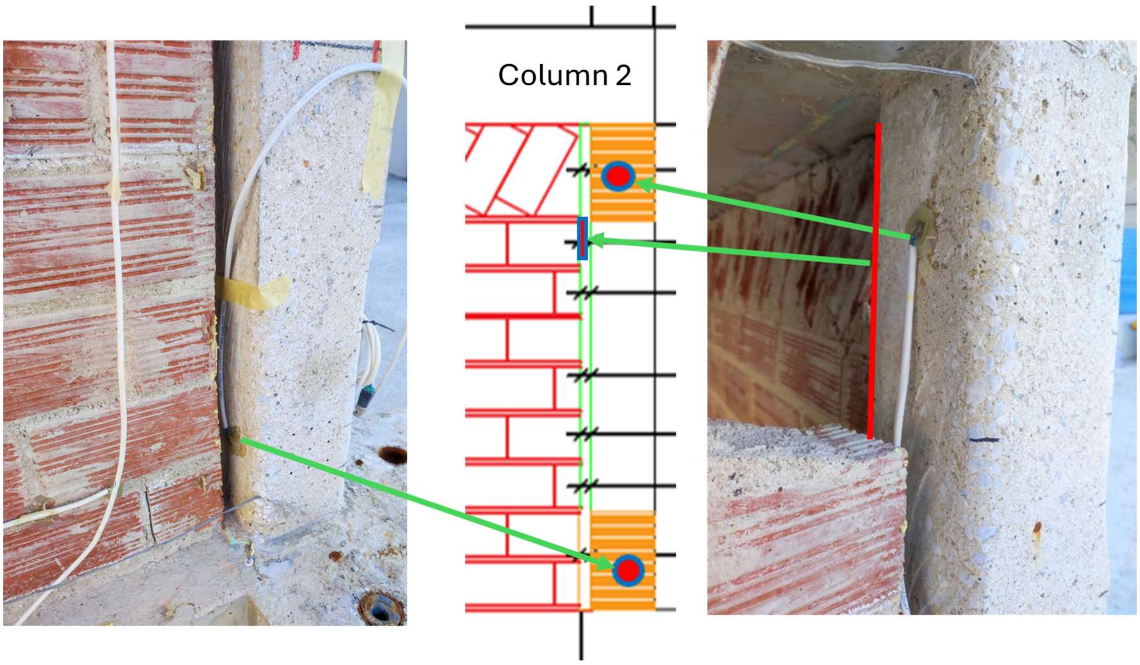

Figure 4.8 Details of the PZT patches installed at the surface of column 2 and at the surface of the infill inside the polyurethane.

The next figure depicts the application of basalt rope for column reinforcement, indicating the locations of PZT patches installed on the basalt ropes using resin at the bottom of Columns 3 and 4.

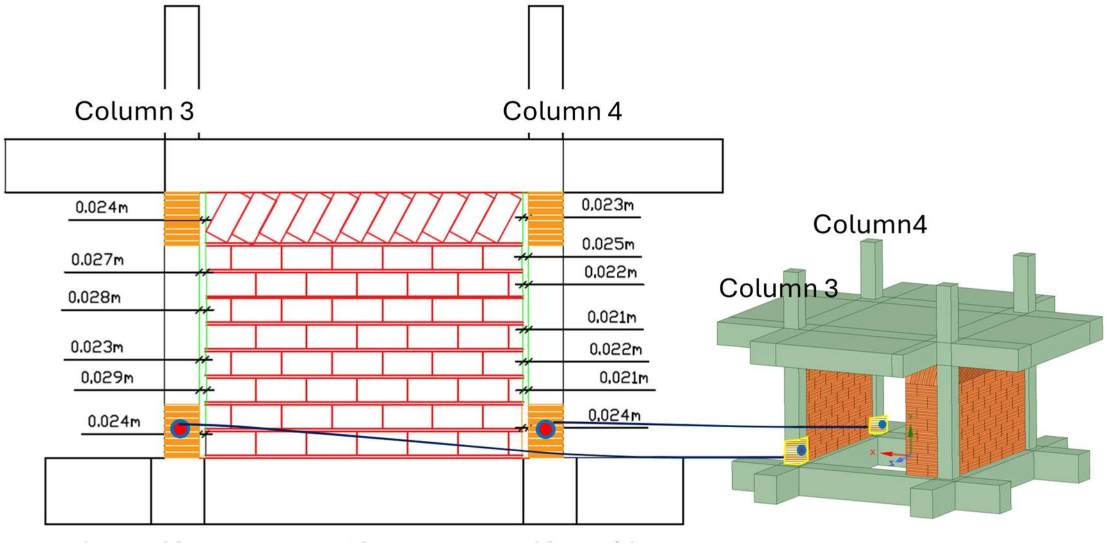

Figure 4.9 Location of the PZT patches installed on Basalt ropes using resin at the bottom of columns 3 and 4.

Figure 4.10 Details of the PZT patches installed on columns 3 and 4.

Next figure illustrates the location and the installation of PZT patches on a basalt rope used to anchor vertical LW steel construction within the slab, where a suitable hole was drilled for rope insertion and a small tension was applied using a special steel device positioned at the upper part of the slab.

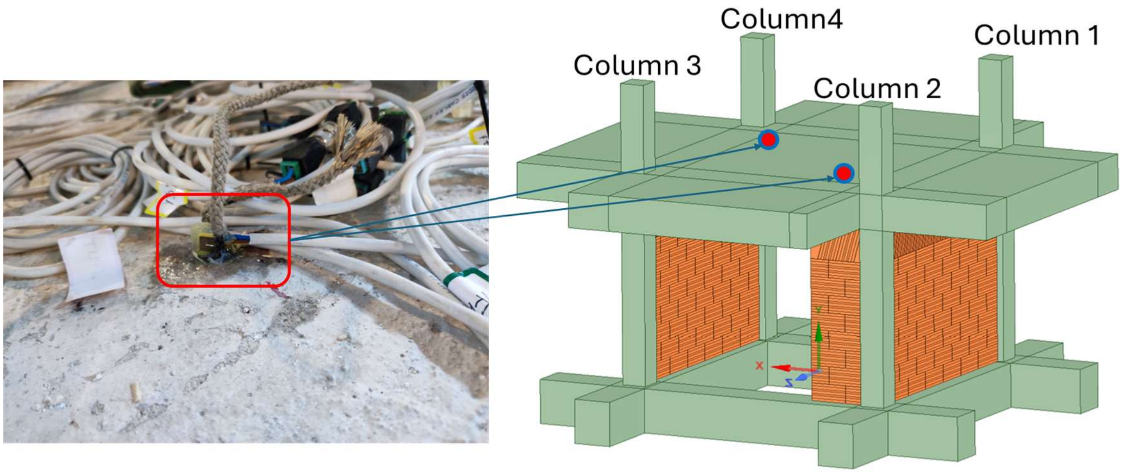

Figure 4.11 Location of the PZT patches installed on Basalt ropes using resin on the roof

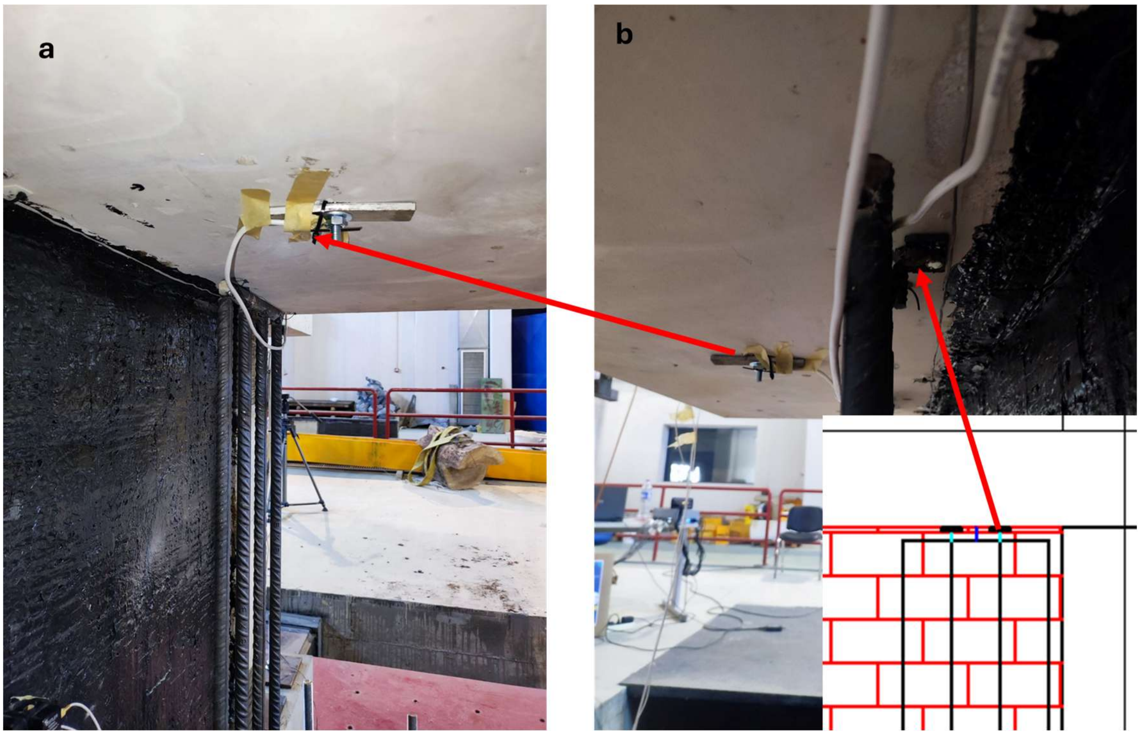

Figure 4.12 PZT patches installed on the anchoring of metal structures for the (a) planter and (b) Living wall structure

5 CONCLUSIONS

This report provides a detailed overview of the design, detailing, and instrumentation of the VF renovated 3D structure. The lightweight local retrofit of the rc columns with basalt fiber ropes, the construction of PUFJ seismic joints between the rc columns and the brick infill walls and the external jacketing of the cracked brick infill walls with FRPU are thoroughly presented.

The retrofitted structure receives additional vertical forest renovations with eight constructions simulating typical vertical living walls (mass and stiffness) with traditional bottom supports and different innovative detailing of top supports with PU pads and basalt ropes to minimize unfavorable interaction with the concrete structure. Finally, 5 concrete planters with wooden sticks simulate heavy tree greenery on top slabs and balconies and assess different anchoring detailing with traditional or basalt rope anchors as well as the effects of PU pads. All different cases of renovation detailing assess innovative green envelopes, compared to traditional ones.

Besides the accelerometers, displacement meters, strain gauges, PZT sensors used during the first phase of testing of as-built structure, the PZT network is further expanded. Together with additional strain gauges, the extra PZTs cover also the retrofits and VF renovations.

REFERENCES

Chalioris, C.E.; Karayannis, C.G.; Angeli, G.M.; Papadopoulos, N.A.; Favvata, M.J.; Providakis, C.P. Applications of Smart Piezoelectric Materials in a Wireless Admittance Monitoring System (WiAMS) to Structures-Tests in RC Elements. Case Stud. Constr. Mater. 2016, 5, 1-18, doi:10.1016/j.cscm.2016.03.003.

Chalioris C, Voutetaki M, Liolios A. Structural Health Monitoring of Seismically Vulnerable RC Frames under Lateral Cyclic Loading. Earthquakes and Structures 2020; 19(1): 29–44.

Chalioris CE, Kytinou VK, Voutetaki ME, Karayannis CG. Flexural Damage Diagnosis in Reinforced Concrete Beams Using a Wireless Admittance Monitoring System—Tests and Finite Element Analysis. Sensors 2021; 21(3). DOI: https://doi.org/10.3390/s21030679.

Gams M, Tomaževič M, Berset T. Seismic strengthening of brick masonry by composite coatings: an experimental study. Bulletin of Earthquake Engineering 2017; 15(10): 4269–4298.

Golias E, Zapris AG, Kytinou VK, Osman M, Koumtzis M, Siapera D, Chalioris CE, Karayannis CG. Application of X-Shaped CFRP Ropes for Structural Upgrading of Reinforced Concrete Beam–Column Joints under Cyclic Loading–Experimental Study. Fibers 2021; 9(7).

Guo R, Zhang H, Chen K, et al. Seismic Performance Analysis of Concrete Columns Reinforced with Prestressed Wire Ropes Embedded in Polyurethane Cement Composites. *Buildings*. 2024 ; 14 (4) : 993. doi:10.3390/buildings14040993.

Haq M., Bhalla S., Naqvi T., Piezo-impedance based fatigue damage monitoring of restrengthened concrete frames, Composite Structures 280 (2022), 114868, https://doi.org/10.1016/J.COMPSTRUCT.2021.114868.

Helman D, Yungstein Y, Mulero G, Michael Y. High-Throughput Remote Sensing of Vertical Green Living Walls (VGWs) in Workplaces. Remote Sensing 2022; 14(14): 3485.

Hojdys Ł, Krajewski P, Kwiecien A, Rousakis T, Vanian V, Marcin T, Viskovic A, Ilki A, Gams M, Rakicevic Z, Zajac B, Bogdanovic A. Quick Repair of Damaged Infill Walls with Externally Bonded FRPU Composites: Shake Table Tests. Journal of Composites for Construction ASCE. Volume 27, Issue 1.February: 2023. https://doi.org/10.1061/(ASCE)CC.1943-5614.0001268

Hou S, Zhang H, Han X, Ou J. Damage monitoring of the RC frame shaking table test and comparison with FEM results. Procedia Engineering 2017; 210: 393–400.

Irga PJ, Torpy FR, Griffin D, Wilkinson SJ. Vertical Greening Systems: A Perspective on Existing Technologies and New Design Recommendation. *Sustainability*. 2023;15(7):6014. doi:10.3390/su15076014.

Karayannis, C.G.; Golias, E.; Naoum, M.C.; Chalioris, C.E. Efficacy and Damage Diagnosis of Reinforced Concrete Columns and Joints Strengthened with FRP Ropes Using Piezoelectric Transducers. Sensors 2022, 22, 8294. https://doi.org/10.3390/s22218294

Karayannis C, Golias E, Kalogeropoulos G, Influence of Carbon Fiber-Reinforced Ropes Applied as External Diagonal Reinforcement on the Shear Deformation of RC Joints, Fibers 2022, 10(3), 28; https://doi.org/10.3390/fib10030028

Karayannis C, Golias E, Full-scale experimental testing of RC beam-column joints strengthened using CFRP ropes as external reinforcement, Engineering Structures, Volume 250, 1 January 2022, 113305, https://doi.org/10.1016/j.engstruct.2021.113305

Karayannis CG, Voutetaki ME, Chalioris CE, Providakis CP, Angeli GM. Detection of flexural damage stages for RC beams using Piezoelectric sensors (PZT). Smart Structures and Systems, An International Journal 2015; 15(4): 997–1018.

Kwiecień A, Gams M, Rousakis T, Viskovic A, Korelc J. Validation of a New Hyperviscoelastic Model for Deformable Polymers Used for Joints between RC Frames and Masonry Infills. Engineering Transactions 2017; 65(1): 113–121.

Kwiecień A. Shear bond of composites-to-brick applied with highly deformable, in relation to resin epoxy, interface materials. Materials and Structures 2014; 47(12): 2005–2020.

Kwiecień A, Zając B. Dynamic response of the cracked masonry building repaired with the flexible joint method – an innovative earthquake protection. In: Brennan MJ, editor. Proceedings of the 7th European Conference on Structural Dynamics, 7-9 July 2008, Southampton: University of Southampton. Institute of Sound & Vibration Research; 2008.

Kwiecień A, de Felice G, Oliveira DV, Zając B, Bellini A, De Santis S, et al. Repair of composite-to masonry bond using flexible matrix. Materials and Structures 2016; 49(7): 2563–2580.

Na, W.S; Baek, J., A Review of the Piezoelectric Electromechanical Impedance Based Structural Health Monitoring Technique for Engineering Structures, Sensors 2018, 18(5), 1307; doi:10.3390/s18051307.

Nakashima M, Nagae T, Enokida R, Kajiwara K. Experiences, accomplishments, lessons, and challenges of E-defense—Tests using world's largest shaking table. *Japan Architectural Review*. 2018;1(1):4-17. doi:10.1002/2475-8876.10020.

Naoum, M.C.; Papadopoulos, N.A.; Voutetaki, M.E.; Chalioris, C.E. Structural Health Monitoring of Fiber-Reinforced Concrete Prisms with Polyolefin Macro-Fibers Using a Piezoelectric Materials Network under Various Load-Induced Stress. Buildings 2023, 13, 2465. https://doi.org/10.3390/buildings13102465

Naoum, M.C.; Papadopoulos, N.A.; Sapidis, G.M.; Chalioris, C.E. Advanced Structural Monitoring Technologies in Assessing the Performance of Retrofitted Reinforced Concrete Elements. Appl. Sci. 2024, 14, 9282. https://doi.org/10.3390/app14209282

Ozden S, Akguzel U, Ozturan T. Seismic strengthening of infilled reinforced concrete frames with composite materials. ACI Structural Journal 2011; 108(4): 414–422.

Padanattil A, Karingamanna J, K.M M. Novel hybrid composites based on glass and sisal fiber for retrofitting of reinforced concrete structures. Construction and Building Materials 2017; 133: 146–153.

Papadopoulos, N.A.; Naoum, M.C.; Sapidis, G.M.; Chalioris, C.E. Cracking and Fiber Debonding Identification of Concrete Deep Beams Reinforced with C-FRP Ropes against Shear Using a Real-Time Monitoring System. Polymers 2023, 15, 473, doi:10.3390/polym15030473.

Providakis C, Tsistrakis S, Voutetaki M, Tsompanakis Y, Stavroulaki M, Agadakos J, Kampianakis E, Pentes G. A new damage identification approach based on impedance-type measurements and 2D error statistics. Structural Monitoring and Maintenance 2015; 2(4): 319–338.

Providakis C, Tsistrakis S, Voutetaki M, Tsompanakis J, Stavroulaki M, Agadakos J, Kampianakis E, Pentes G, Liarakos E. An Innovative Active Sensing Platform for Wireless Damage Monitoring of Concrete Structures. Current Smart Materials 2016; 1(1): 49–62.

Rouka D, Kaloudaki A, Rousakis T, Fanaradelli T, Anagnostou E, Kwiecień A, et al. Response of RC buildings with Low-strength Infill Walls Retrofitted with FRP sheets with Highly Deformable Polymer-Effects of Infill Wall Strength. 25th International Conference on Composites/Nano Engineering, Rome 2017.

Rousakis TC, Tourtouras IS. RC columns of square section – Passive and active confinement with composite ropes. Composites Part B: Engineering 2014; 58: 573–581.

Rousakis TC. Reusable and recyclable nonbonded composite tapes and ropes for concrete columns confinement. Composites Part B: Engineering 2016; 103: 15–22.

Rousakis T, Ilki A, Kwiecien A, Viskovic A, Gams M, Triller P, Ghiassi B, Benedetti A, Rakicevic Z,Colla C, Halici OF, Zając B, Hojdys Ł, Krajewski P, Rizzo F, Vanian V, Sapalidis A, Papadouli E, Bogdanovic A. Deformable Polyurethane Joints and Fibre Grids for Resilient Seismic Performance of Reinforced Concrete Frames with Orthoblock Brick Infills. Polymers 2020; 12(12). DOI: https://doi.org/10.3390/polym12122869.

Rousakis T, Anagnostou E, Fanaradelli T. Advanced Composite Retrofit of RC Columns and Frames with Prior Damages—Pseudodynamic Finite Element Analyses and Design Approaches. Fibers 2021a; 9(9).

Rousakis T, Vanian V, Fanaradelli T, Anagnostou E. 3D FEA of Infilled RC Framed Structures Protected by Seismic Joints and FRP Jackets. Applied Sciences 2021b; 11(14).

Rousakis TC, Panagiotakis GD, Archontaki EE, Kostopoulos AK. Prismatic RC columns externally confined with FRP sheets and pre-tensioned basalt fiber ropes under cyclic axial load. Composites Part B: Engineering 2019; 163: 96–106. DOI: https://doi.org/10.1016/j.compositesb.2018.11.024.

Rousakis T, Tourtouras I. RC columns of square section – Passive and active confinement with composite ropes. *Composites Part B: Engineering*. 2014;58:573-581. doi:10.1016/j.compositesb.2013.11.011.

Rousakis T, Macha M. External Confinement with Basalt Fiber Ropes in Existing Reinforced Concrete Structures. *ce papers*. 2023;6(5):277-285. doi:10.1002/cepa.2109.

Sam-Daliri, O.; Faller, L.M.; Farahani M.; Roshanghias, A.; Araee, A.; Baniassadi, M.; Oberlercher, H.; Zangl, H., Impedance analysis for condition monitoring of single lap CNT-epoxy adhesive joint. International Journal of Adhesion and Adhesives, 88, 59-65, doi:10.1016/j.ijadhadh.2018.11.003.

Sam-Daliri, O.; Faller, L.M.; Farahani M.; Zangl, H., Structural health monitoring of adhesive joints under pure mode I loading using the electrical impedance measurement. Engineering Fracture Mechanics, 245, 107585, doi:10.1016/j.engfracmech.2021.107585.

Sharma R, Hsiao FP, Liu KY, Pon CE. Shaking table test of a half-scale three-story non-ductile RC building subjected to near-fault ground motions: Experimental and numerical modeling. *Structures*. 2022;45:721-747. doi:10.1016/j.istruc.2022.09.041.

Talakokula V, Bhalla S, Gupta A. Corrosion assessment of reinforced concrete structures based on equivalent structural parameters using electro-mechanical impedance technique. Journal of Intelligent Material Systems and Structures 2014; 25(4): 484–500. DOI: https://doi.org/10.1177/1045389X13498317.

Talakokula V, Bhalla S. Reinforcement corrosion assessment capability of surface bonded and embedded piezo sensors for reinforced concrete structures. Journal of Intelligent Material Systems and Structures 2015; 26(17): 2304–2313. DOI: https://doi.org/10.1177/1045389X14554133.

Tedeschi C, Kwiecień A, Valluzzi MR, Zając B, Garbin E, Binda L. Effect of thermal ageing and salt decay on bond between FRP and masonry. Materials and Structures 2014; 47(12): 2051–2065.

Triantafillou TC, Papanicolaou CG, Zissimopoulos P, Laourdekis T. Concrete confinement with textile- reinforced mortar jackets. ACI Structural Journal 2006; 103(1): 28.

Voutetaki ME, Papadopoulos NA, Angeli GM, Providakis CP. Investigation of a new experimental method for damage assessment of RC beams failing in shear using piezoelectric transducers. Engineering Structures 2016; 114: 226–240. DOI: https://doi.org/10.1016/j.engstruct.2016.02.014.

Voutetaki ME, Naoum MC, Papadopoulos NA, Chalioris CE. Cracking Diagnosis in Fiber- Reinforced Concrete with Synthetic Fibers Using Piezoelectric Transducers. Fibers 2022; 10(1).

Yuksel E, Ilki A, Erol G, Demir C, Karadogan HF. Seismic retrofit of infilled reinforced concrete frames with cfrp composites. In: Wasti ST, Ozcebe G, editors. Advances in Earthquake Engineering for Urban Risk Reduction, Dordrecht: Springer Netherlands; 2006.